STEREOISOMERS RESULTING FROM THE HINDERED ROTATION IN N-(*o*-ARYL)-2,4-OXAZOLIDINEDIONE DERIVATIVES

by

Öznur Demir

BS. in Chem., Abant İzzet Baysal University, 1998

Submitted to the Institute for Graduate Studies in
Science and Engineering in partial fulfillment of
the requirements for the degree of
Master of Science
in
Chemistry

Boğaziçi University
2001

STEREOISOMERS RESULTING FROM THE HINDERED ROTATION IN

N-(*o*-ARYL)-2,4-OXAZOLIDINEDIONE DERIVATIVES

APPROVED BY:

Prof. İlknur Doğan . . . . . .

(Thesis Supervisor)

Prof. Hadi Özbal . . . . . .

Prof. Süheyla Uzman . . . . . .

DATE OF APPROVAL . . . 11-06-2001 . .

To all people who believe in science

ACKNOWLEDGMENT

I would like to express my sincere gratitude to my thesis supervisor Prof. İlknur Doğan for her help, advice, encouragement and guidance in every stage of this work. It was a great pleasure for me to work with her.

I wish to thank the members of my examination committee: Prof. Hadi Özbal and Prof. Süheyla Uzman for their advices and comments on the final manuscript of my thesis.

I would like to express my heartfelt thanks to my laboratory partner Funda Oğuz for her invaluable help, understanding and motivation.

I would like to thank Esra Altıner for her endless support and love, Esra Müjde Yılmaz for her friendship and Mustafa Yılmaz for his help with computer programs. I wish to thank all my friends Sinan Şen, Türkan Çetinceviz, Zeynep Taner, Ümit Turan and Güler Avcı for their moral support.

I would like to extend my thanks to all the members of the chemistry department who were always most helpful during my study. I wish to thank especially to Hülya Metiner for her readiness to help and share the problems.

I would like to thank Assoc. Prof. Nihat Çelebi for endearing organic chemistry to me, Prof. Yüksel İnel for allowing me to use his HPLC instrument and Muhittin Çergel for patiently recording the NMR spectra.

My special thanks are for my fiance Bülent Ordu for his understanding, support and love during my study.

My greatest thank is to my family, who were always behind me, with their endless love, encouragement and support during my whole life.

ABSTRACT

STEREOISOMERS RESULTING FROM THE HINDERED ROTATION IN N-(*o*-ARYL)-2,4-OXAZOLIDINEDIONE DERIVATIVES

In this study, sterically hindered 5-methyl-3-(*o*-aryl)-2,4-oxazolidinediones and 5,5-dimethyl-3-(*o*-aryl)-2,4-oxazolidinediones have been synthesized by the reaction of the *o*-aryl isocyanates with (S)-(-)-ethyllactate or ethyl α-hydroxyisobutyrate, respectively.

Diastereomeric isomers of the 5-methyl-3-(*o*-aryl)-2,4-oxazolidinediones have been detected by using ^{1}H NMR. Enantiomeric isomers of the 5,5-dimethyl-3-(*o*-aryl)-2,4-oxazolidinediones have been identified by ^{1}H NMR and ^{13}C NMR, also in the presence of the chiral auxiliary. Activation barriers to hindered rotation around C-N single bond have been determined for *o*-methyl and *o*-chloro substituted enantiomers by using DNMR.

The conformational preferences of the diastereomers have been investigated by ^{1}H NMR and by HPLC on an optically active sorbent.

The rotation in the *o*-fluoro derivatives was found to be too fast to make the rotational isomers observable by NMR, whereas the rotational isomers of the *ortho* bromo compounds were found to be separable at room temparature. Using HPLC on cellulose carbamate the isomers were separated and for the diastereomeric isomers of 5-methyl-3-(*o*-bromophenyl)-2,4-oxazolidinedione, the equilibrium constant and the energy barrier for the conversion of the less stable conformation to the more stable one were determined by following the equilibration of the isomers at constant temperature.

In addition, the reactions of halogen substituted 5-methyl-3-(*o*-aryl)-2,4-oxazolidinediones with methanol have been studied. The compounds were found to react with methanol, causing a ring opening reaction. The products were identified by ^{1}H NMR.

ÖZET

N-(*o*-ARİL)-2,4-OXAZOLİDİNDİON TÜREVLERİNİN DÖNME ENGELLİ STEREOİZOMERLERİ

Bu çalışmada sterik engelli 5-metil-3-(*o*-aril)-2,4-oxazolidindion ve 5,5-dimetil-3-(*o*-aril)-2,4-oxazolidindion türevleri *o*-arilizosiyanatın sırasıyla (S)-(-)-etillaktat ve etil α-hidroksiizobütirat ile olan reaksiyonundan elde edilmiştir.

5-metil-3-(*o*-aril)-2,4-oxazolidindion bileşiklerinin diastreomerik izomerleri ^{1}H NMR kullanılarak tespit edildi. 5,5-dimetil-3-(*o*-aril)-2,4-oxazolidindion bileşiklerinin enantiomerik izomerleri ^{1}H NMR , ^{13}C NMR ve (S)-(+)-1-(9-antril)-2,2,2-trifloroetanol kullanılarak belirlendi. *O*-methyl ve *o*-chloro sübstitüenti olan enantiomerlerin sterik dönme için aktivasyon enerjileri dinamik NMR kullanılarak belirlendi.

Diastereomerlerin conformasyonel seçicilikleri ^{1}H NMR ve optikçe aktif HPLC kolonu kullanılarak bulundu.

Billeşiklerin *o*-flor türevlerindeki dönme, conformasyonel izomerlerin NMR ile belirlenmesini önleyecek derecede hızlıyken, *o*-brom türevlerinin conformasyonel izomerlerinin oda sıcaklığında ayrı olarak bulunduğu tespit edildi. Selüloz karbamet dolgu maddeli HPLC kolonu kullanılarak bu izomerler birbirinden ayrıldı. Sabit sıcaklıkta isomerlerin dengeye gelmesi HPLC yardımı ile izlenerek, denge sabiti ve daha az kararlı conformasyonun daha kararlı olana dönüşme için gereken aktivasyon enerjisi hesaplandı.

Ayrıca, 5-metil-3-(*o*-aril)-2,4-oxazolidindion bileşiklerinin metanol ile olan reaksiyonları incelenerek, 5-metil-3-(*o*-florofenil)-2,4-oxazolidindion, 5-metil-3-(*o*-chlorofenil)-2,4-oxazolidindion ve 5-metil-3-(*o*-bromofenil)-2,4-oxazolidindion bileşiklerinin metanol ile reaksiyona girdiği bulundu. Halkanın açılması ile oluşan ürünler 60 MHz ^{1}H NMR kullanılarak tespit edildi.

TABLE OF CONTENTS

LIST OF FIGURES

LIST OF TABLES

LIST OF SYMBOLS/ABBREVIATIONS

$\Delta G^{\#}$	Free energy of activation
ΔG^{o}	Standard free energy change
h	Planck's constant
ΔH^{o}	Standard enthalpy change
J	Coupling constant
K	Equilibrium constant
k'	Capacity factor
k_b	Boltzmann constant
k_c	Rate constant at coalesence temperature
k_f	Rate constant for the forward reaction
k_r	Rate constant for the reverse reaction
ΔS^{o}	Standard entropy change
t	Retention time
α	Separation factor
δ	Chemical shift
$\Delta\nu$	The difference in hertz
APT	Attached proton technique
CA	Chiral auxiliary
HPLC	High pressure liquid chromatography
(S)-(+)-TFAE	(S)-(+)-1-(9-anthryl)-2,2,2-trifluoroethanol

1. INTRODUCTION

The search for the presence of stereoisomerism in certain substituted molecules containing rings of an aromatic type is a natural development from the study of biphenyl compounds (Figure 1.1). In the biphenyl compounds, the presence of stereoisomerism is due to the hindered internal rotation around C sp^2- C sp^2 single bond [1-3].

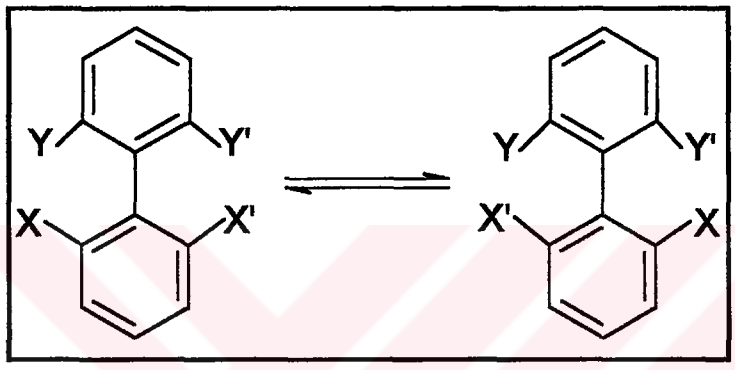

Figure 1.1. Stereoisomers of hindered biphenyl derivatives

After the synthesis of sterically hindered biphenyl derivatives, a number of scientists have been interested in the synthesis of and the determination of the barrier to rotation about the C-N bond of some heterocyclic analogues of biphenyl [4-12]. The resolution and the separation of rotational isomers have been studied by different methods in the past [13-19].

In 1931, Bock and Adams succeeded in separating the enantiomers of 1-(2-carboxyphenyl)-2,5-dimetylpyrole-3-carboxylic acid (Figure 1.2) by the formation of the brucine salt [4].

Adams *et al.* studied the resolution of N-phenylpyroles and N,N'-dipyrryls (Figure 1.3) in 1931. The results of their investigation proved that optical isomerism is due to the restricted rotation between the rings [5,6].

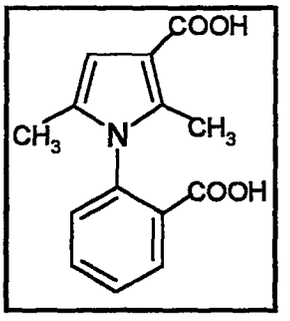

Figure 1.2. The structure of 1-(2-carboxyphenyl)- 2,5-dimetylpyrole-3-carboxylic acid

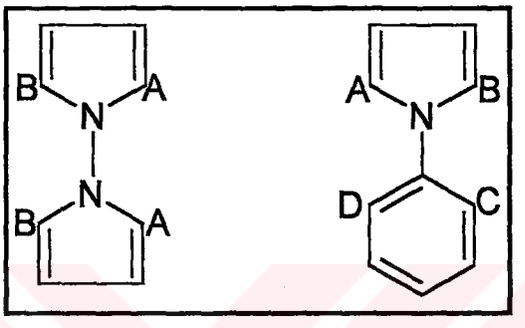

Figure 1.3. The general structures of N,N'-dipyrryls and N-phenylpyroles

In 1970, Bentz, Colebrook and Fehlner studied hindered rotation about C-N bond of 5-methyl-3-α-naphtyl-2-thiohydantoin (Figure 1.4). The equilibration of diastereomeric rotational isomers has been followed by integration of their NMR signals and their activation parameters for hindered rotation about C-N bond have been calculated [7].

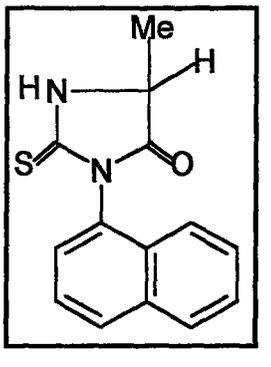

Figure 1.4. The structure of 5-methyl-3-α-naphtyl-2-thiohydantoin

In 1972, Colebrook, Giles, and Rosowsky calculated the barriers to internal rotation in aryl substituted heterocyclic compounds lacking bulky ortho substituents by DNMR [8].

Another DNMR study for the determination of the internal rotation barriers around the aryl C-N bond was done by Icli *et al.* in 1972. In this research, they studied the reversal of the effective sizes of methyl and chlorine in 1-arylhydantoins, 3-arylhydantoins and 3-aryl-2-thiohydantoins (Figure 1.5) [9].

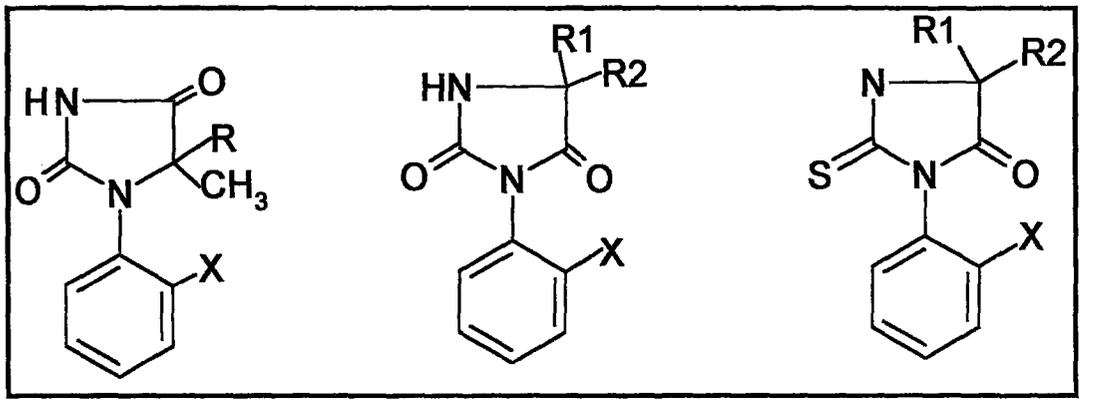

Figure 1.5. The structures of 1-Arylhydantoins, 3-Arylhydantoins and 3-Aryl-2-thiohydantoins

Up to 1966, it was well known that the solute-solvent interactions could be detected by NMR spectroscopy, therefore, several groups of workers considered the possibility of distinguishing the enantiomeric molecules in the presence of an optically active solvent. After the suggestion of the possibility of distinguishing enantiomeric molecules in the presence of an optically active solvent by Mislow and Raban [10], Colebrook, Icli and Hund studied enantiomeric internal rotational isomers of 1- and 3-arylhydantoins (Figure 1.5) in chiral solvents [11].

In 1992, Dogan *et al.* synthesized the sterically hindered 2-thioxo-4-oxazolidinones and rhodanines (Figure 1.6) forming enantiomers by rotation about the C-N bond. In their study, the enantiomers showed proton NMR shift differences in the presence of (S)-(+)-1-(9-anthryl)-2,2,2- trifluoroethanol as a chiral solvent [12].

Mannschreck and his coworkers worked on the separation of enantiomers of some heterocyclic compounds by liquid chromatography on triacetylcellulose. In their research, the barrier to rotation about the C-N bond was determined by thermal racemization [13,15,17].

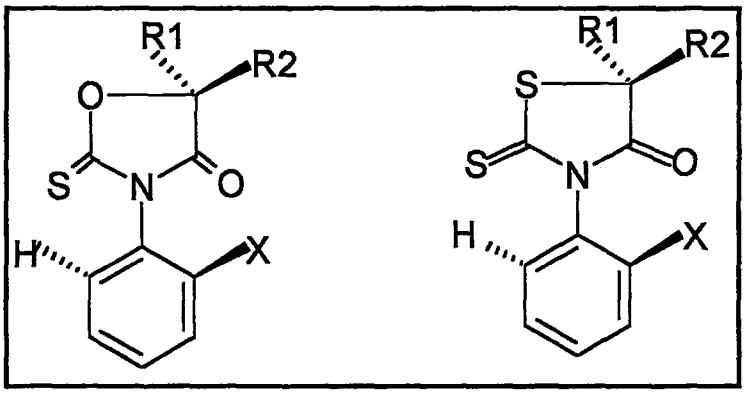

Figure 1.6. Sterically hindered 2-thioxohydantoins and rhodanines

In 1986, Roussel and Djafri resolved the enantiomers of *m*-substituted N-phenyl-Δ-4-thiazoline-2-thiones (Figure 1.7) on microcrystalline triacetylcellulose (TAC) and determined the enantiomerization rates by polarimetry at different temperatures [14].

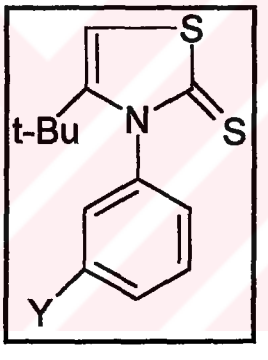

Figure 1.7. The structure of *m*-substituted N-phenyl-3-t-butyl-4-Δ-4-thiazolinethiones

Roussel, Stein and Beauvais measured the kinetics of racemization of thiazoline-2-thiones (Figure 1.8) where the kinetic data were obtained from enantiomerically enriched samples on triacetylcellulose by monitoring the decrease of the polarimetric detection at a given temperature [16].

In 1993, Dogan *et al.* enriched the enantiomers of the sterically hindered heterobiaryls semi-preparatively by liquid chromatography on triacetylcellulose and tribenzoylcellulose. In this work, the circular dicroism spectra were used to provide the relative configuration of enriched enantiomers [18].

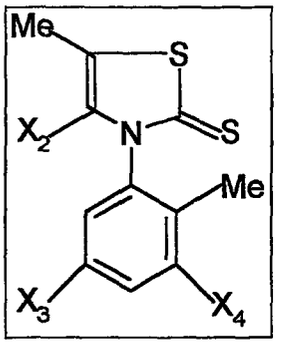

Figure 1.8. The structure of thiazoline-2-thione derivative

In 1979, 60 MHz ^{1}H NMR and ^{13}C NMR studies of some 3-aryl-2,4-oxazolidinediones were done by Içli, where the magnetic non-equivalence of diastereotopically and diastereomerically related protons and ^{13}C nuclei were investigated. Not all diastereomerically and diastereotopically related protons were observed in the 60 MHz ^{1}H NMR spectra [19].

In this study, hindered rotation leading to the formation of diastereomeric and enantiomeric compounds has been investigated on 2,4-oxazolidinedione derivatives (Figure 1.9). The compounds which have been synthesized for the project are shown in Figure 1.10 and Table 1.1.

These compounds are of interest for two reasons:

- As part of an on going study of restricted internal rotation about the C-N bond in aryl substituted heterocyclic compounds.
- The *o*-substituted 2,4-oxazolidinediones have been examined for some pharmaceutical activities in recent years. Therefore, the study of the stereochemistry, the separation and the reactions of these compounds may be expected to contribute to the research in pharmaceutical chemistry as well.

The pharmaceutical activities of 2,4-oxazolidinedione derivatives are their uses as herbicides and anticonvulsants.

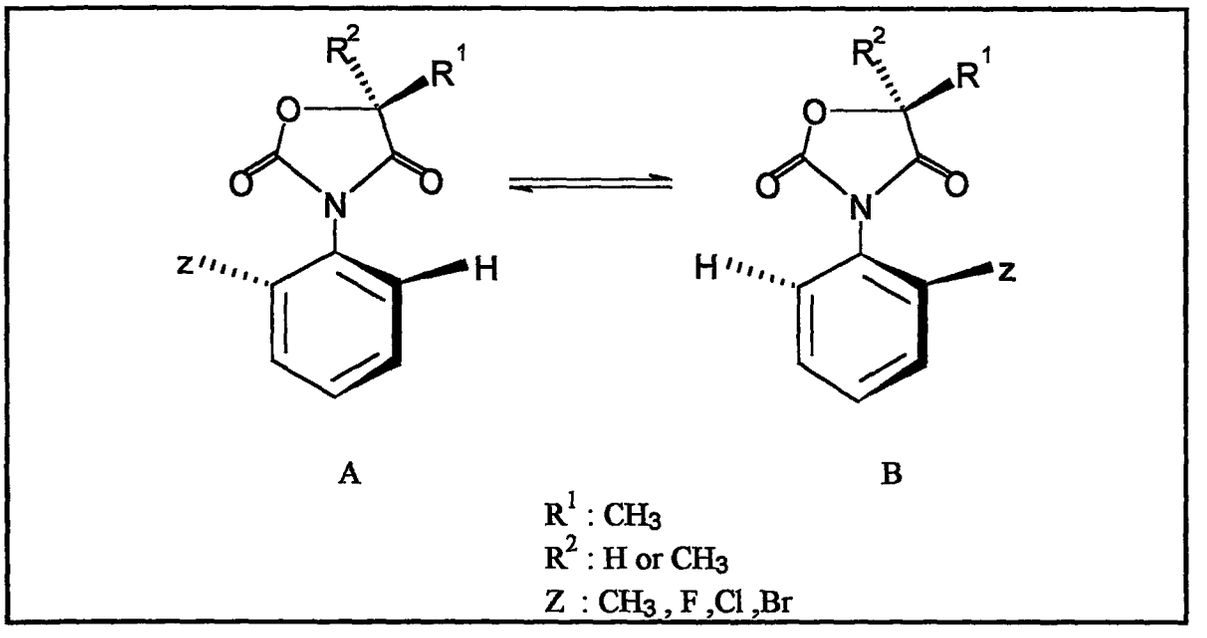

Figure 1.9. Sterically hindered heterocyclic compounds studied

In recent years, the scientists working in research centers examined some 2,4-oxazolidinedione derivatives for plant growth regulating activity. In 1963, Levy *et al.* tested some derivatives of 2,4-oxazolidinediones for growth regulation (e.g. tomato, mustard, radish, green peas). In 1978, Walter and his coworkers found that a certain derivative protected soybean plants against *cercospara personata*. Another study was done by Hirai *et al.* in 1990. In this study, they investigated the herbicidal activities of some 2,4-oxazolidinedione derivatives. All these researches received patents for their work.

In 1959, Shapiro and his coworkers synthesized a series of 2,4-oxazolidinedione derivatives. They examined the effect of the structural variation on anticonvulsant activity as well. In this research, it was found that the best compound of the series was 3-(4-chloro-2-methylphenyl)-2,4-oxazolidinedione. Structure-activity relationships indicated that best activities were noted when the 3-substituent was aralkyl or *o*-substituted phenyl compounds (e.g. 5,5-dimethyl-3-(*o*-tolyl)-2,4-oxazolidinedione, 5,5-dimethyl-3-(2-ethoxyphenyl)-2,4-oxazolidinedione and 5,5-dimethyl-3-(2-methoxyphenyl)-2,4-oxazolidinedione [20].

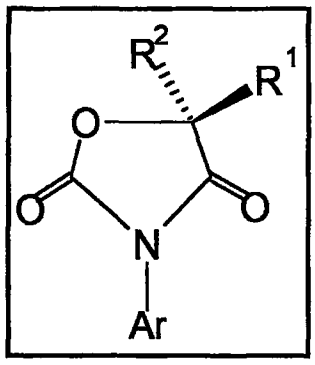

Figure 1.10. The general structure for 3-(*o*-aryl)-2,4-oxazolidinediones

Table 1.1. The synthesized 3-(*o*-aryl)-2,4-oxazolidinediones

No	Ar	R^1	R^2
1S	*o*-Tolyl	CH_3	H
2	*o*-Tolyl	CH_3	CH_3
3S	2-Chlorophenyl	CH_3	H
4	2-Chlorophenyl	CH_3	CH_3
5S	2-Fluorophenyl	CH_3	H
6	2-Fluorophenyl	CH_3	CH_3
7S	2-Bromophenyl	CH_3	H
8	2-Bromophenyl	CH_3	CH_3

The aims of this project are the followings:

- To synthesize 3-(o-aryl)-2,4-oxazolidinedione derivatives.
- If the rotation at room temperature is slow enough to enable isolation, to separate rotational enantiomers by liquid chromatography on an optically active sorbent.
- To separate diastereomers by crystallization or by liquid chromatography.
- To differentiate enantiomers with an optically active auxiliary compound in ^1H NMR and ^{13}C NMR.
- To determine the rotational barriers by thermal racemization and by DNMR.
- To investigate the reactivity of the heterocyclic ring at the C-5 position.

2. THEORY

2.1. Isomerism: Constitutional Isomers and Stereoisomers

Isomers are different compounds that have the same molecular formula. They can be classified into two categories:

- Constitutional isomers
- Stereoisomers

Constitutional isomers are isomers that differ because their atoms are connected in a different order.

Stereoisomers are isomers that have their constituent atoms connected in the same way and that differ only in the arrangement of their atoms in space.

2.2. The Stereogenic Unit and Chirality

A unit within a molecule which gives rise to the existence of stereoisomers is called a stereogenic unit. The chirality of most chiral molecules is associated with the presence of one or more stereogenic units. However, the presence of a stereogenic unit is not in itself a sufficient condition for chirality. An object is said to be chiral if it cannot be superimposed upon its mirror image. In a chemical context, chirality is applied to the three-dimensional structure of molecules.

Simple chiral molecules can be classified into three types according to the type of stereogenic unit present: central, axial and planar. A centrally chiral molecule is chiral by virtue of the arrangement of atoms or groups about a stereogenic center (asymmetric center or chiral center). The most familiar example is a tetrahedral carbon atom bearing four different groups like in Figure 2.1. This is the most common class of chiral molecule.

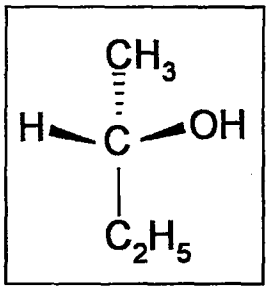

Figure 2.1. A tetrahedral carbon atom possessing four different groups

An axially chiral molecule is chiral because of the arrangement of atoms or groups about a stereogenic axis (chiral axis). An example is provided by the sterically hindered biphenyl derivatives (Figure 1.1). The final type, planar chirality is due to the arrangement of atoms or groups with respect to a stereogenic plane (chiral plane).

2.3. Enantiomers

Many compounds may be obtained in two different forms in which the molecular structures are constitutionally identical but differ in the three-dimensional arrangement of atoms such that they are related as mirror images. In such a case the two possible forms are called enantiomers and are said to be enantiomeric with each other. To take a simple example, the amino acid alanine (Figure 2.2) can be obtained in two forms that are related as nonsuperimposable mirror images.

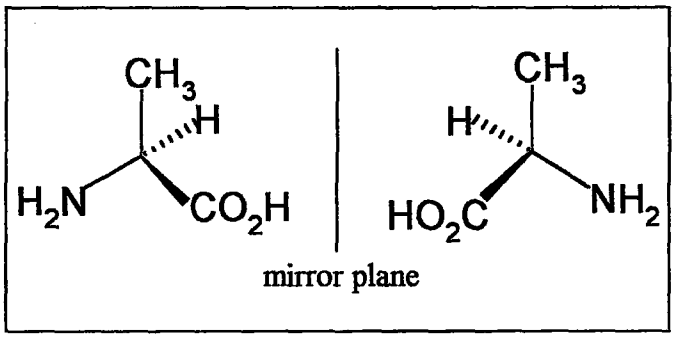

Figure 2.2. The enantiomers of the amino acid alanine

Enantiomers have identical chemical and physical properties in the absence of an external chiral influence. This means the enantiomers have the same melting point,

solubility, chromatographic retention time and IR and NMR spectra as each other. Therefore they are not separable in achiral media.

One observable way in which enantiomers differ is in their behaviour toward plane-polarized light. When a beam of plane-polarized light passes through an enantiomer, the plane of polarization rotates. Moreover, separate enantiomers rotate the plane-polarized light equal amounts but in opposite directions. Because their effect on plane-polarized light, separate enantiomers are said to be optically active compounds.

2.4. Diastereomers

Diasteromers are stereoisomers whose molecules are not mirror images of each other. Diastereomeric pair of (+)-allo-threonine and (-)-threonine (Figure 2.3) can be given as an example of diastreomers.

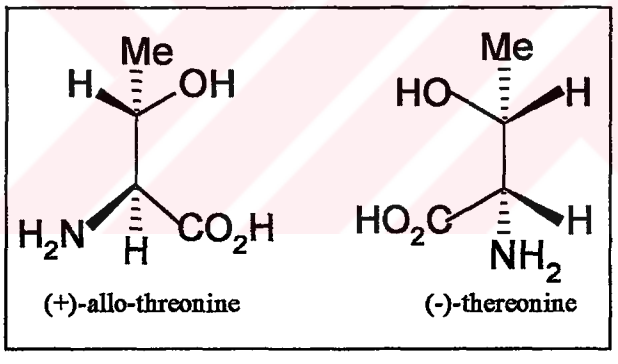

Figure 2.3. Diastereomeric pair of (+)-allo-threonine and (-)-threonine

Compounds that are diastreomeric with each other have completely different chemical and physical properties. Their melting points, densities and solubilities differ. The liquids have different boiling points, refractive indices, densities and viscosities. They differ in all of their spectral properties (UV, IR, NMR, mass spectra). Because of these differences in physical and spectral properties, they can be separated by chromatography, distillation, crystallization and other separation techniques.

2.5. Rotational Isomers and Stereochemistry of 2,4-Oxazolidinediones

Isomers that may be interconverted by torsion around a single bond are referred to as rotational isomers or atropisomers. The atropisomerism arises due to hindered rotation about a C-C single bond. Atropisomerism is commonly encountered among the biphenyls (Figure 1.1). In these types of compounds, interconversion of stereoisomers is rendered difficult by the necessity of forcing bulky *ortho* substituents (in the example cited, X, X', Y, Y') passing one another in the transition state.

The stereoisomerism in 2,4-oxazolidinedione derivatives that are analogous of biphenyls is caused by the restricted rotation around C-N single bond. The restricted rotation is due to the steric interference between the *ortho* substituents on the 3-aryl group and the carbonyl oxygen on the heterocyclic moiety (Figure 2.4). In these molecules, the substituents are too large to pass each other, resulting in configurational stability. Therefore the aryl group in the ground states of the molecules is expected to be orthogonal (or nearly orthogonal) to the heterocyclic ring. The transition state structures during the conversion of one rotamer to the other one are expected to be planar like either in T_1 or T_2 as shown in Figure 2.4.

The ortho aryl substitution (Z) brings dissymmetry to the molecule as well as causing the hindered rotation. Since the configurational difference is provided by restricted rotation around a single bond, they are called axially chiral compounds, the C-N single bond being chiral axis. If $R^1=R^2$, (A) and (B) are enantiomers of each other. If another asymmetric center exists in the molecule i.e. $R^1 \neq R^2$, then (A) and (B) are diastereomers of each other.

2.6. Nomenclature

The chiralty of the axially chiral molecules is defined in terms of their helicities **M** and **P** in the Chan, Ingold, Prelog system [21]. In this system, first an axis is drawn through the single bond around which conformation is defined and the smallest torsion angle formed between the carbon atoms bearing the groups of the highest priority is used to

define the helix. A resulting clockwise rotation is denoted as " **P** " (plus) and the counter clockwise rotation is denoted as " **M** " (minus).

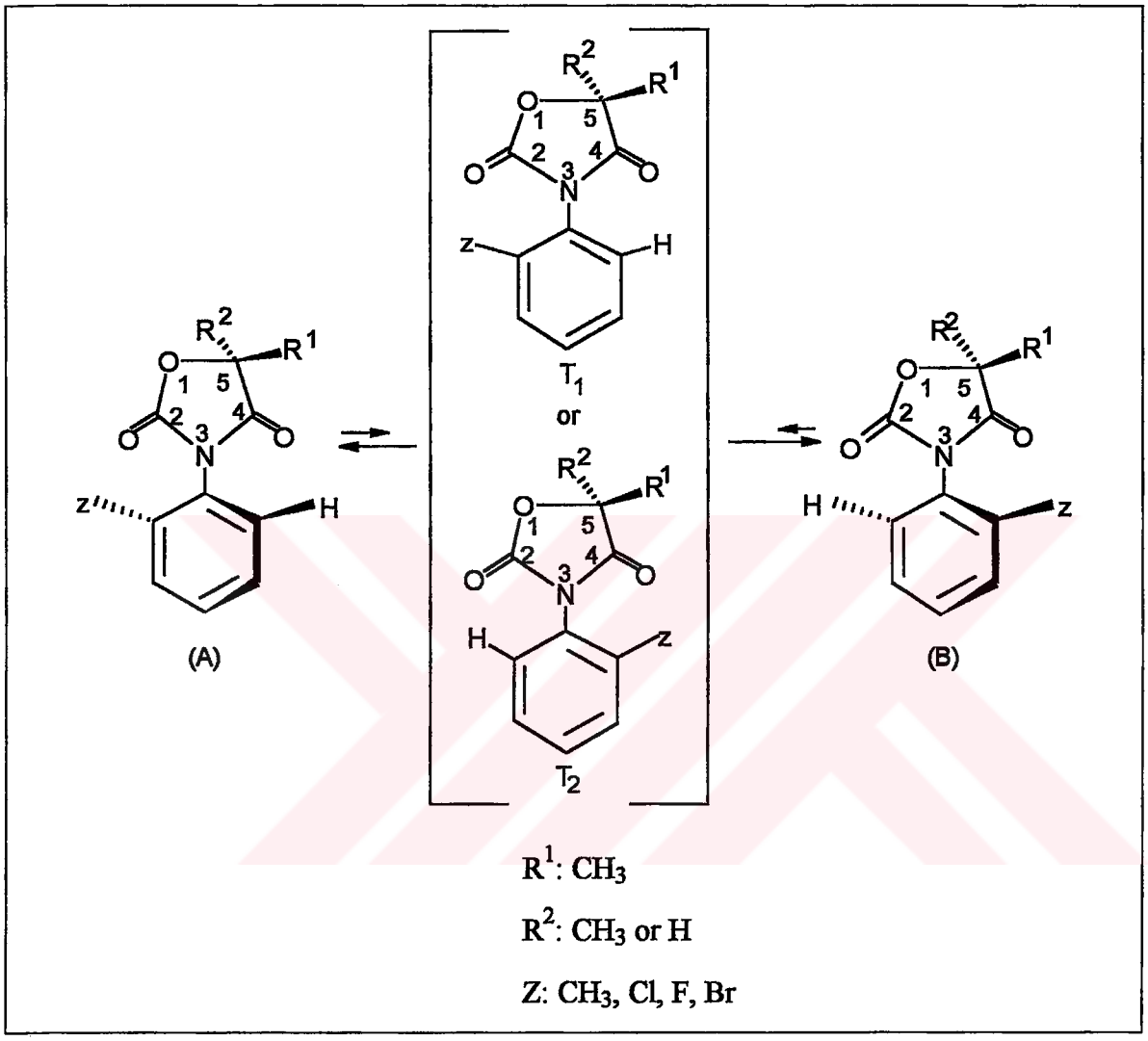

Figure 2.4. Rotational isomers resulting from 180° rotation around the C-N single bond

2.7. Detection of the Enantiomers of N-(*o*-Aryl)-2,4-oxazolidinediones by NMR

Enantiomeric nuclei are equally screened by environments in achiral solvents and they exhibit the same NMR chemical shifts. However, in the presence of an optically active auxiliary compound, the enantiomers are expected to give different NMR spectra, if the auxiliary compound is able to make diastereomeric association complexes with the enantiomers. As a result, the various portions of the solute molecules will bear different spatial relationship with respect to the complexed auxiliary molecules. Therefore, they will

experience different magnetic environments associated with any long range effects due to the auxiliary molecules. Diamagnetic anisotropy and dipolar interactions would enhance the long range effects, thus magnify the chemical shift differences of diastereomeric nuclei in the association complex.

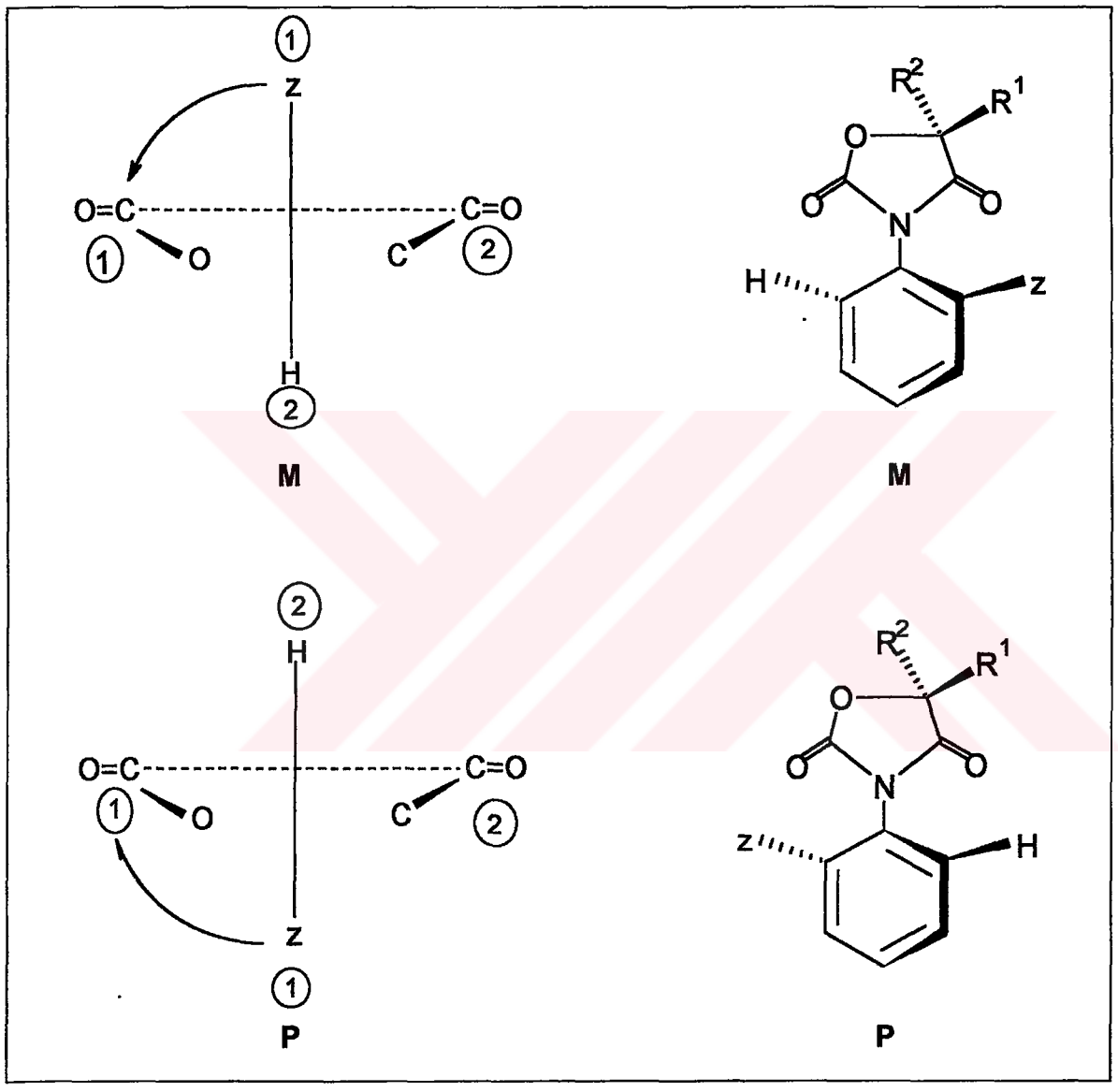

Figure 2.5. Descriptors for the axially chiral 5-methyl-3-(*o*-aryl)-2,4-oxazolidinediones

In this study, ^{1}H NMR spectra were taken in the presence of the chiral auxiliary (S)-(+)-1-(9-anthryl)-2,2,2-trifluoroethanol (Figure 2.6). The auxiliary forms a diastereomeric association complex with the enantiomers. The hydroxyl group in the auxiliary compound is capable of making strong intermolecular hydrogen bonds with the carbonyl oxygen of the enantiomers (Figure 2.7). Thus a close contact between enantiomers and the auxiliary

molecules can be provided and diastereomeric association complexes can be formed. Therefore chemical shift difference is induced between certain nuclei of the enantiomers of the racemic mixture, which may be identified by NMR spectroscopy and this will in turn prove the chirality of the molecules. In addition, the presence of the strongly anisotropic anthryl group is expected to enhance the difference in average magnetic environments of nuclei in enantiomers.

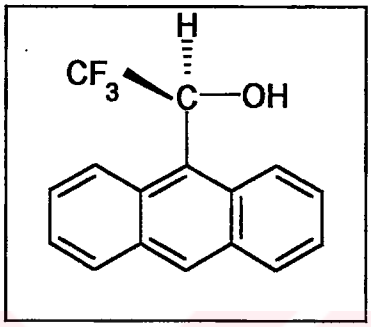

Figure 2.6. The structure of (S)-(+)-1-(9-anthryl)-2,2,2-trifluoroethanol

2.7.1. The Chiral Auxiliary (CA)

The chiral auxiliary compound forms a diastereomeric association complex with the enantiomers. The differences in magnetic environment of the nuclei are generated by diastereomeric complexes that form and dissociate rapidly on the NMR time scale (Equation 2.1 where (S)-A and (R)-A stand for the enantiomers of the substrate and (S)-X stands for a chiral auxiliary). The NMR shifts observed are thus average shifts of the complexed (right-hand side of the Equations 2.1 and 2.2) and uncomplexed (left-hand side of the equations) species.

$$\text{(S)-A} + \text{(S)-X} \underset{}{\overset{K_{SS}}{\rightleftharpoons}} \text{(S)-A . (S)-X} \qquad (2.1)$$

$$\text{(R)-A} + \text{(S)-X} \underset{}{\overset{K_{RS}}{\rightleftharpoons}} \text{(R)-A . (S)-X} \qquad (2.2)$$

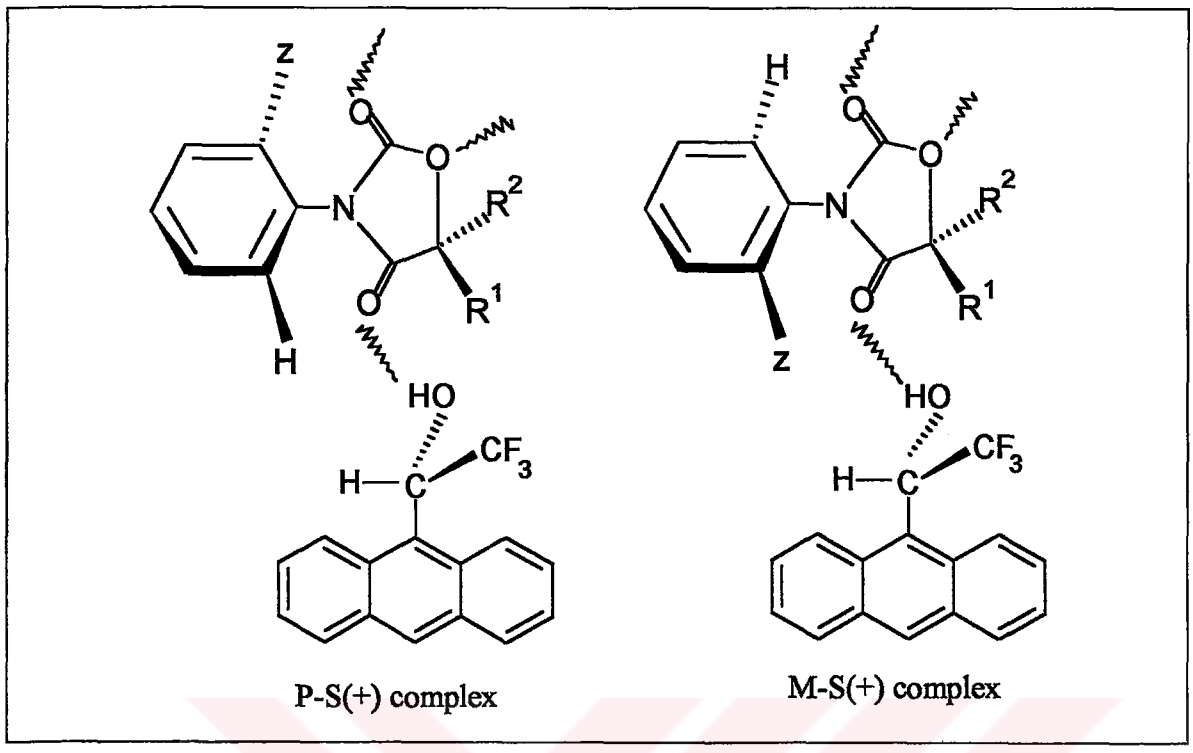

Figure 2.7. Intermolecular hydrogen bonding between the auxiliary and the enantiomers

There are two reasons why the equilibria in Equations 2.1 and 2.2 taking place in the presence of CA lead to differently shifted signals:

- Intrinsic: (S)-A . (S)-X and (R)-A . (S)-X are diastereomers and therefore have, at least in principle, different chemical shifts.
- Differential stability of diastereomeric solvates: $K_{SS} \neq K_{RS}$, since the species on the right side of the two equations are diastereomers, and hence may not be equally stable (the species on the left hand side, in contrast, have equal stability). Thus complexing may not be same for the two enantiomers; other things being equal, the more complexed enantiomer is likely to present the larger chemical shift change by the CA [22].

When this equilibria are fast on the NMR time scale a single average species is observed for each of the two systems. Besides the solute enantiomers might themselves associate, thus forming different type of diastereomeric complex. The spectral consequences of solute-solute interactions contribute to the time-averaged nonequivalence pool. Solute-solute association is second (or higher) order in solute concentration, whereas

solute-CA association is first order in solute concentration of each solute enantiomer, even if K_{SS} and K_{RS} are equal. In general, the effects of solute-solute interaction are minimal and can be ignored, especially when an excess of a strongly solvating CA is employed. Hence, the overall nonequivalence that is observed is a function of the differences between the spectra of the diastereomeric solvates and the uncomplexed enantiomers, and of their relative populations (hence the component concentrations and equilibrium constants K_{SS} and K_{RS}).

2.7.2. Solvent Effect of CA

The earliest studies of diastereomeric solvates verified the importance of hydrogen bonding to the CA-solute interaction. For example, although fluorine nonequivalence is observed for racemic 2,2,2-trifluoro-1-phenylethanol in optically active 1-(α-naphtyl) ethylamine, no nonequivalence is observed for its methyl ether under same conditions. Association is also much stronger (and nonequivalence accordingly larger) in nonpolar solvents. Addition of even a small quantity of a polar material will severely reduce or eliminate nonequivalence to the extent that the polar material competes with the solute for CA or to extent that it alters conformations of the solvates give rise to non-equivalence [23, 24].

2.7.3. Concentration Effect of CA

The concentration of CA (for a given solute concentration) also substantially influences the nonequivalence. The nonequivalence increases with an increase in CA concentration until the solute is completely solvated by the CA. The concentration required to produce this effect depends on the interaction strength of the solvent-solute pair, with fluoroalcohols [22].

An achiral diluent is essential if a solid CA is to be used, and its use is preferable even with liquid CA. Nonequivalece decreases with increased dilution at constant CA-solute ratio, since CA concentration is the important factor.

2.7.4. Configuration of Association Complex

Complex formation results primarily from hydrogen bonding between the chiral alcohol and a carbonyl group of the 2,4-oxazolidinedione derivatives. Secondary attractive interactions between the Π-electron systems of phenyl and anthryl groups appear to be responsible for determining for the conformation of the complex. In order to maximize the Π- Π interactions between the solute and the auxiliary molecules, the corresponding anthryl ring would tend to stay parallel to the phenyl ring in the ground state conformations of the diastreomeric solvates (Figure 2.8).

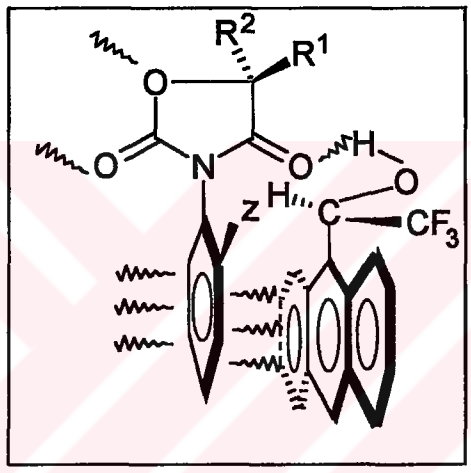

Figure 2.8. Configuration of association complex formed between the CA and 2,4-oxazolidinedione derivatives

2.8. Determination of the Activation Energies for Hindered Rotation of the 2,4-Oxazolidinedione Derivatives by Dynamic NMR

If two groups of chemically equivalent nuclei (for example; the two methyl groups bonded to the nitrogen in Figure 2.9) are exchanged by an intermolecular process, the NMR spectrum is a function of the difference in their resonance frequencies, $\Delta\nu$, and of the rate of exchange, k. At low temperatures the exchange is slow and $k << \Delta\nu$. Therefore, at 55° and below two resonances appear for the two N-methyl groups. At high temperatures the exchange is fast; i.e. $k >> \Delta\nu$ and a single sharp peak is observed. There is also an intermediate temperature range over which the spectrum consists of two significantly broadened overlapping lines. This temperature is referred to as the coalescence

temperature, Tc. Above Tc the signal, which now belongs to both N-methyl groups, becomes increasingly sharp.

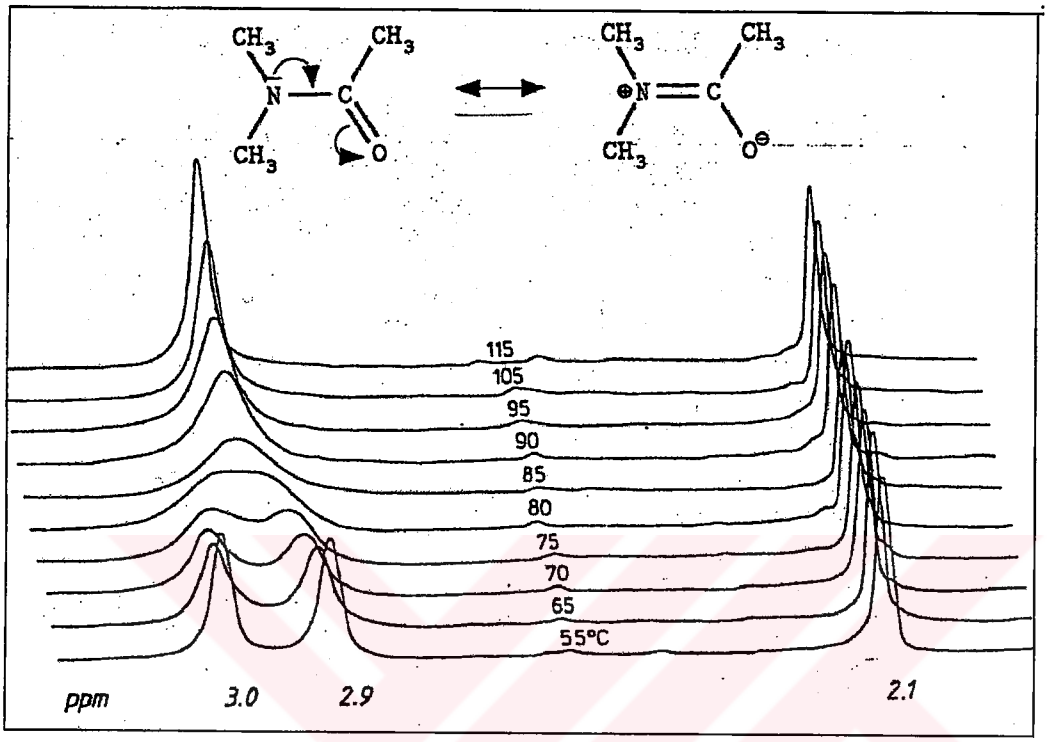

Figure 2.9. The ^{1}H NMR spectrum of N,N-dimethylacetamide and its dependence on temperature

The temperature-dependent position and profile of the N-methyl signal result from amide canonical formulae shown in Figure 2.9. The CN bond is partial double bond; this hinders rotation of the N,N-dimethylamino group. One methyl group is now cis (δ_B = 3.0 ppm) and the other is trans (δ_A = 2.9 ppm) to the carboxamide oxygen. At low temperatures (55° C), the N-methyl protons slowly exchange positions in the molecule (slow rotation, slow exchange). If energy is increased by heating (to above 90 ° C), then the N,N-dimethyamino group rotates so that the N-methyl protons exchange their position with a high frequency (free rotation, rapid exchange), and one single, sharp N-methyl signal of double imtensity appears with the average shift ($\delta_A + \delta_B$)/ 2.

The dimethylamino group rotation follows a first-order rate law; the exchanging methyl protons show no coupling and their singlet signals are of the same intensity. Under these conditions, Equation 2.3 affords the rate constant k_c, at the coalecence point Tc:

$$k_c = \pi (\upsilon_A - \upsilon_B) / \sqrt{2} = \pi \, \Delta\nu / \sqrt{2} \approx 2.22 \Delta\nu \qquad (2.3)$$

where $\Delta\nu$ is the full width at half-maximum of the signal at the coalesence point T_c; it corresponds to the difference in chemical shift ($\upsilon_A - \upsilon_B$) observed during slow exchange.

According to the Eyring Equation 2.4, the exchange frequency k_c decreases exponentially with the free molar activation enthalpy $\Delta G^{\#}$:

$$k_c = (k_b \, T_c / h) \, e^{-\Delta G^{\#} / RT} \qquad (2.4)$$

where R is the gas constant, k_b is the Boltzmann constant and h is the Planck's constant. Equations 2.3 and 2.4 illustrate the value of temperature-dependent NMR for the investigation of molecular dynamics: following substitution of the fundamental constants, they give Equation 2.5 for the free molar activation enthalpy $\Delta G^{\#}$ for the first order exchange process:

$$\Delta G^{\#} = 19.1 \, T_c \, [10.32 + \log (Tc / k_c)] \times 10^{-3} \text{ kJ / mol} \qquad (2.5)$$

In this study, the activation barriers for hindered rotation around C-N single bond were calculated for compounds **2** and **4** (Figure 2.10) by following the temperature-dependent ^{1}H NMR spectra of the two diastereotopic protons on C-5 in these compounds.

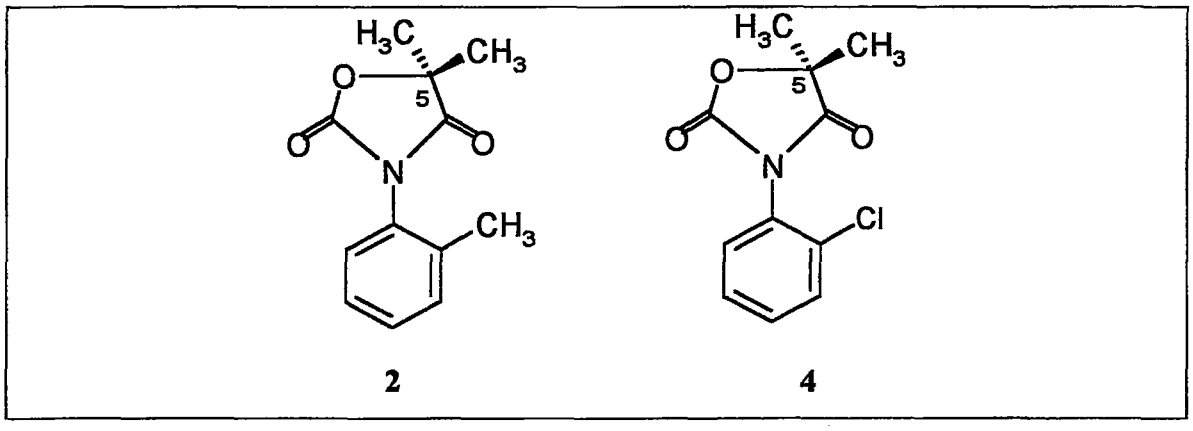

2 **4**

Figure 2.10. The structures of the compounds **2** and **4** for which the activation barriers were calculated

2.9. Chromatographic Separation of Stereoisomers

2.9.1. A Review of Basic Chromatographic Theory

The concept of chromatography relies basically on the distribution of a compound between two phases, one of which (the mobile phase) is moving respect to the other (the stationary phase). The various modes of chromatography depend on the respective nature of the two phases. The two phases are chosen so that the components of the sample distribute themselves between the mobile and stationary phase to varying degrees. Those components that are strongly retained by the stationary phase move slowly with the flow of the mobile phase. In contrast, components that are weakly held by the stationary phase travel rapidly.

The retention of a compound on a column can be expressed by its retention time (t_R), retention volume ($V_R = t_R F$, where F is the flow rate) or the capacity ratio (k'), which is directly related to its equilibrium distribution constant (K) in the stationary-mobile phase system. The capacity ratio is defined by:

$$k' = A_s/A_m \qquad (2.6)$$

where A_s and A_m denote the amount of the compound in the stationary and the mobile phase, respectively. Let V_s and V_m be the volumes of the respective phases; then

$$k' = C_s V_s/C_m V_m = K V_s/V_m \qquad (2.7)$$

V_m is commonly written as V_0 and represents the dead volume in the column, which does not contribute to the separation. Consequently, the net retention volume, V_n, can be written as $V_n = V_R - V_0$, since $K = V_n/V_s$, combination with Equation 2.7 gives:

$$k' = (V_R - V_0)/V_0 \qquad (2.8)$$

This expression permits the determination of the capacity factor from the chromatogram.

The chromatographic separation of two components (1 and 2) depends on the separation factor (α) of a column. It can be written as $k_2'/k_1' = K_2/K_1 = \alpha$. From Equation 2.8, α can be formulated as:

$$\alpha = (V_{R2}-V_0)/(V_{R1}-V_0) \qquad (2.9)$$

Thus the separation factor is simply the ratio of the net retention volumes of the two components. If the dead volume V_0, has been determined, the separation factor is easily calculated from Equation 2.9.

2.9.2. Separating Isomers and Chiral Stationary Phases

Enantiomers and diastereomers can be separated by chromatographic methods such as gas chromatography (GC), high pressure liquid chromatography (HPLC) or column chromatography.

HPLC or column chromatography over a stationary phase of silica or alumina allows the physical separation of substantial quantities of material. For many diastereomers, the separation does not cause a problem, because they have different physical and chemical properties.

To accomplish separation of enantiomers on an analytical scale GC or HPLC columns packed with chiral material are available. The chiral stationary phase will interact to different extents with the two enantiomers to form transient, diastereomerically related molecular complexes. The chiral stationary phase will adsorb enantiomers dissolved in the eluent to different extents. The more tightly bound enantiomer will elute more slowly.

The separation of enantiomeric compounds on chiral stationary phases is due to the differences in energy between temporary diasteromeric complexes formed between the solute isomers and the chiral stationary phases.; the larger the difference, the greater the separation. To completely resolve a mixture of two components, they must differ in the free energy of interaction with the stationary phase by as little as 0.025 kj/mol, which corresponds to the column selectivity value of $\alpha = 1.01$.

The association of the complexes is a function of the magnitudes of the binding as well as of the repulsive interactions involved. The latter are usually steric, although dipole-dipole repulsions may also occur, whereas various kinds of binding interactions may operate. These include hydrogen bonding, electrostatic and dipole-dipole attractions, charge-transfer interaction and hydrophobic interaction (in aqueous systems).

For enantiomeric resolution, the large number of chiral phases present in the market are polysaccharide phases, ligand-exchange phases and protein bonded-phases. Polysaccharide derivatives were found to exhibit an excellent ability of chiral recognition as a stationary phase for liquid chromatography. It is widely believed that an inclusion complex should be formed for chiral recognition to be possible in these kinds of chiral stationary phases. In this case, the solutes enter into the chiral cavities within the chiral stationary phase to form inclusion complexes.

In this study, cellulose tris-(3,5-dimethyl)phenylcarbamate which was a polysaccharide phase were used as chiral stationary phase. Although the mechanism of chiral recognition by carbamate has not been clarified, it is believed that the chiral attractive interaction results from the urethane linkages. Some chiral space like a concave or a ravine existing on the chiral stationary phase may also enable chiral separation.

2.10. Determination of the Kinetic and Thermodynamic Constants of the Internal Rotation Process for 5-Methyl-3-(*o*-bromophenyl)-2,4-oxazolidinedione

5-Methyl-3-(*o*-bromophenyl)-2,4-oxazolidinedione (Figure 2.11) was obtained as diastereomeric mixture, in which one conformation was yielded in excess. If the one conformation is enriched in one of the diastereomers in solution, the enriched diasteromer thermally interconverts to the other one with time through rotation around the C-N bond and finally reaches the equilibrium (Figure 2.11). The conformation may be quite stable at room temperature, however at elevated temperatures rotation becomes faster and the diastereomers may be equilibrated in a shorter time.

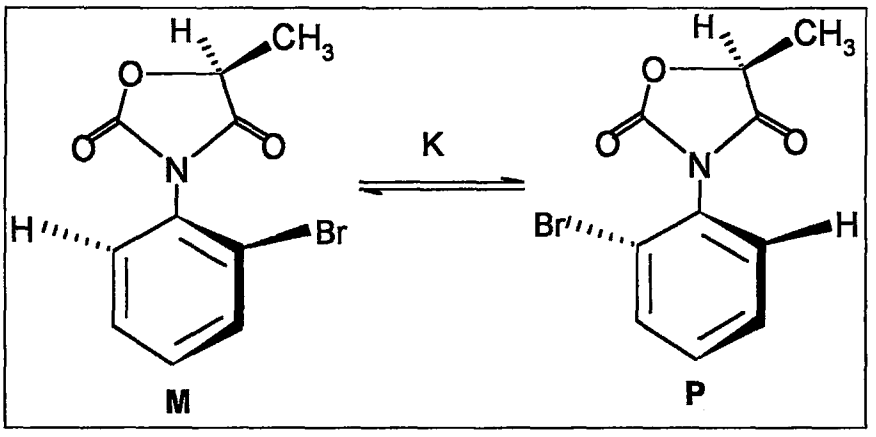

Figure 2.11. The internal rotation between two rotamers

The reversible reaction M $\rightleftharpoons$ P is first order in both the forward (f) and reverse (r) direction, so that $r_f = k_f[M]$ and $r_r = k_r[P]$. If $(d[M]/dt)_f$ denotes the rate of change of [M] due to the forward reaction, then $-(d[M]/dt)_f = r_f = k_f[M]$. The rate of formation of [M] by the reverse reaction is $(d[M]/dt)_r = r_r = k_r[P]$. Then,

$$(d[M]/dt) = -k_f[M] + k_r[P] \qquad (2.10)$$

We have $\Delta[P] = -\Delta[M]$, so $[P]-[P]_0 = -([M]-[M]_0)$. Substitution of $[P] = [P]_0 + [M]_0 - [M]$ into Equation 2.10 gives,

$$d[M]/dt = k_r[P]_0 + k_r[M]_0 - (k_f + k_r)[M] \qquad (2.11)$$

At equilibrium, the rates of the forward and reverse reactions become equal, the concentration of each species being constant, thus d[M]/dt is 0. Let $[M]_{eq}$ be the equilibrium concentration of M. Setting d[M]/dt=0 and $[M] = [M]_{eq}$ in Equation 2.11, we get,

$$k_r[P]_0 + k_r[M]_0 = (k_f + k_r)\,t \qquad (2.12)$$

The use of Equation 2.12 in Equation 2.11 gives $d[M]/dt = (k_f + k_r)([M]_{eq} - [M])$. Using the identity $\int (x+s)^{-1} dx = \ln(x+s)$ to integrate this equation, we get,

$$\ln ([M]-[M]_{eq}/ [M]_{o}-[M]_{eq})= (k_f+k_r)t \quad (2.13)$$

The equilibrium constant $K= k_f / k_r$ for the conversion process (Figure 2.11) can be determined from the integration of the peaks in the chromatograms given as percentage of the two isomers. By using Equation 2.13, a plot of $\ln ([M]- [M]_{eq}/[M]_{0}-[M]_{eq}$ versus time gives a straight line, the slope being equal to k_f+k_r having determined the k_f and k_r, the free energy of activation ($\Delta G^{\#}_{,forward}$) (the energy barrier for interconversion in Figure 2.12) can be calculated using the Eyring Equation 2.14,

$$\Delta G^{\#}_{,forward} = RT\ln(k_b .T/ k_f.h) \quad (2.14)$$

where R= 8.3143 J/mol.K, T= temperature (Kelvin) at which the interconversion took place, k_b (Boltzmann constant) = $1.3805.10^{-23}$ J/K, h (Planck constant)= $6.6256.10^{-34}$ J.s, k_f= the rate constant for the forward reaction.

Moreover, at temperature T, the standard free energy change for the process (Figure 2.12), ΔG^{o} is given by,

$$\Delta G^{o}= -RT\ln K= \Delta H^{o}- T\,\Delta S^{o} \quad (2.15)$$

where K is the equilibrium constant at temperature T (K). ΔH^{o} is the standard enthalpy change and ΔS^{o} is the standard entropy change. Thus,

$$\ln K= - \Delta H^{o}/ RT + \Delta S^{o}/R \quad (2.16)$$

Assuming that ΔH^{o} and ΔS^{o} are constant in the temperature range studied, by plotting lnK values versus 1/T, ΔH^{o} and ΔS^{o} of the process can be obtained.

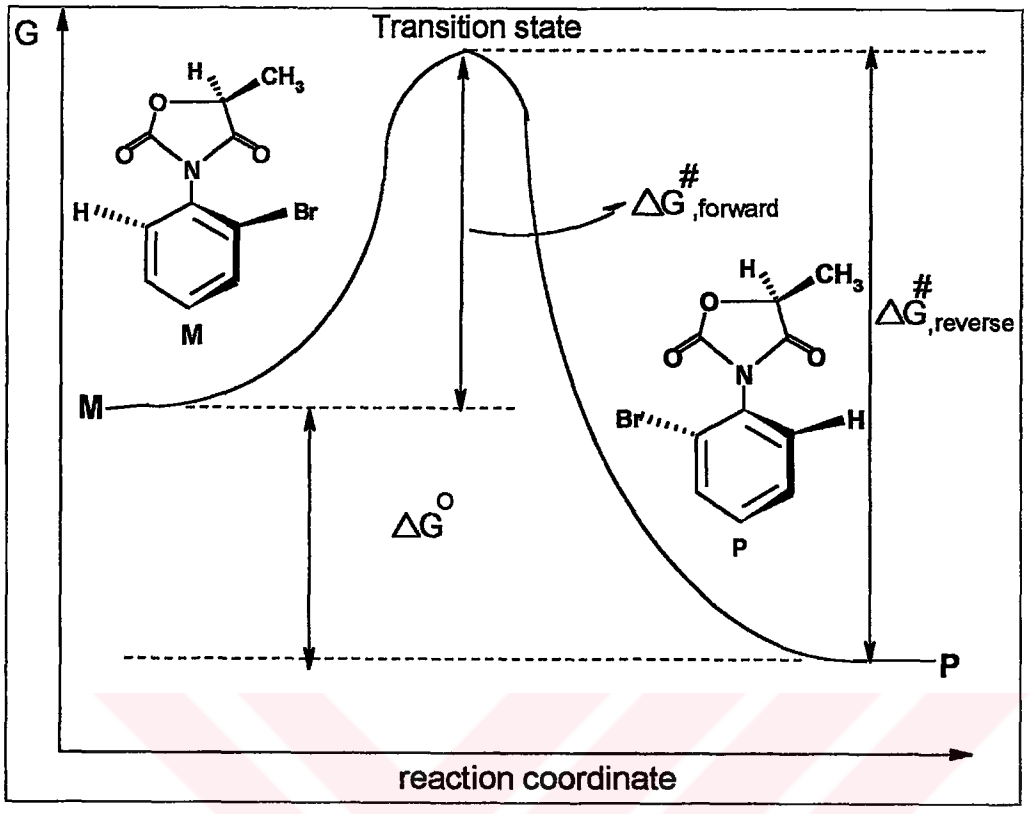

Figure 2.12. The graph illustrates the energy barrier for interconversion, $\Delta G^{\#}$, and the standard free energy change, ΔG^{o}, for the interconversion of rotamers

3. ORGANIC SYNTHESIS

3.1. The Synthesis of 5-Methyl-3-(*o*-aryl)-2,4-oxazolidinediones

3.1.1. The General Procedure

The 5-methyl-3-(*o*-aryl)-2,4-oxazolidinediones were synthesized by the reaction of (S)-(-)-ethyl lactate and *o*-aryl isocyanates in the presence of sodium metal in toluene (Figure 3.1).

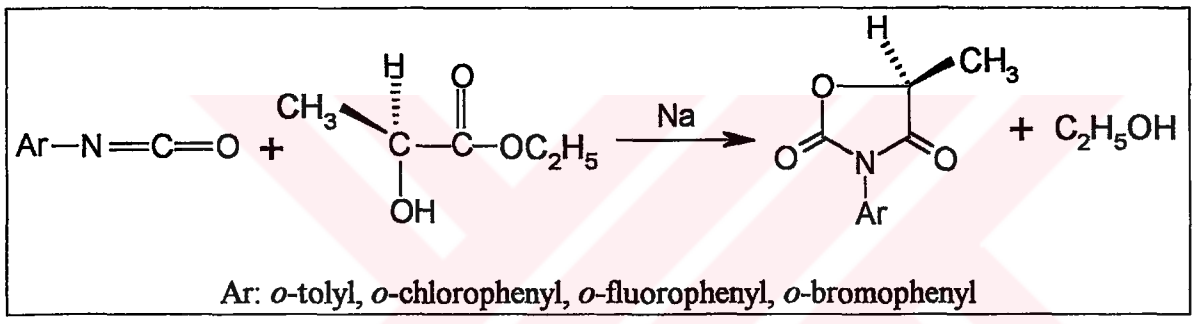

Figure 3.1. The synthesis of 5-methyl-3-(*o*-aryl)-2,4-oxazolidinediones

In a 100 ml three-necked flask, fitted with a thermometer and a reflux condenser, *o*-aryl isocyanate and S-(-)-ethyl lactate were mixed in toluene. Sodium metal was added prior to the heating in small pieces. After the addition of sodium, the mixture was heated for 10 hours at about 80 ° C then the temperature was raised to 100-110 ° C for one hour. At the end of this period, the reaction was stopped and the solvent was removed by evaporation in hood. 5-Methyl-3-(*o*-aryl)-2,4-oxazolidinediones were purified by recrystallization from ethanol.

3.1.1.1. 5-Methyl-3-(*o*-tolyl)-2,4-oxazolidinedione. Starting materials: 3.99 g (0.03 mole) *o*-tolyl isocyanate, 3.54 g (0.03 mole) S-(-)-ethyl lactate, 0.1379 g (0.006 mole) sodium metal, 15 ml toluene.

The compound has been prepared according to the general procedure. At the end of the 11-hour reflux process, a dark-orange crude product was obtained. After dissolving in

ethanol, 5-methyl-3-(*o*-tolyl)-2,4-oxazolidinedione was purified as white crystals and identified based on its ^1H spectrum and elemental analysis.

Yield: 2.07 g, 33.57 %

Melting point: 100.8-101.8 ° C

^1H NMR (200 MHz) Data in C_6D_6:

Methyl protons at C-5: δ= 1.02 ppm (d, J= 6.75 Hz), 1.03 ppm (d, J= 7.21 Hz), (3H)

Methine proton at C-5: δ= 4.07 ppm (q, J= 6.93 Hz), 4.02 ppm (q, J= 7.12 Hz), (1 H)

o-Methyl protons: δ= 1.99 (s), 1.92 ppm (s), (3H)

Aromatic protons: δ= 6.91-6.99 ppm (m), (4H)

Elemental Analysis Data:

Found: C, 64.50 %; H, 5.92 %; N, 6.51 %

Calculated for $C_{11}H_{11}O_3N$: C,64.38%; H, 5.4 %; N, 6.83 %

IR Data:

ν_{-Ar-H}: 3066 cm^{-1}, aromatic C-H stretching

ν_{-C-H}: 2989, 2935 cm^{-1}, alkyl C-H stretching

$\nu_{-C=O}$: 1749 cm^{-1}, carbonyl stretching

ν_{-C-H}: 1498, 1404 cm^{-1}, alkyl C-H bending

ν_{-C-H}: 768 cm^{-1}, *o*-disubstituted aromatic C-H out-of-plane bending

ν_{-C-O}: 1177 cm^{-1}, -C-O stretching

3.1.1.2. 5-Methyl-3-(*o*-chlorophenyl)-2,4-oxazolidinedione. Starting materials: 1.54 g (0.01 mole) *o*-chlorophenyl isocyanate, 1.18 g (0.01 mole) S-(-)-ethyl lactate, about 0.023 g (0.001 mole) sodium metal, 15 ml toluene.

The compound has been prepared according to the general procedure. At the end of the 11-hour reflux process, a dark-orange crude product was obtained. After dissolving in ethanol, 5-methyl-3-(*o*-chlorophenyl)-2,4-oxazolidinedione was purified as white crystals and identified based on its ^1H spectrum and elemental analysis.

Yield: 0.30 g, 6.73 %

Melting point: 81-81.7 ° C

^{1}H NMR (200 MHz) Data in C_6D_6:

Methyl protons at C-5: δ= 1.10 ppm (d, J= 7.19 Hz), 1.00 ppm (d, J= 7.22 Hz), (3H)

Methine proton at C-5: δ= 4.13 ppm (q, J= 6.81 Hz), 4.06 ppm (q, J= 7.22 Hz), (1H)

Aromatic protons: δ= 6.60-7.00 ppm (m), (4H)

Elemental Analysis Data:

Found: C, 53.93 %; H, 3.78 %; N, 5.59 %

Calculated for $C_{10}H_8O_3NCl$: C, 53.23 %; H,3.57 %; N, 6.21 %

IR Data:

ν_{-Ar-H}: 3073 cm^{-1}, aromatic C-H stretching

ν_{-C-H}: 2990, 2939 cm^{-1}, alkyl C-H stretching

$\nu_{-C=O}$: 1755 cm^{-1}, carbonyl stretching

ν_{-C-H}: 1489, 1407 cm^{-1}, alkyl C-H bending

ν_{-C-H}: 764 cm^{-1}, *o*-disubstituted aromatic C-H out-of-plane bending

ν_{-C-O}: 1179 cm^{-1}, -C-O stretching

3.1.1.3. 5-Methyl-3-(*o*-fluorophenyl)-2,4-oxazolidinedione. Starting materials: 6.86 g (0.05 mole) *o*-fluorophenyl isocyanate, 5.91 g (0.05 mole) S-(-)-ethyl lactate, about 0.11 g (0.005 mole) sodium metal, 15 ml toluene.

The compound has been prepared according to the general procedure. At the end of the 11-hour reflux process, a dark-orange crude product was obtained. After dissolving in ethanol, 5-methyl-3-(*o*-fluorophenyl)-2,4-oxazolidinedione was purified as white crystals and identified based on its ^{1}H spectrum and elemental analysis.

Yield: 1.55 g, 14.83 %

Melting point: 79.6-80.6 ° C

^{1}H NMR Data (200 MHz) in C_6D_6:

Methyl protons at C-5: δ= 0.95 ppm, (d, J= 7.1) (3H)

Methine proton at C-5: δ= 3.97 ppm (q, J= 7.1) (1H)

Aromatic protons: δ= 6.60-7.00 ppm (m) (4H)

Elemental Analysis Data:

Found: C, 57.73 %; H, 4.21 %; N, 6.80 %

Calculated for $C_{10}H_8O_3NF$: C, 57.42 %; H, 3.85 %; N, 6.70 %

IR Data:

ν_{-Ar-H}: 3072 cm^{-1}, aromatic C-H stretching

ν_{-C-H}: 2992, 2939 cm^{-1}, alkyl C-H stretching

$\nu_{-C=O}$: 1755 cm^{-1}, carbonyl stretching

ν_{-C-H}: 1514, 1462, 1409 cm^{-1}, alkyl C-H bending

ν_{-C-H}: 765 cm^{-1}, *o*-disubstituted aromatic C-H out-of-plane bending

ν_{-C-O}: 1174 cm^{-1}, -C-O stretching

3.1.1.4. 5-Methyl-3-(*o*-bromophenyl)-2,4-oxazolidinedione. Starting materials: 2.38 g (0.012 mole) *o*-bromophenyl isocyanate, 1.42 g (0.012 mole) S-(-)-ethyl lactate, 0.028 g (0.0012 mole) sodium metal, 15 ml toluene.

The compound has been prepared according to the general procedure. At the end of the 11-hour reflux process, a dark-orange crude product was obtained. After dissolving in ethanol, 5-methyl-3-(*o*-bromophenyl)-2,4-oxazolidinedione was purified as white crystals and identified based on its ^1H spectrum and elemental analysis.

Yield: 0.82 g, 25.17 %

Melting point: 95.3-95.9 ° C

^1H NMR (200 MHz) Data in C_6D_6:

Methyl protons at C-5: δ= 1.02 ppm (d, J= 7.08 Hz), 1.16 ppm (d, J= 6.86 Hz), (3H)

Methine proton at C-5: δ= 4.2 ppm (q, J= 7.12 Hz), 4.08 ppm (d, J= 6.71 Hz), (1H)

Aromatic protons: δ= 6.50-7.2 ppm (m), (4H)

Elemental Analysis Data:

Found: C, 44.07 %; H, 2.95 %; N, 4.73 %

Calculated for $C_{10}H_8O_3NBr$: C, 44.47 %; H, 2.99 %; N, 5.19 %

IR Data:

ν_{-Ar-H}: 3078 cm^{-1}, aromatic C-H stretching

ν_{-C-H}: 2992 cm^{-1}, alkyl C-H stretching

$\nu_{-C=O}$: 1749 cm^{-1}, carbonyl stretching

ν_{-C-H}: 1483, 1406 cm^{-1}, alkyl C-H bending

ν_{-C-H}: 773 cm^{-1}, *o*-disubstituted aromatic C-H out-of-plane bending

ν_{-C-O}: 1178 cm^{-1}, -C-O stretching

3.2. The Synthesis of 5,5-Dimethyl-3-(*o*-aryl)-2,4-oxazolidinediones

3.2.1. The General Procedure

The 5,5-dimethyl-3-(*o*-aryl)-2,4-oxazolidinediones were synthesized by the reaction of ethyl α-hydroxyisobutyrate and *o*-aryl isocyanates in the presence of sodium metal in toluene (Figure 3.2).

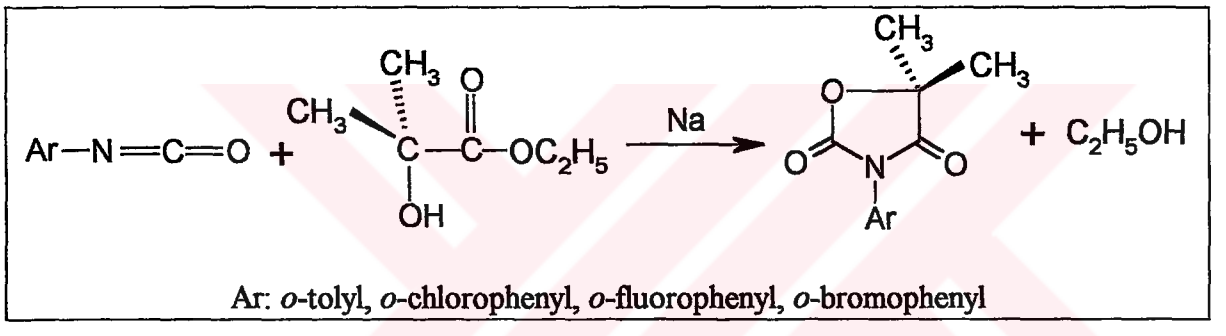

Ar: *o*-tolyl, *o*-chlorophenyl, *o*-fluorophenyl, *o*-bromophenyl

Figure 3.2. The synthesis of 5,5-dimethyl-3-(*o*-aryl)-2,4-oxazolidinediones

In a 100 ml three-necked flask, fitted with a thermometer and reflux condenser, *o*-aryl isocyanate and ethyl α-hydroxyisobutyrate were mixed in toluene. Sodium metal was added prior to heating in small pieces. After the addition of sodium, the mixture was heated for 10 hours at about 80 ° C then the temperature was raised to 100-110 ° C for one hour. At the end of this period, the reaction was stopped and the solvent was removed by evaporation in hood. The 5,5-dimethyl-3-(*o*-aryl)-2,4-oxazolidinediones were purified by recrystallization from ethanol.

3.2.1.1. 5,5-Dimethyl-3-(*o*-tolyl)-2,4-oxazolidinedione. Starting materials: 3.87 g (0.029 mole) ethyl α-hydroxyisobutyrate, 3.90 g (0.029 mole) *o*-tolyl isocyanate, 0.12 g (0.0052 mole) sodium metal, 15 ml toluene.

The compound has been prepared according to the general procedure. At the end of the 11-hour reflux process, a dark-orange crude product was obtained. After dissolving in

ethanol, 5,5-dimethyl-3-(*o*-tolyl)-2,4-oxazolidinedione was purified as white crystals and identified based on its ^{1}H and ^{13}C NMR spectra and elemental analysis.

Yield: 3.28 g, 51.55 %

Melting point: 91.2-92.2 ° C

^{1}H NMR (200 MHz) Data in C_6D_6:

Diastereotopic methyl protons at C-5: δ= 1.15 ppm (s, 3H), 1.17 ppm (s, 3H)

o-Methyl protons: δ= 1.97 ppm (s, 3H)

aromatic protons: δ= 6.88-7.03 ppm (m, 4H)

^{13}C NMR (200 MHz) Data in C_6D_6:

Carbonyl carbons in the heterocyclic ring: 174.8 ppm, 153.1 ppm

Diastereotopic methyl carbons: 23.0 ppm, 23.7 ppm

Methine carbon (C-5) in the heterocyclic ring: 83.5 ppm

o-Methyl carbon: 17.4 ppm

Aromatic carbons: 127.1, 128.54, 129.8, 130.5, 131.3, 136.2 ppm

Elemental Analysis Data:

Found: C, 64.61 %; H, 5.93 %; N, 5.57 %

Calculated for $C_{12}H_{13}O_3N$: C, 65.74 %; H, 5.98 %; N, 6.39 %

IR Data:

ν_{-Ar-H}: 3066 cm^{-1}, aromatic C-H stretching

ν_{-C-H}: 2985, 2934, 2875 cm^{-1}, alkyl C-H stretching

$\nu_{-C=O}$: 1749 cm^{-1}, carbonyl stretching

ν_{-C-H}: 1498, 1463, 1405 cm^{-1}, alkyl C-H bending

ν_{-C-H}: 767 cm^{-1}, *o*-disubstituted aromatic C-H out-of-plane bending

ν_{-C-O}: 1173 cm^{-1}, -C-O stretching

3.2.1.2. 5,5-Dimethyl-3-(*o*-chlorophenyl)-2,4-oxazolidinedione. Starting materials: 1.54 g (0.01 mole) *o*-chlorophenyl isocyanate, 1.32 g (0.01 mole) ethyl α-hydroxyisobutyrate, 0.023 g (0.001 mole) sodium metal, 15 ml toluene.

The compound has been prepared according to the general procedure. At the end of the 11-hour reflux process, a dark-orange crude product was obtained. After dissolving in

ethanol, 5,5-dimethyl-3-(*o*-chlorophenyl)-2,4-oxazolidinedione was purified as white crystals and identified based on its ^{1}H and ^{13}C NMR spectra and elemental analysis.

Yield: 0.58 g, 24.25 %

Melting point: 94.9-95.6 ° C

^{1}H NMR (200 MHz) Data in C_6D_6:

Diastereotopic methyl protons at C-5: δ= 1.16 ppm (s, 3H), 1.25 ppm (s, 3H)

Aromatic protons: δ= 6.60-7.00 ppm (m, 4H)

^{13}C NMR (200 MHz) Data in C_6D_6:

Carbonyl carbons in the heterocyclic ring: 174.2 ppm, 152.3 ppm

Diastereotopic methyl carbons at C-5: 22.9 ppm, 23.8 ppm

Methine carbon (C-5) in the heterocyclic ring: 84.1 ppm

Aromatic carbons: 127.8, 129.2, 130.4, 131.1, 132.9 ppm

Elemental Analysis Data:

Found: C, 53.94 %; H, 4.14 %; N, 4.99 %

Calculated for $C_{11}H_{10}O_3NCl$: C, 55.13 %; H, 4.21 %; N, 5.84 %

IR Data:

ν_{-C-H}: 2987 cm^{-1}, alkyl C-H stretching

$\nu_{-C=O}$: 1745 cm^{-1}, carbonyl stretching

ν_{-C-H}: 1488, 1406 cm^{-1}, alkyl C-H bending

ν_{-C-H}: 772 cm^{-1}, *o*-disubstituted aromatic C-H out-of-plane bending

ν_{-C-O}: 1171 cm^{-1}, -C-O stretching

3.2.1.3. 5,5-dimethyl-3-(*o*-fluorophenyl)-2,4-oxazolidinedione. Starting materials: 2.06 g (0.015 mole) *o*-fluorophenyl isocyanate, 1.98 g (0.015 mole) ethyl α-hydroxyisobutyrate, 0.03 g (0.0013 mole) sodium metal, 15 ml toluene.

The compound has been prepared according to the general procedure. At the end of the 11-hour reflux process, a dark-orange crude product was obtained. After dissolving in ethanol, 5,5-dimethyl-3-(*o*-fluorophenyl)-2,4-oxazolidinedione was purified as white crystals and identified based on its ^{1}H and ^{13}C NMR spectra and elemental analysis.

Yield: 1.17 g, 34.70 %

Melting point: 114.1-114.8 ° C

^{1}H NMR (200 MHz) Data in C_6D_6:

Diastereotopic methyl protons at C-5: δ= 1.11 ppm (s, 6H)

Aromatic protons: δ= 6.60-7.48 ppm (m, 4H)

^{13}C NMR (200 MHz) Data in C_6D_6:

Carbonyl carbons in the heterocyclic ring: 174.2 ppm, 160.5 ppm, 155.4 ppm, 152.4 ppm

Diastereotopic carbons at C-5: 23.3 ppm

Aromatic carbons: 124.8,125.7,129.2, 129.6, 131.3, 131.4, 116.9, 116.5 ppm

Elemental Analysis Data:

Found: C, 59.78 %; H, 4.84 %; N, 6.33 %

Calculated for $C_{11}H_{10}O_3NF$: C, 59.19 %; H, 4.54 %; N, 6.28 %

IR Data:

ν_{-Ar-H}: 3078 cm^{-1}, aromatic C-H stretching

ν_{-C-H}: 2992, 2942 cm^{-1}, alkyl C-H stretching

$\nu_{-C=O}$: 1744 cm^{-1}, carbonyl stretching

ν_{-C-H}: 1508, 1410 cm^{-1}, alkyl C-H bending

ν_{-C-H}: 774 cm^{-1}, *o*-disubstituted aromatic C-H out-of-plane bending

ν_{-C-O}: 1170 cm^{-1}, -C-O stretching

3.2.1.4. 5,5-dimethyl-3-(*o*-bromophenyl)-2,4-oxazolidinedione. Starting materials: 1.98 g (0.01 mole) *o*-bromophenyl isocyanate, 1.32 g (0.01 mole) ethyl α-hydroxyisobutyrate, 0.02 g (0.00087 mole) sodium metal, 15 ml toluene.

The compound has been prepared according to the general procedure. At the end of the 11-hour reflux process, a dark-orange crude product was obtained. After dissolving in ethanol, 5,5-dimethyl-3-(*o*-bromophenyl)-2,4-oxazolidinedione was purified as white crystals and identified based on its ^{1}H and ^{13}C NMR spectra and elemental analysis.

Yield: 1.24 g, 43.68 %

Melting point: 91.7-92.4 ° C

^{1}H NMR (200 MHz) Data in C_6D_6:

Diastereotopic methyl protons at C-5: δ= 1.2 ppm (s, 3H), 1.3 ppm (s, 3H)

Aromatic protons: δ= 6.5-7.2 ppm (m, 4H)

^{13}C NMR (200 mHz) Data in C_6D_6:

Carbonyl carbons in the heterocyclic ring: 174.1 ppm, 152.3 ppm

Diastereotopic methyl carbons at C-5: 22.9 ppm, 23.8 ppm

Methine carbon (C-5) in the heterocyclic ring: 84.2 ppm

Aromatic carbons: 122.9, 128.6, 129.2, 130.5, 131.4, 133.5 ppm

Elemental Analysis Data:

Found: C, 46.78 %; H, 3.79 %; N, 4.61 %

Calculated for $C_{11}H_{10}O_3NBr$: C, 46.5 %; H, 3.55 %; N, 4.93 %

IR Data:

ν_{-Ar-H}: 3067 cm^{-1}, aromatic C-H stretching

ν_{-C-H}: 2986, 2937 cm^{-1}, alkyl C-H stretching

$\nu_{-C=O}$: 1749 cm^{-1}, carbonyl stretching

ν_{-C-H}: 1485, 1411 cm^{-1}, alkyl C-H bending

ν_{-C-H}: 763 cm^{-1}, *o*-disubstituted aromatic C-H out-of-plane bending

ν_{-C-O}: 1180 cm^{-1}, -C-O stretching

3.3. The Synthesis of *o*-Aryl Isocyanates

3.3.1. The General Procedure

o-Aryl isocyanates which were used as starting materials to synthesize 2,4-oxazolidinedione derivatives were formed from the reaction of the corresponding acid chloride with sodium azide by the Curtius rearrangement of the acyl azide. The reaction was carried out in toluene that allowed the isolation of *o*-aryl isocyanates (Figure 3.3).

The sodium azide was mixed with acid chloride in a 250 ml round bottomed flask and toluene was added into the flask. The reaction mixture was refluxed for 11 hours. Isocyanates formed at the end of this period were taken away from the reaction mixture by

vacuum distillation and purified by fractional distillation under vacuum. The isocyanates were identified by their IR spectra.

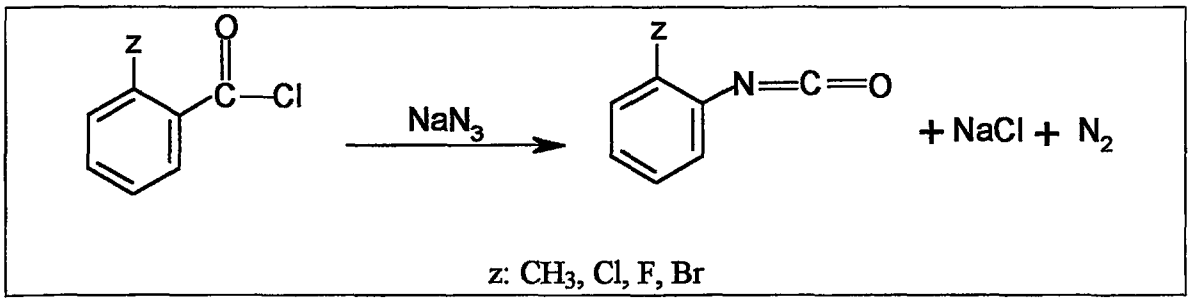

Figure 3.3. The synthesis of *o*-aryl isocyanates

3.3.1.1. *o*-Tolyl Isocyanate. Starting materials: 7.15 g (0.11 mole) sodium azide, 12.40 g (0.08 mole) 2-methylbenzoyl chloride, 75 ml toluene.

Yield: 8.18 g, 76.82 %

Boiling point: 110 ° C (35 mmHg)

IR Data:

$\nu_{-N=C=O}$: 2275 cm^{-1} (cumulative -N=C=O stretching vibration)

3.3.1.2. *o*-Chlorophenyl Isocyanate. Starting materials: 7.80 g (0.12 mole) sodium azide, 17.50 g (0.10 mole) 2-chlorobenzoyl chloride, 75 ml toluene.

Yield: 8.18 g, 53.28 %

Boiling point: 113 ° C (35 mmHg)

IR Data:

$\nu_{-N=C=O}$: 2264 cm^{-1} (cumulative -N=C=O stretching vibration)

3.3.1.3. *o*-Fluorophenyl Isocynate. Starting materials: 8.45 g (0.13 mole) sodium azide, 17.50 g (0.11 mole) 2-fluorobenzoyl chloride, 75 ml toluene.

Yield: 13.76 g, 91.22 %

Boiling point: 108 ° C (35 mmHg)

IR Data:

$\nu_{-N=C=O}$: 2269 cm^{-1} (cumulative -N=C=O stretching vibration)

3.3.1.4. *o*-Bromophenyl Isocyanate. Starting materials: 2.60 g (0.04 mole) sodium azide, 4.39 g (0.02 mole) 2-bromophenylbenzoyl chloride, 30 ml toluene.

Yield: 3.18 g, 80.41 %

Boiling point: 128 ° C (35 mmHg)

IR Data:

$\nu_{-N=C=O}$: 2264 cm^{-1} (cumulative -N=C=O stretching vibration)

3.4. Reactions of 5-Methyl-3-(*o*-aryl)-2,4-oxazolidinediones with Methanol

The 5-methyl-3-(*o*-aryl)-2,4-oxazolidinediones was found to react with methanol, causing a ring opening of the 5-membered heterocyclic ring.

3.4.1. Reaction of 5-Methyl-3-(*o*-tolyl)-2,4-oxazolidinedione with Methanol

The 5-Methyl-3-(*o*-tolyl)-2,4-oxazolidinedione (0.024 g, 0.00012 mole) was dissolved in 2 ml methanol and refluxed for 5 days. At the end of the reflux process, methanol was removed by evaporation in the hood.

3.4.2. Reaction of 5-Methyl-3-(*o*-bromophenyl)-2,4-oxazolidinedione with Methanol

The 5-methyl-3-(*o*-bromophenyl)-2,4-oxazolidinedione (0.026 g, 0.000096 mole) was refluxed in 2 ml methanol for 5 days. At the end of the reflux process, methanol was removed by evaporation in hood.

3.4.3. Reaction of 5-Methyl-3-(*o*-chlorophenyl)-2,4-oxazolidinedione with Methanol

The 5-methyl-3-(*o*-chlorophenyl)-2,4-oxazolidinedione (0.0759 g, 0.00034 mole) was refluxed in 2 ml methanol for 5 days. At the end of the reflux process, methanol was removed by evaporation in hood.

3.4.4. Reaction of 5-Methyl-3-(*o*-fluorophenyl)-2,4-oxazolidinedione with Methanol

The 5-methyl-3-(*o*-fluorophenyl)-2,4-oxazolidinedione (0.0788 g, 0.00038 mole) was refluxed in 2 ml methanol for 5 days. At the end of the reflux process, methanol was removed by evaporation in hood. The product was identified by 60 MHz ^{1}H NMR.

3.5. Materials and Apparatus

The list of chemicals used in this work, together with the names of suppliers are briefly described in Table 3.1.

Table 3.1. Chemicals used in the study

Name	Formula	Supplier	% Purity
Toluene	C_7H_8	Merck	>99%
(S)-(-)-Ethyllactate	$C_5H_{10}O_3$	Merck	>99%
Ethyl α-hydroxyisobutyrate	$C_6H_{12}O_3$	Fluka	>97%
Sodium azide	NaN_3	Merck	>99%
2-Methylbenzoyl chloride	C_8H_7ClO	Merck	>97%
2-Fluorobenzoyl chloride	C_7H_4ClFO	Aldrich	99%
2-Bromobenzoyl chloride	C_7H_4BrClO	Merck	>98%
2-Chlorobenzoyl chloride	$C_7H_4C_2lO$	Merck	98%
Sodium metal	Na	Riedel-de haen	99.50%
Methanol	CH_3OH	Merck	>99.50%
Deutorochloroform	$CDCl_3$	Merck	99%
Ethanol	C_2H_5OH	Delta	98.50%
Carbontetrachloride	CCl_4	Aksın	purified
Hexane for HPLC	C_6H_{14}	Merck	>98.00%
Absolute ethanol for HPLC	C_2H_5OH	Panreac	>99.80%
(S)-(+)-1-(9-Anthryl)-2,2,2-trifluoro ethanol	$C_{16}H_{11}F_3O$	Aldrich	>98%

3.5.1. Apparatus

^{1}H NMR spectra were recorded on an varian T-60A spectrometer (60 MHz, 24 °C), on a Bruker AC-200L (200 MHz, 22 °C).

^{13}C-(APT) NMR spectra were recorded on a Bruker AC-200L (50 MHz, T=22 °C).

Elemental analysis were performed on Carlo Erba 1106.

Melting points were recorded using Electrothermal 9100 melting point apparatus.

The IR analyses were performed on a Mattson Genesis II FTIR using KBr discs or NaCl windows.

The OD-H column (Daicel Ltd.) used in HPLC, filling with cellulose tris-(3,5-dimethyl)phenyl-carbamate have the following dimentions: partical size: 5 μm, column size: 250+4.6 mm).

4. RESULTS AND DISCUSSION

4.1. ^{1}H NMR Spectra of the Compounds

The 5-methyl-3-(*o*-aryl)-2,4-oxazolidinedione and 5,5-dimethyl-3-(*o*-aryl)-2,4-oxazolidinedione molecules are expected to have two relatively stable conformations, corresponding to the ground states for internal rotation about the C-N single bond. Steric interactions between the *o*-aryl groups and the heterocyclic moiety are likely to result in large dihedral angles between the two groups in the ground states (Figure 1.9). In these molecules, C-N single bond around which conformational difference is provided is the chiral axis. If the substituents on C-5 are identical (**2, 4, 6, 8**) the rotational isomers of the *o*-substituted compounds are enantiomeric, and expected to exhibit identical NMR spectra in achiral solvents. However, the C-5 substituents are diasteriotopically related and should be, in principle, magnetically non-equivalent, provided that the rate of internal rotation is slow on the NMR time scale. If another asymmetric center exist in the molecule i.e. the groups on the C-5 are different, the rotational isomers (**1S, 3S, 5S, 7S**) are diastereomers, and should have distinctly different NMR spectra, provided that the internal rotation is sufficiently slow. In particular, corresponding pairs of nuclei in the two diastereomeric rotamers should show chemical shift differences. The magnitude of the chemical shift differences must be related to factors such as the steric effects which determine dihedral angles, and the rate of internal rotation, anisotropic and electronic effect of the substituents.

For the compounds **2**, **4**, and **6** the chemical shift difference between diastereotopic methyl protons on C-5 was not large enough to be distinctly measured in the 60 MHz NMR spectrometer. In the spectra taken by the 60 MHz NMR instrument only a singlet around 1.7 ppm was seen instead of two singlets. The integral ratios were as expected based on the structures of 5,5-dimethyl-3-(*o*-aryl)-2,4-oxazolidinedione derivatives. When the *ortho* aryl substituent was Br (**8**), the diastereotopic methyl protons on C-5 are distinguishable in the 60 MHz ^{1}H NMR spectrum. The spectrum of **8** in Figure 4.9a shows evidence for the polar influence of a large *ortho* bromo substituent, since, in this case, the signals of the 5-methyl protons were distinguishable. The greater chemical shift difference observed between the two diastereomeric methyl groups of the bromo substituted

oxazolidinedione than the other groups was attributed, in part, to the repulsive interaction between the bromine atom and the carbonyl oxygen atom of the heteroring, and partially to the larger size of the bromine atom (Table 4.1) [25], with a consequent effect of a relatively larger dihedral angle between the two rings. Since bromine atom is larger than the other groups, the steric influence is more noticeable on the NMR time scale.

Table 4.1. Van der Waals radii of several atoms and groups

Atom/group	Van der Waals radii (Å)
F	1.47
Cl	1.75
Br	1.85
CH_3	2

To obtain a better resolution, an NMR instrument with a higher operational frequency (200 MHz) was used. This time the spectra were taken in hexadeutorobenzene instead of CCl_4 or $CDCl_3$ since it is a better solvent to observe the shift differences due to the anisotropy effect of the benzene ring [12]. The spectrum of the compound **2** taken in C_6D_6 is shown in the Figures 4.3 and 4.4, that of compound **4** in Figures 4.5 and 4.6, that of compound **6** in Figure 4.7 and that of compound **8** in Figures 4.8 and 4.9. The compounds **2, 4** and **8** exhibited proton spectra with additional splittings expected for the each diastereotopic methyl protons on C-5. Therefore, it was concluded that the rates of internal rotation in these compounds are slow on the NMR time scale at 22 °C. However, for compound **6**, the two singlets of diastereotopic methyl protons were still not observed. Because florine atom is very small compared with the other groups (Table 4.1), not much steric repulsion is expected between the florine and the carbonyl oxygen atom. Therefore, in this case, the pair of signals produced by the diastereotopic nuclei collapsed to a singlet due to the fast internal rotation about C-N single bond on the NMR time scale.

In compounds **2, 4** and **8**, diastereotopically related methyl groups on C-5 displayed magnetic non-equivalence. The chemical shift differences between the methyl groups were sufficient to be observed, therefore, it was concluded that the rate of internal rotation was slow on the NMR time scale. Since the rate of rotation depends on the interaction between

the subsitutents and the carbonyl oxygen atom in the transition state (Figure 2.4), an increase in the size of the substituents is expected to decrease the rate of rotation. In compound **4**, the substituent is chlorine atom, and it possesses lone pair electrons that interact with the electrons of carbonyl oxygen atom in the transition state and cause steric repulsion. This repulsion rendered the rotation slow on the NMR time scale, and made the methyl groups non-equivalent. Therefore, the chemical shift difference ($\Delta\delta$= 0.0867 ppm) was more compared with that of compound **2**, where the substituent was methyl ($\Delta\delta$= 0.0165 ppm). Although the *o*-methyl group in compound **2** possesses a larger van der Waals radius (Table 4.1), it does not have lone pair electrons which interact with the electrons of carbonyl oxygen atom. Therefore, in this case, the rate of rotation was faster than that of compound **4**, and the chemical shift difference ($\Delta\delta$) was only 0.0165 ppm. In compound **8**, since the bromo substituent, because it is larger than the chloro substituent, causes more steric repulsion. The rate of rotation of this compound is very slow, and the chemical shift difference ($\Delta\delta$= 0.1217 ppm) is the largest in the series studied.

All the 5-methyl-3-(*o*-aryl)-2,4-oxazolidinedione derivatives (**1S**, **3S**, **5S** and **7S**) were obtained as diastereomeric mixtures which were differentiated in the ^{1}H NMR spectra taken by using 200 MHz instrument in C_6D_6. The 60 MHz spectrometer was used for the initial identification of the compounds synthesized.

The chemical shift differences between the diastereomeric signals of the compounds **1S**, **3S**, and **7S** increased with an increase in the expected dihedral angle between the two rings. The magnitude of the dihedral angle depends on the steric repulsion between the *o*-substituents and the carbonyl oxygen atom in the transition state. Since, *o*-bromo and *o*-chloro substituents possessed lone pair electrons that interacted with that of carbonyl oxygen in the transition state, the chemical shift differences were higher than the others. Therefore, for compound **7S** where the *o*-bromo substitution was present, the chemical shift differences were the largest in the series studied and the values of two diastereomeric methyl and methine protons were 0.14 ppm and 0.12 ppm, respectively (Figures 4.15, 4.16 and 4.17). Since the van der Waals radius of o-chloro substituent was less than that of o-bromo (Table 4.1), smaller chemical shift differences (0.10 ppm and 0.07 ppm) were observed for compound **3S**, compared to **7S** as expected (Figures 4.13 and 4.14). Although the van der Waals radius of *o*-methyl group was the largest one (Table 4.1), because of the

absence of lone pair electrons to cause more steric repulsion in the transition state, a smaller dihedral angle was expected for compound **1S** and the chemical shift differences were accordingly less than that of **3S** and **7S**. For doublets, quartets and singlets, the chemical shift differences were 0.0087 ppm, 0.051 ppm and 0.066 ppm, respectively (Figures 4.10, 4.11 and 4.12). Because *o*-fluoro substitution was the smallest in the series studied, the rotation was fast on the NMR time scale and (the dihedral angle was very small), no chemical shift difference was observed. As a result, only one doublet for diastereomeric methyl protons and only one quartet for the diastereomeric methine protons were seen in the 200 MHz ^{1}H NMR spectrum (Figures 4.18, 4.19 and 4.20).

In conclusion, the existence of hindered rotation around C-N single bond in all compounds except for *o*-fluoro derivative was proved by studying ^{1}H NMR spectra. The spectral assignments are given in Table 4.2 and Table 4.3.

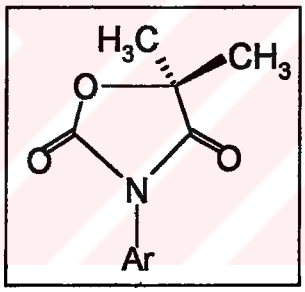

Figure 4.1. The general structure for the 5,5-dimethyl-3-(o-aryl)-2,4-oxazolidinediones

Table 4.2. 200 MHz ^{1}H NMR spectral data for the 5,5-dimethyl-3-(o-aryl)-2,4-oxazolidinediones

Compound No	Ar	ppm C-5 Methyl	ppm *o*-Methyl
2	*o*-Tolyl	1.15 and 1.17 [a]	1.97
4	*o*-Chlorophenyl	1.16 and 1.25 [a]	-
6	*o*-Fluorophenyl	1.11 [b]	-
8	*o*-Bromophenyl	1.19 and 1.31 [a]	-

[a]: Two values refer to two diastereotopic methyl groups
[b]: Only one singlet was observed

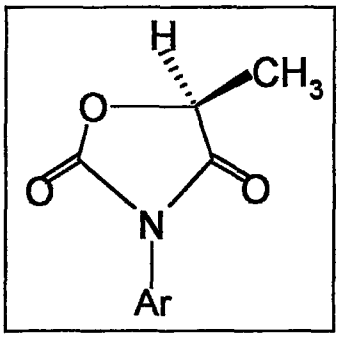

Figure 4.2. The general structure for the 5-methyl-3-(o-aryl)-2,4-oxazolidinediones

Table 4.3. 200 MHz ^{1}H NMR spectral data for the 5-methyl-3-(o-aryl)-2,4-oxazolidinediones

Compound No	Ar	δ (ppm), C-5 methyl [a]	δ (ppm), C-5 methine [a]	δ (ppm), *o*-methyl [a]
1S	*o*-Tolyl	1.016 and 1.025	4.02 and 4.07	1.92 and 1.99
3S	*o*-Chlorophenyl	1.00 and 1.10	4.06 and 4.13	-
5S	*o*-Fluorophenyl	0.95 [b]	3.97 [b]	-
7S	*o*-Bromophenyl	1.02 and 1.16	4.08 and 4.20	-

[a]: Two values refer to two diastereomers
[b]: Only one doublet and one quartet were observed

4.2. ^{1}H NMR Spectra of the Compounds in the Presence of Chiral Auxiliary

5,5-Dimethyl-3-(*o*-aryl)-2,4-oxazolidinediones exist in two enantiomeric forms as a result of restricted rotation about the C-N single bond . The geminal dimethyl groups in the 5 position of the heterocycle are diastereotopic, and for compounds **2, 4** and **8**, they are anisochronous at 22 °C, giving rise to two separable singlets with the chemical shift differences of 0.0165 ppm, 0.0867 ppm and 0.1217 ppm, respectively. For compound **6**, because of the fast rotation around C-N single bond, only one singlet was observed instead of two singlets.

In order to prove the presence of two enantiomeric species, ^{1}H NMR spectra of these compounds were also taken in the presence of the chiral auxiliary (S)-(+)-1-(9-anthryl)-2,2,2-trifluoroethanol (TFAE) by using 200 MHz NMR spectrometer. The chiral auxiliary was chosen for the reason that a close interaction between solute and auxiliary molecules can be provided by means of strong intermolecular hydrogen bonding. Moreover, the presence of the strongly anisotropic anthryl group enhances the difference in average magnetic environments of nuclei in the rotamers (Figure 2.8). That is, it is expected that it will associate with the enantiomers and form two diastereotopic, and in principle, NMR distinguishable complexes in solution (Figure 2.7).

For the C-5 diastereotopic methyl protons of the compound studied, four singlets were expected in the presence of (S)-(+)-TFAE. When the spectrum of the compound **2** was taken in C_6D_6 in the presence of eight equivalents of (S)-(+)-TFAE, only three singlets with chemical shift differences 0.0121 and 0.0179 ppm were observed instead of four singlets (Figure 4.21). However, the signal was like a triplet. Therefore, it was concluded that two of the singlets that had similar chemical shifts overlapped into one singlet (Figure 4.21). Moreover, two singlets with a chemical shift difference of 0.011 ppm for *o*-methyl protons of the two diastereomeric complexes formed between the CA and compound **2** were observed in the presence of CA (Figure 4.21). The spectrum of compound **2** was also taken in the presence of six equivalents of (S)-(+)-TFAE. In this case, the *o*-methyl protons was observed as two singlets with a chemical shift difference of 0.005 ppm (Figure 4.22). Therefore, it was concluded that the concentration of the CA may be influencial in exerting a chemical shift difference between the signals of the diastereomeric association complex.

When the 200 MHz ^{1}H NMR spectrum of compound **4** was taken in C_6D_6 in the presence of six equivalents of (S)-(+)-TFAE, the expected four singlets were observed (Figure 4.23) with chemical shift differences of 0.005 and 0.012 ppm.

The 200 MHz ^{1}H NMR spectrum of compound **8** was also taken in the presence of six equivalents of (S)-(+)-TFAE in C_6D_6. In this case, three singlets were observed instead of four. A chemical shift difference of 0.0102 ppm has been observed for one pair, whereas the other could not be resolved and appeared as a shoulder only (Figure 4.24).

In the spectrum of compound **6**, only two singlets were observed with a chemical shift difference 1.735 ppm (Figure 4.25). The singlets of diastereotopic methyl groups in each conformation may be overlapped and observed as only one singlet. The overlapping may be due to the fast rotation around C-N single bond in this compound, which reduces the four-singlet system into two-singlet. The fast rotation was also the reason for the observation for one singlet in the spectrum of compound **6** taken in the absence of the CA (Figure 4.7).

In the spectrum of compound **2** (Figure 4.22), taken in the presence of six equivalents of (S)-(+)-TFAE in $CDCl_3$, since the singlets of the diastereomeric *o*-methyl protons had the same intensity (7.7:7.12), it was concluded that the two diastereomeric association complex were present in equal amounts. Two more spectra were taken after keeping this solution of the association complex at 35 °C for 2 and 5.5 hours. However, no change in intensities (also in amounts) was observed. After keeping the solution for 3 weeks at room temperature (25 °C), it was seen that (Figure 4.26) the two singlets of diastereomeric *o*-methyl protons overlapped and a small change was observed in the intensities of the other singlets. When this solution was further kept at 35 °C for 7.5 hours, the three singlets changed to two singlets (Figure 4.27). This observation may be due to the fast rotation around C-N single bond or a shift towards the unassociated species in the equilibrium (2.1 and 2.2) involving the enantiomers, the CA and the diastereomeric association complexes. In a similar way, when the solution of the association complex formed between the CA and compound **4** was kept at 35 °C for 2 and 6 hours, no change was observed in the intensities of four singlets.

In the spectra of the compounds **2**, **4**, **6**, and **8** in the presence of (S)-(+)-TFAE (Figures 4.22, 4.23, 4.25, 4.24), it can be seen that the observed singlets were shielded (with the chemical shift differences 0.0556 ppm, 0.0554 ppm, 0.0453 ppm and 0.0498 ppm, respectively) compared with the singlets in the absence of chiral auxiliary. The shielding might have resulted from the large anisotropy effect of the anthryl group. A plausible structure of the association complex formed between the CA and the one of the conformation of the enantiomers is shown in Figure 2.8.

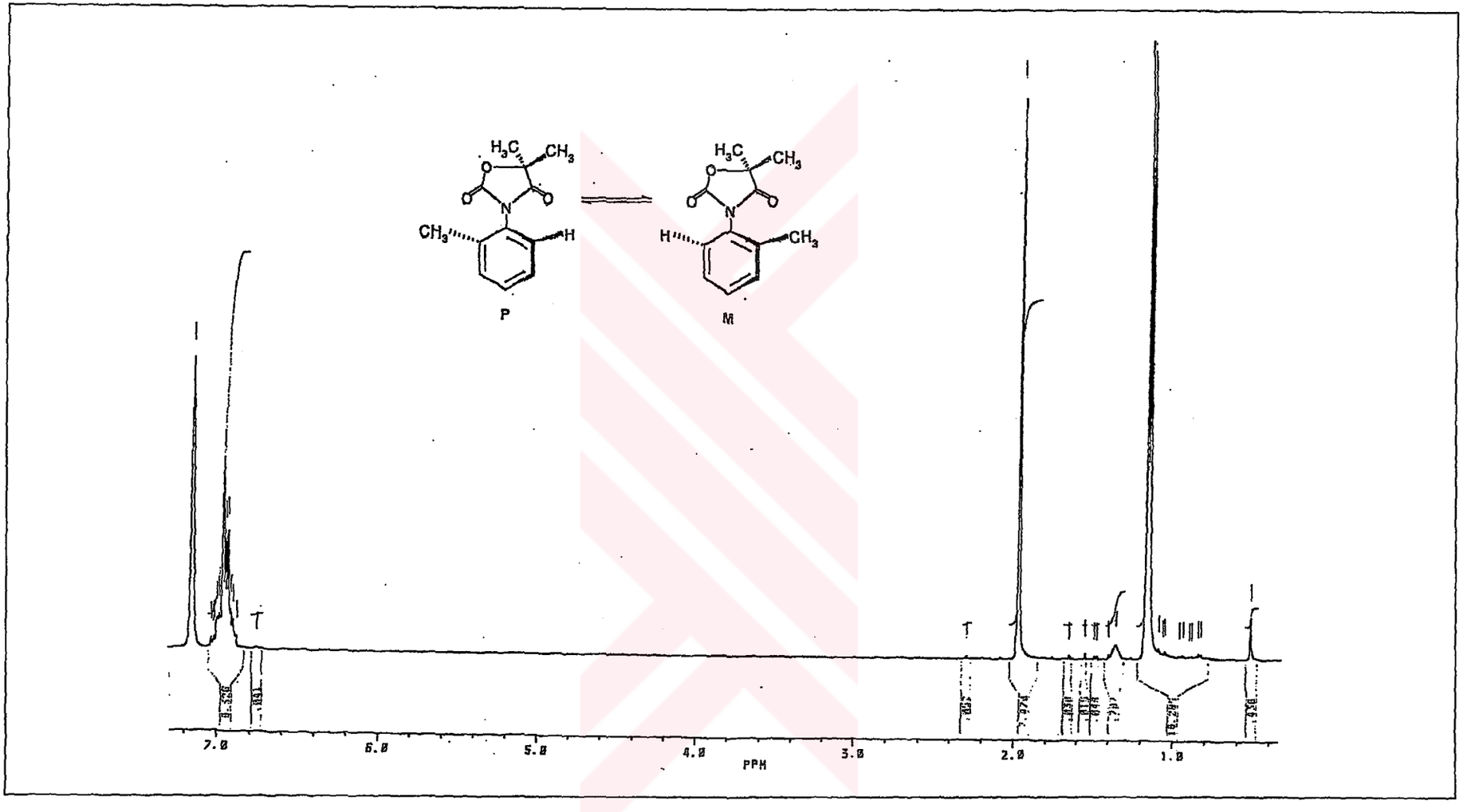

Figure 4.3. The 200 MHz ^{1}H NMR spectrum of compound **2** in deutorobenzene

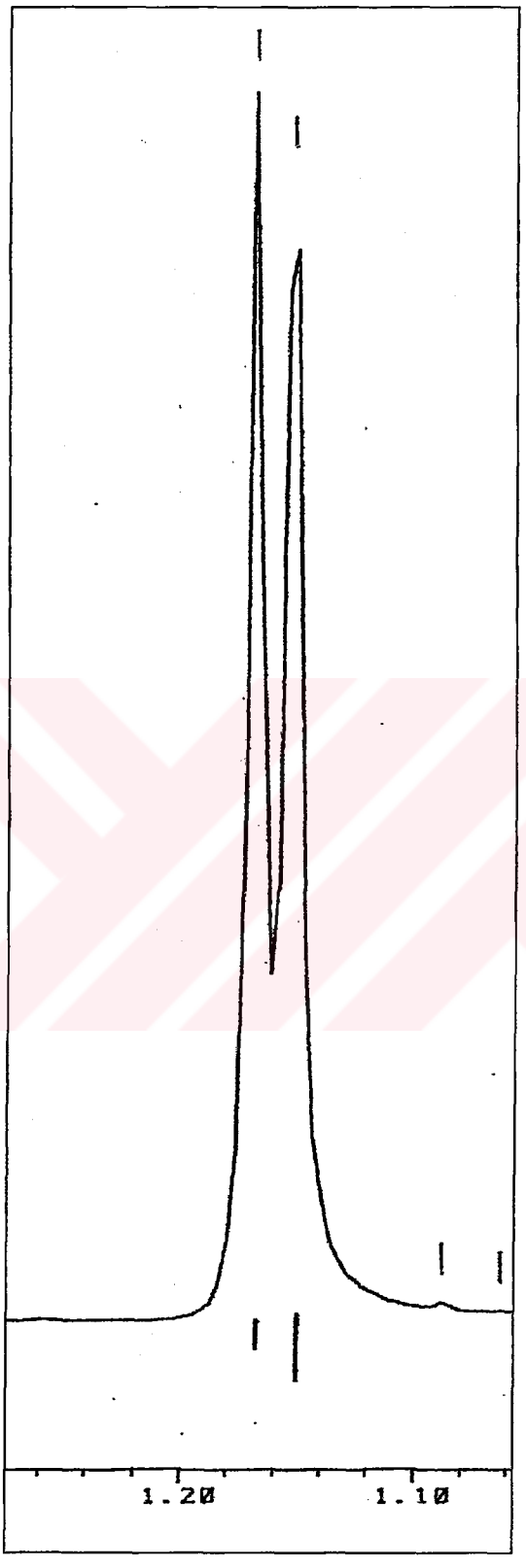

Figure 4.4. The two methyl singlets of 5,5-dimethyl-3-(*o*-tolyl)-2,4-oxazolidinedione (**2**).
The full spectrum is shown in Figure 4.3

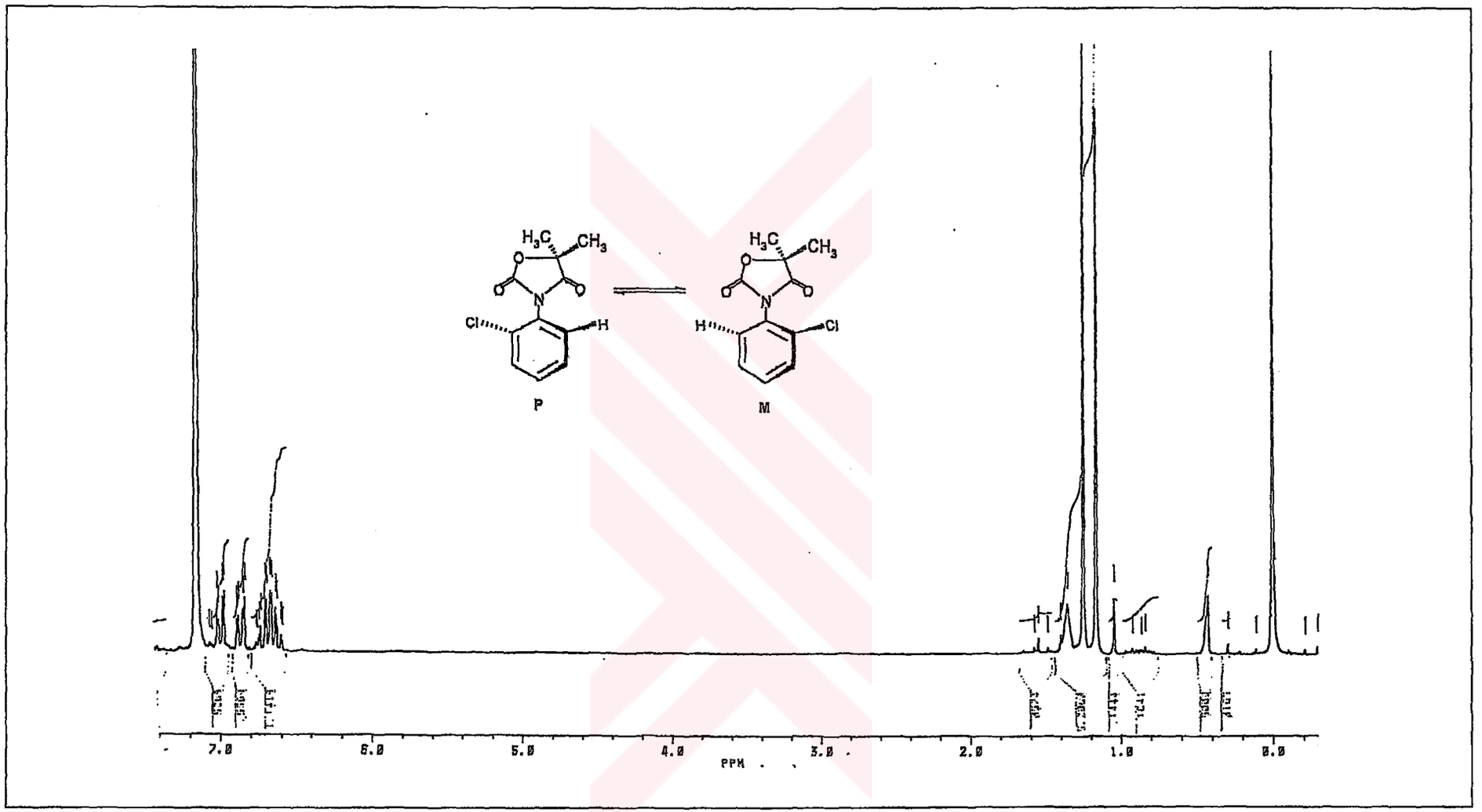

Figure 4.5. The 200 MHz ^{1}H NMR spectrum of compound **4** in deutorobenzene

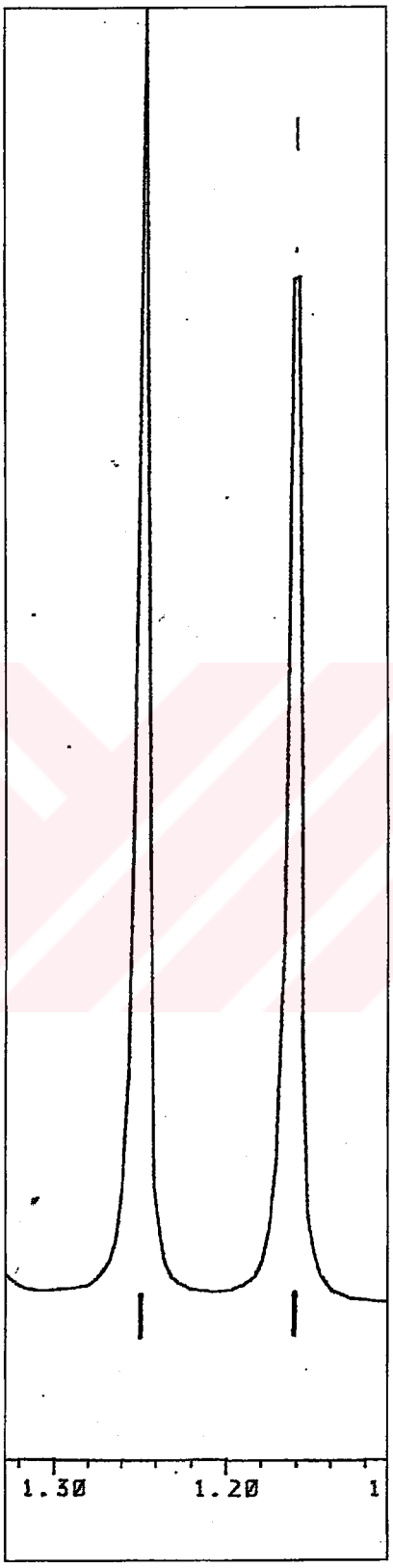

Figure 4.6. The two methyl singlets of 5,5-dimethyl-3-(*o*-chlorophenyl)-2,4-oxazolidinedione (**4**). The full spectrum is shown in Figure 4.5

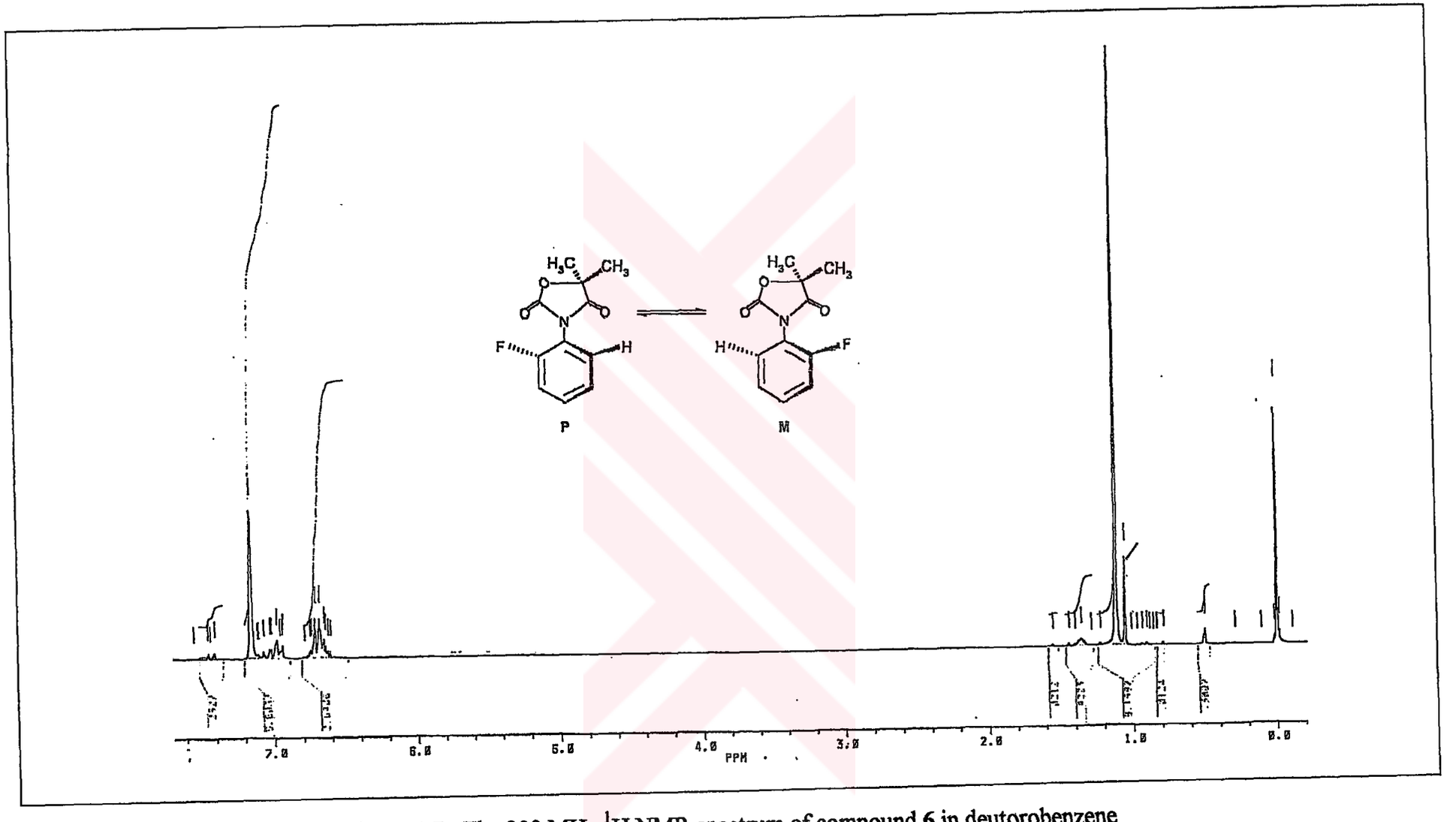

Figure 4.7. The 200 MHz ^{1}H NMR spectrum of compound **6** in deutorobenzene

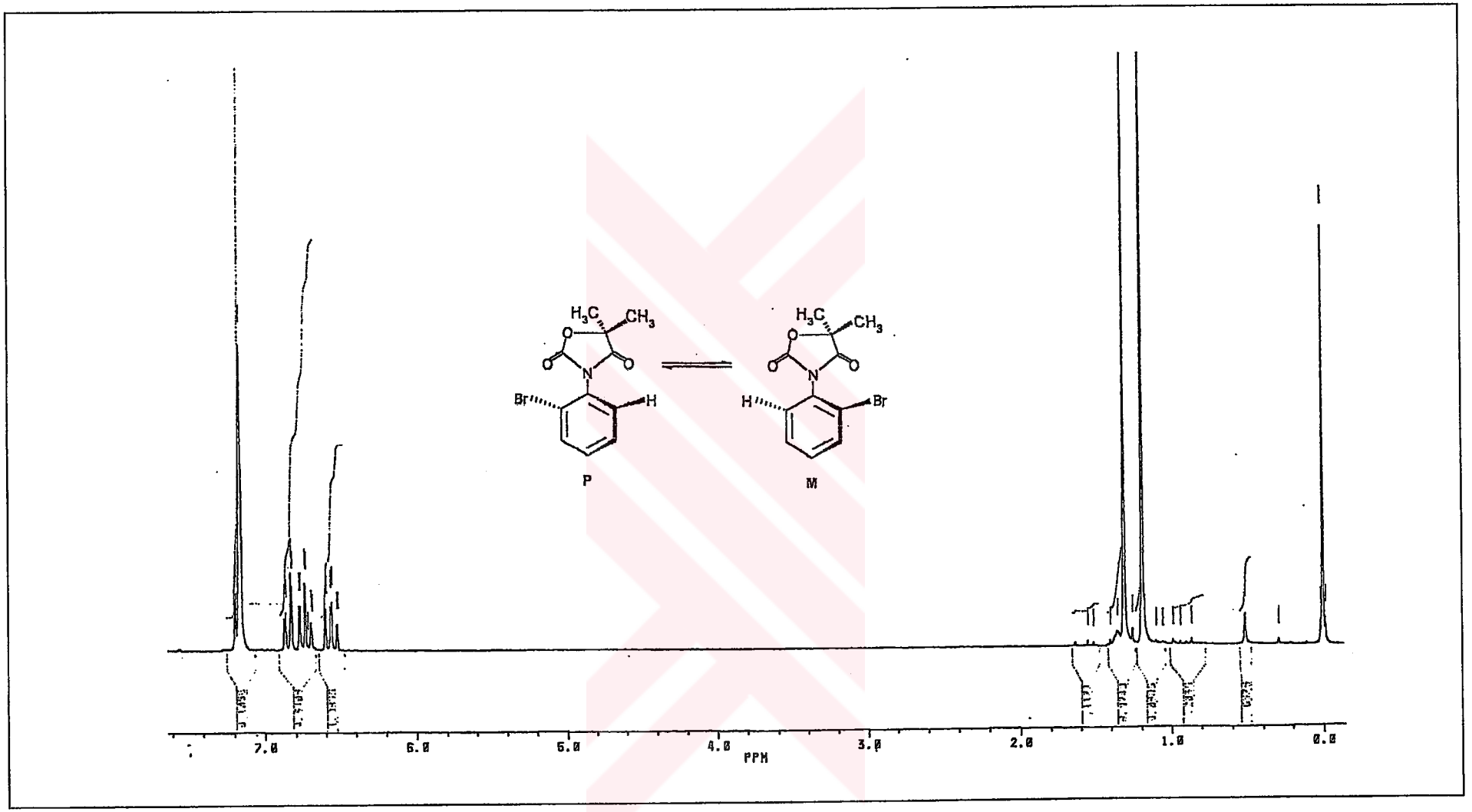

Figure 4.8. The 200 MHz ^{1}H NMR spectrum of compound **8** in deutorobenzene

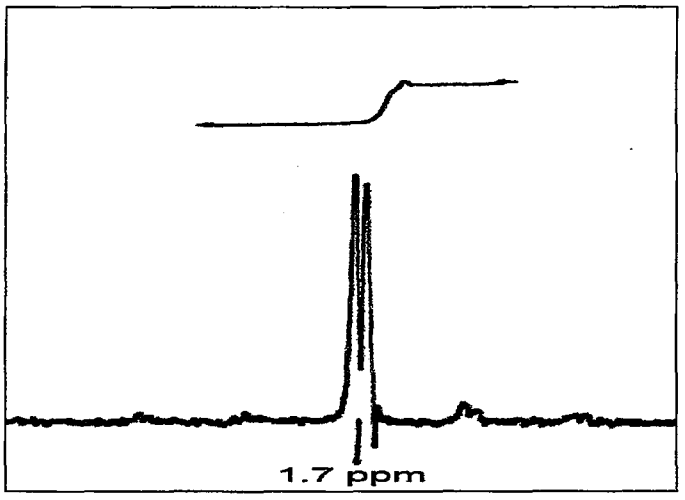

(a)

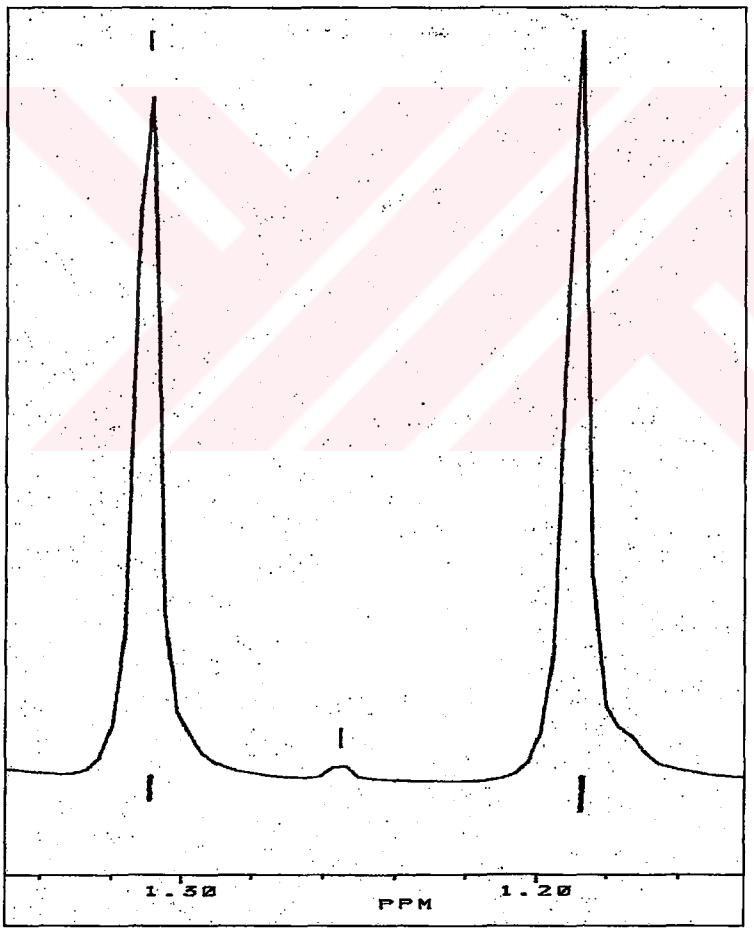

(b)

Figure 4.9. The two ^{1}H NMR methyl singlets of 5,5-dimethyl-3-(*o*-bromophenyl)-2,4-oxazolidinedione (**8**) (a) at 60 MHz, (b) at 200 MHz.

The full spectrum is shown in Figure 4.8

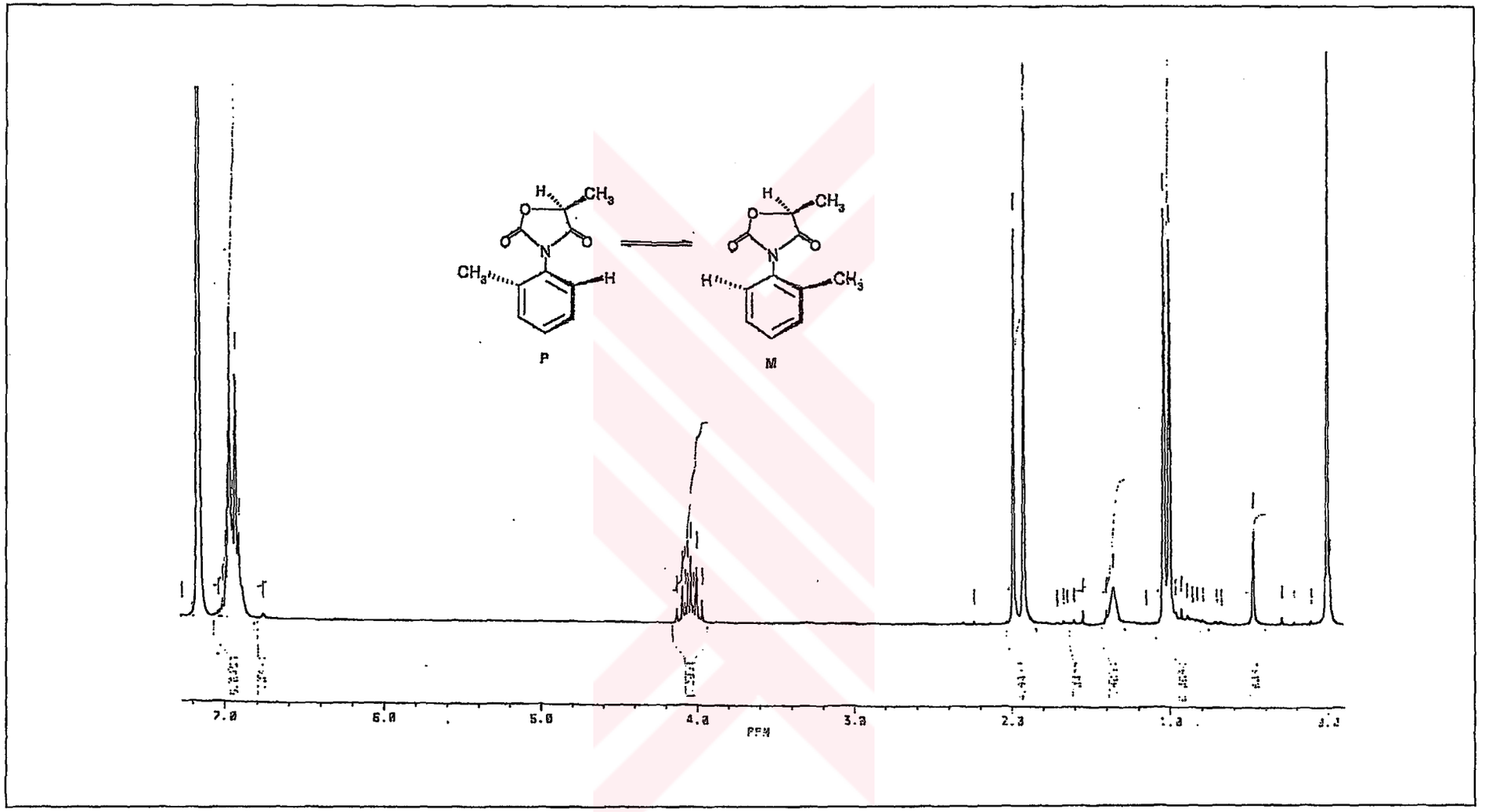

Figure 4.10. The 200 MHz ^{1}H NMR spectrum of compound **1S** in deutorobenzene

Figure 4.11. The two doublets of 5-methyl-3-(*o*-tolyl)-2,4-oxazolidinedione (**1S**). The full spectrum is shown in Figure 4.10

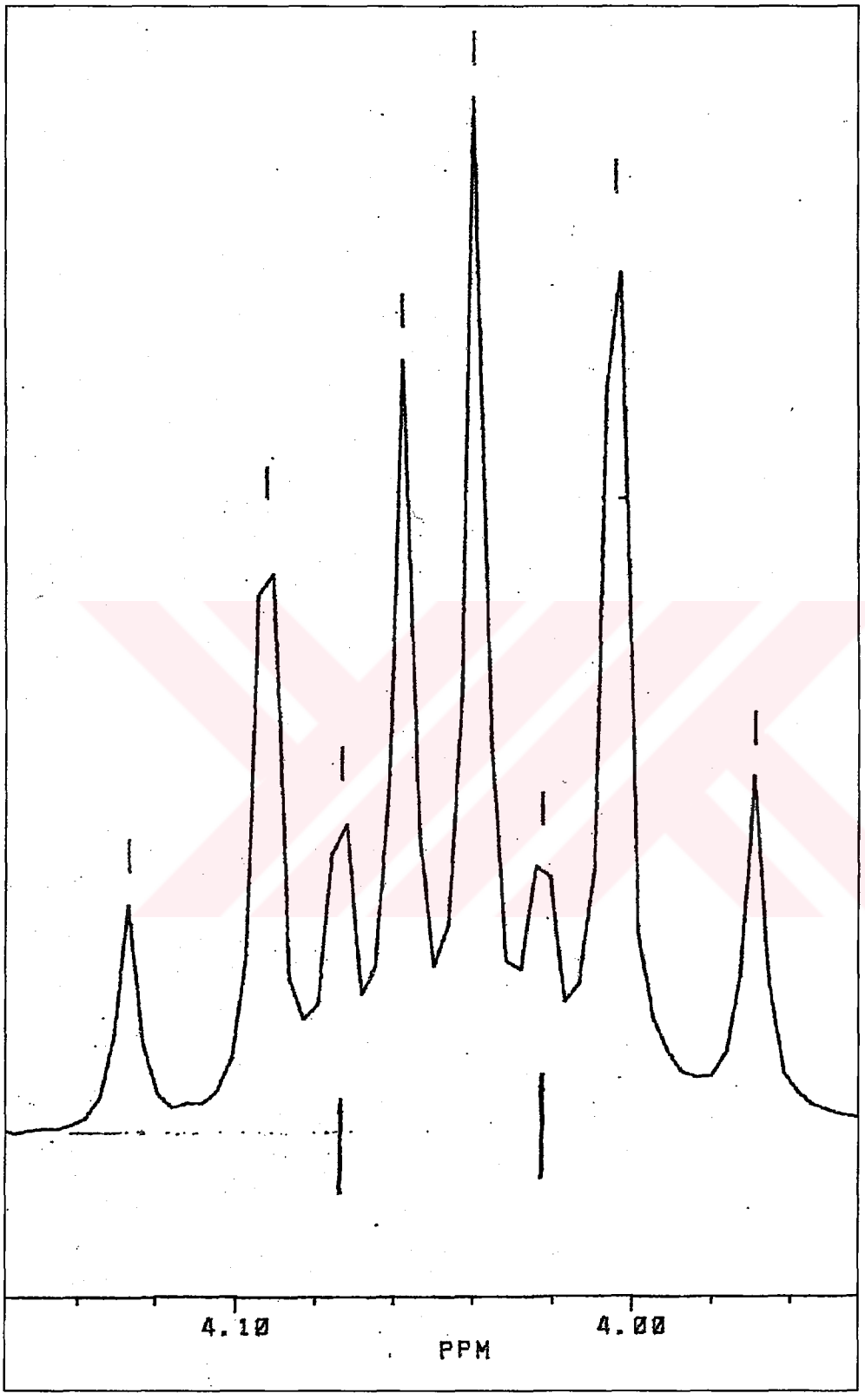

Figure 4.12. The two quartets of 5-methyl-3-(*o*-tolyl)-2,4-oxazolidinedione (**1S**). The full spectrum is shown in Figure 4.10

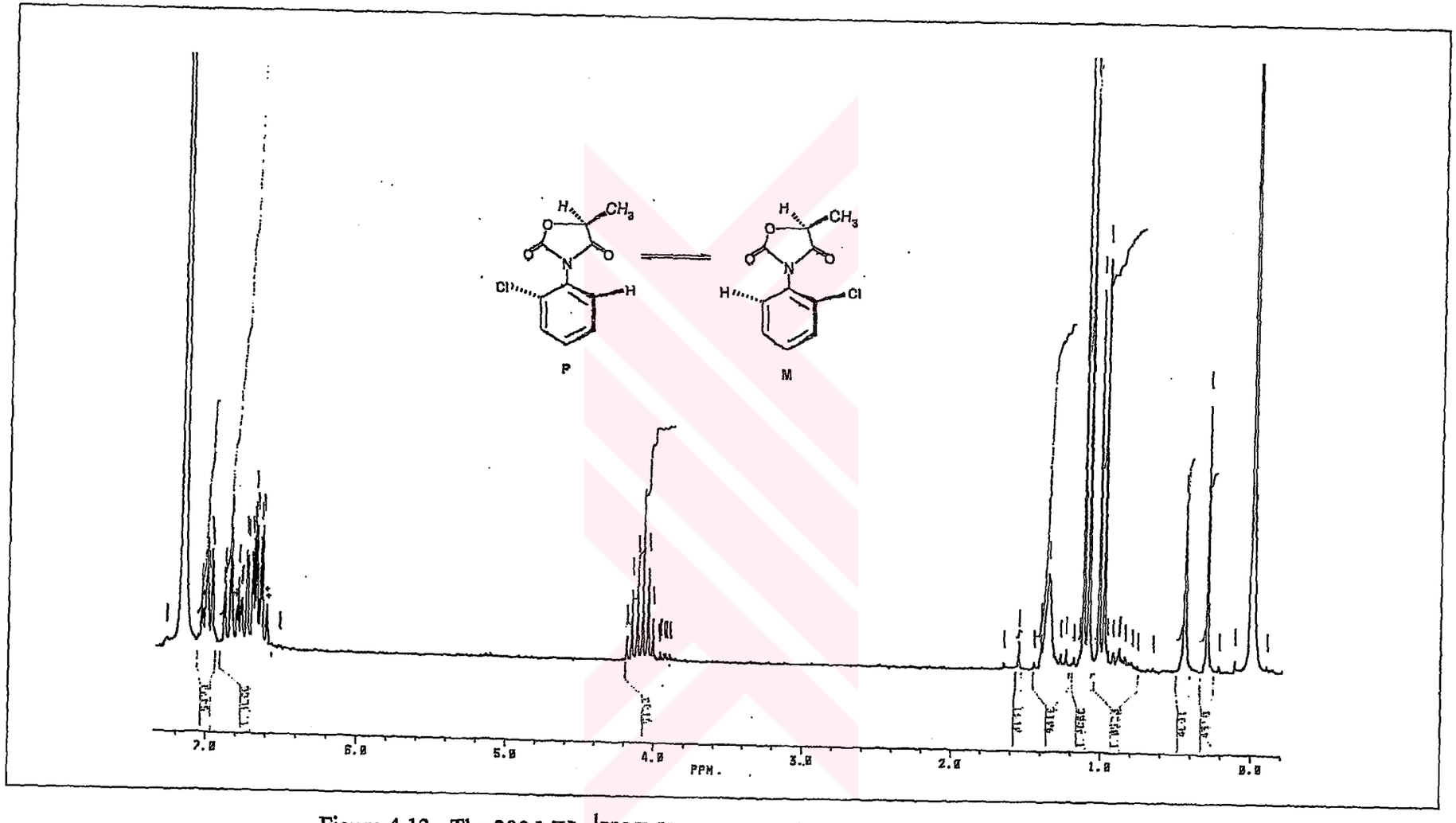

Figure 4.13. The 200 MHz ^{1}H NMR spectrum of compound **3S** in deutorobenzene

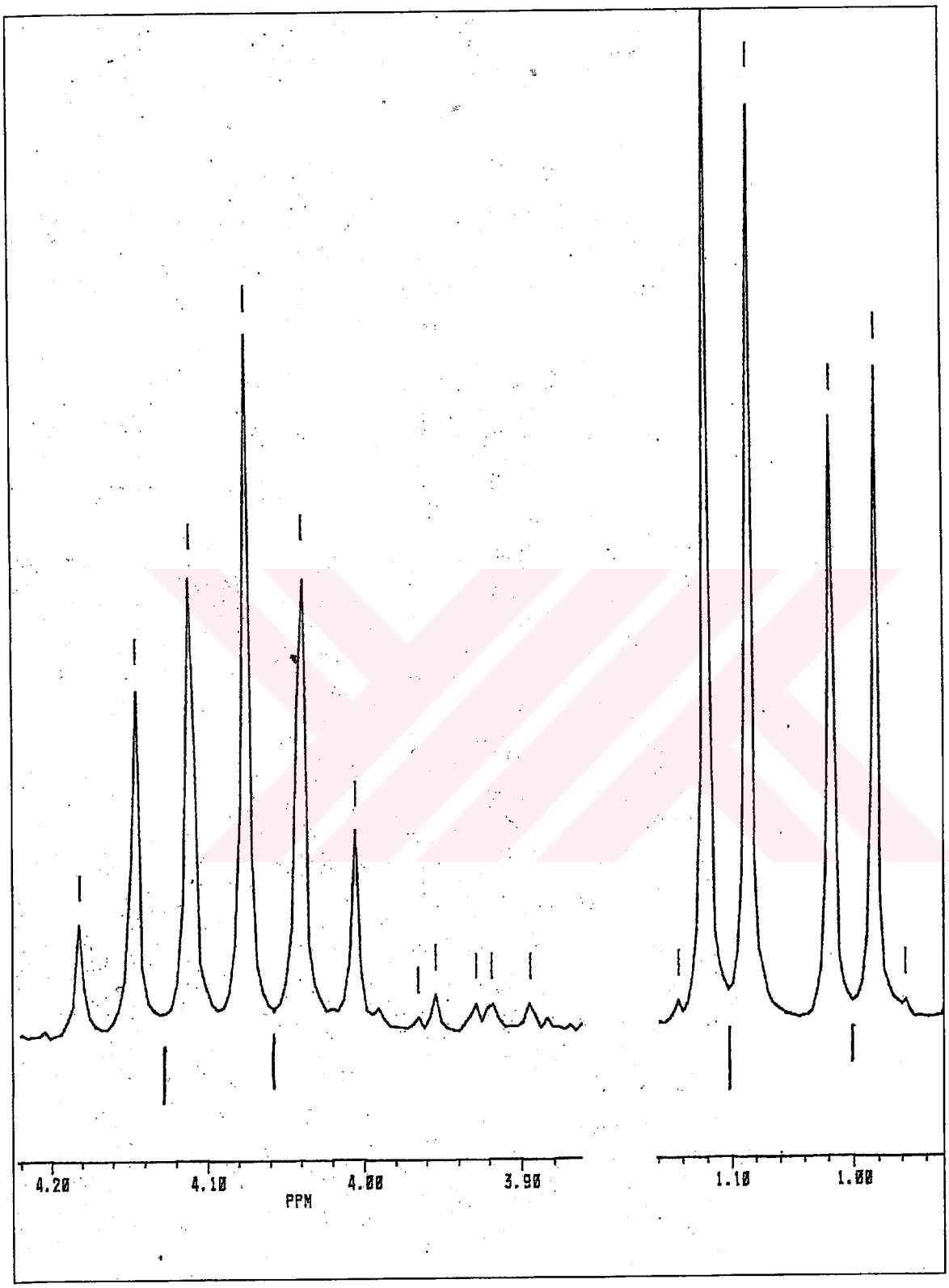

Figure 4.14. The two doublets and quartets of 5-methyl-3-(*o*-chlorophenyl)-2,4-oxazolidinedione (**3S**). The full spectrum is shown in Figure 4.13

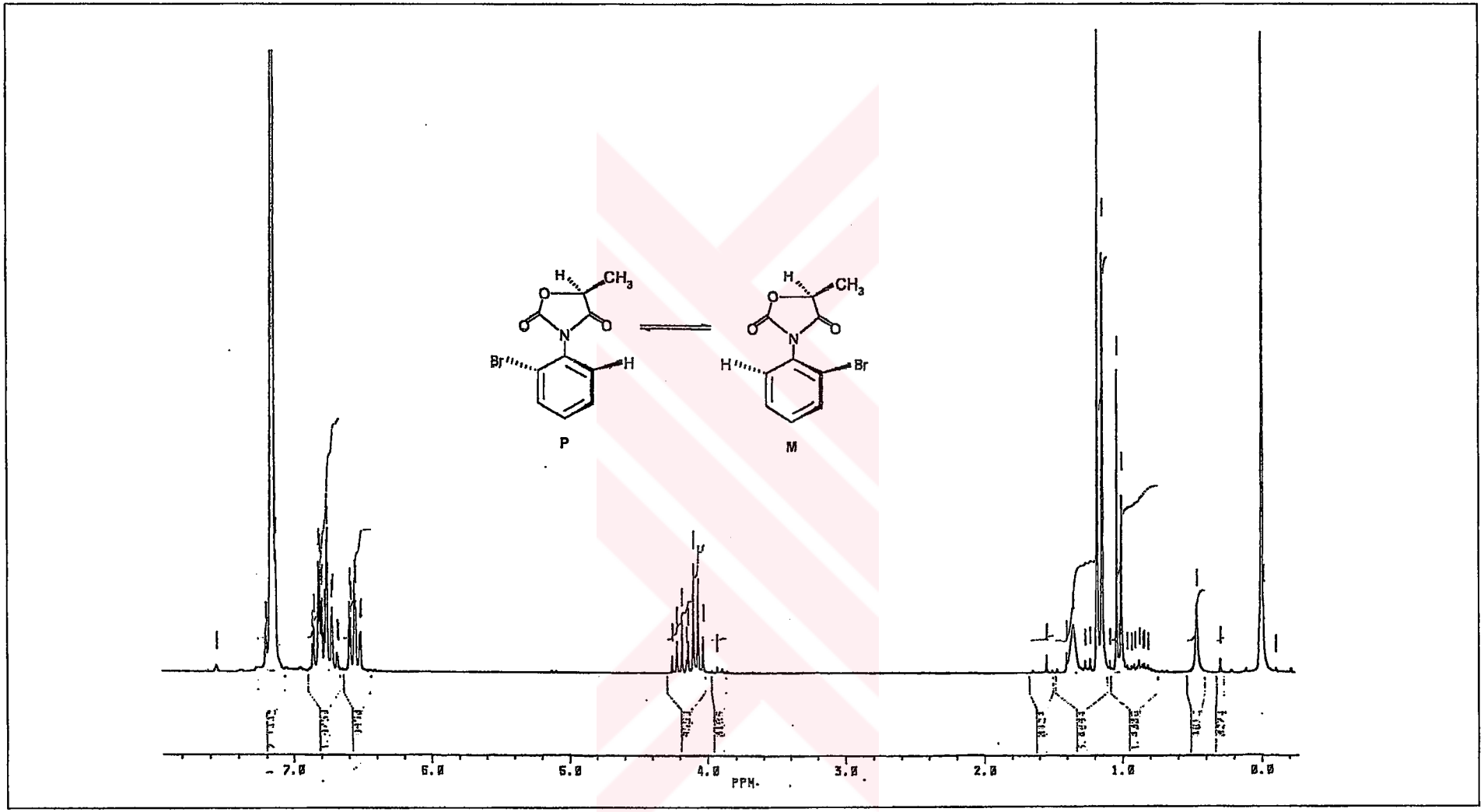

Figure 4.15. The 200 MHz ^{1}H NMR spectrum of compound **7S** in deutorobenzene

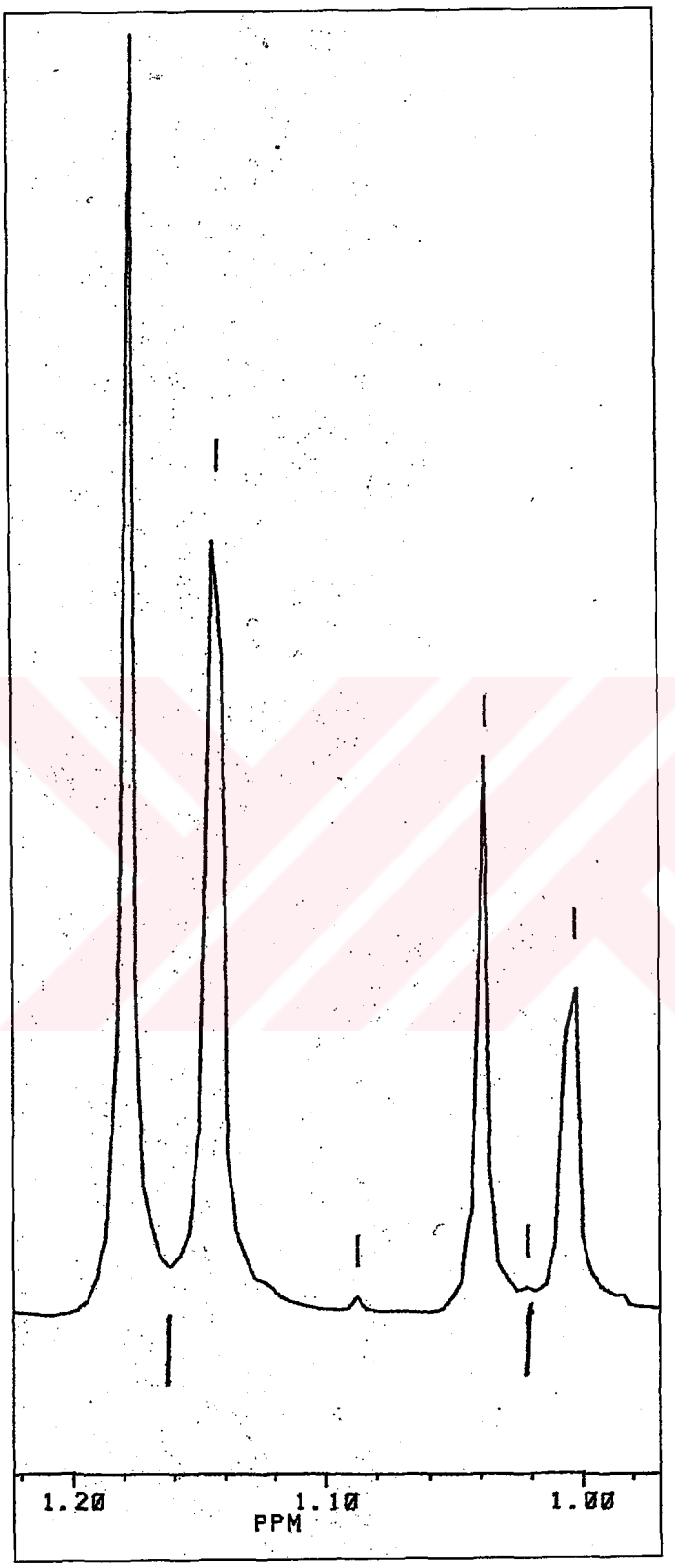

Figure 4.16. The two doublets of 5-methyl-3-(*o*-bromophenyl)-2,4-oxazolidinedione (**7S**).

The full spectrum is shown in Figure 4.15

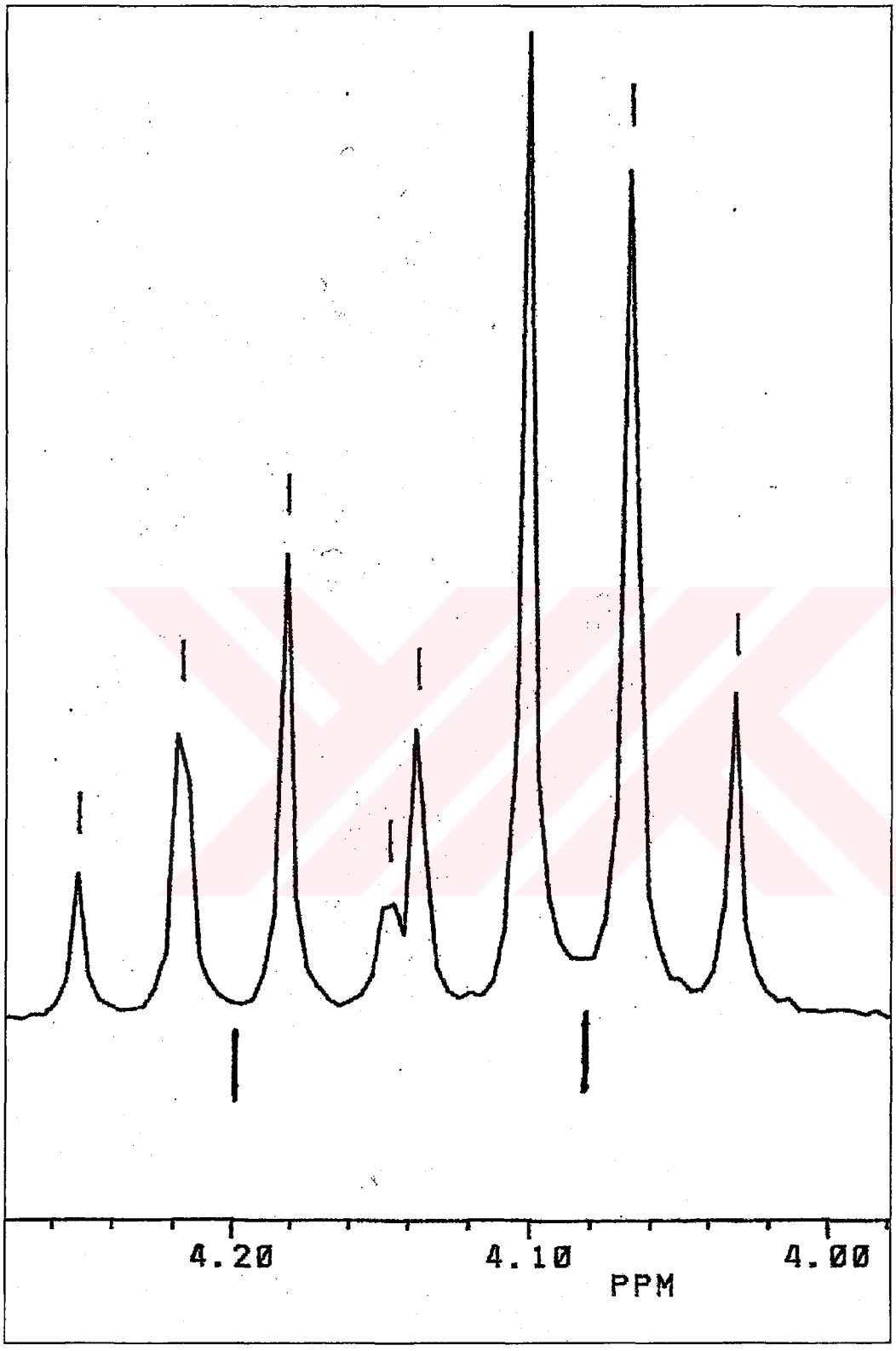

Figure 4.17. The two quartets of 5-methyl-3-(*o*-bromophenyl)-2,4-oxazolidinedione (**7S**).

The full spectrum is shown in Figure 4.15

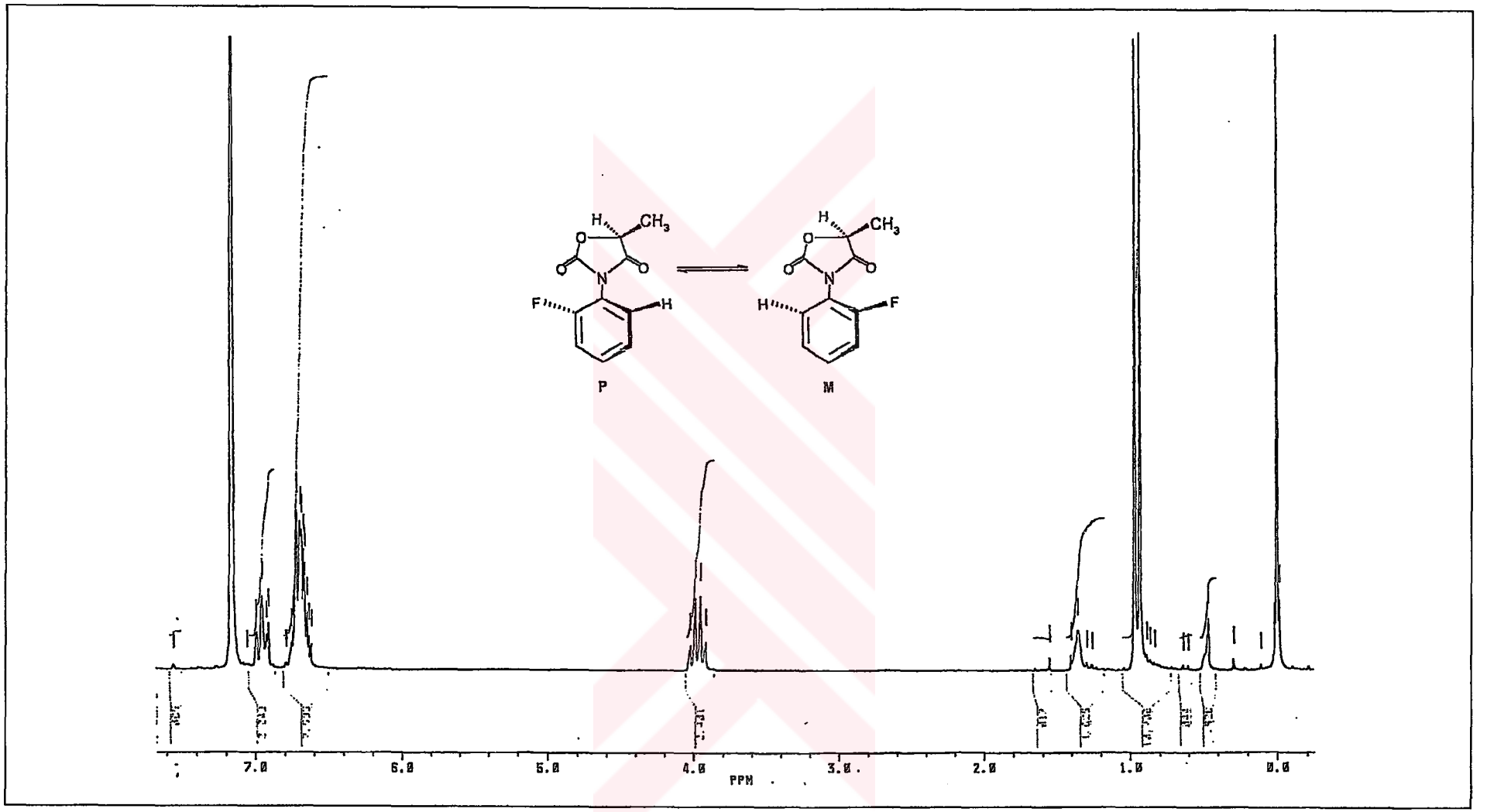

Figure 4.18. The 200 MHz ^{1}H NMR spectrum of compound **5S** in deutorobenzene

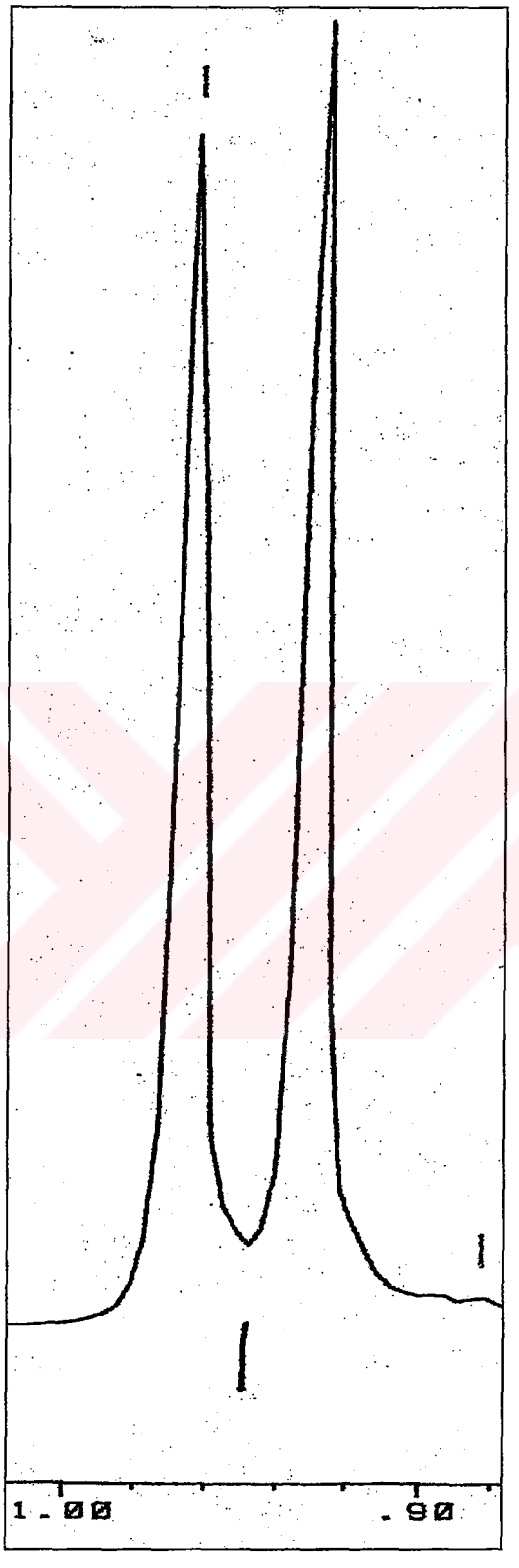

Figure 4.19. The doublet of 5-methyl-3-(*o*-fluorophenyl)-2,4-oxazolidinedione (**5S**).

The full spectrum is shown in Figure 4.18

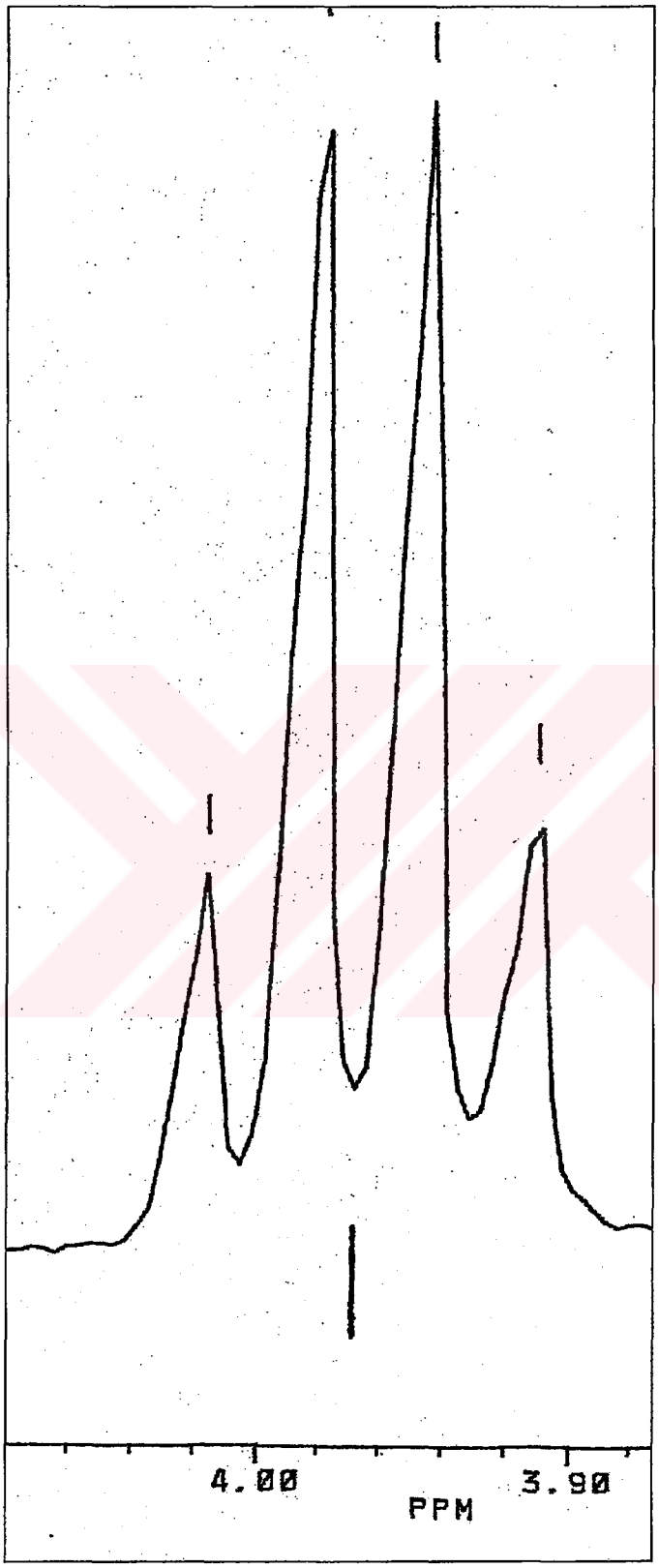

Figure 4.20. The quartet of 5-methyl-3-(*o*-fluorophenyl)-2,4-oxazolidinedione (**5S**).
The full spectrum is shown in Figure 4.18

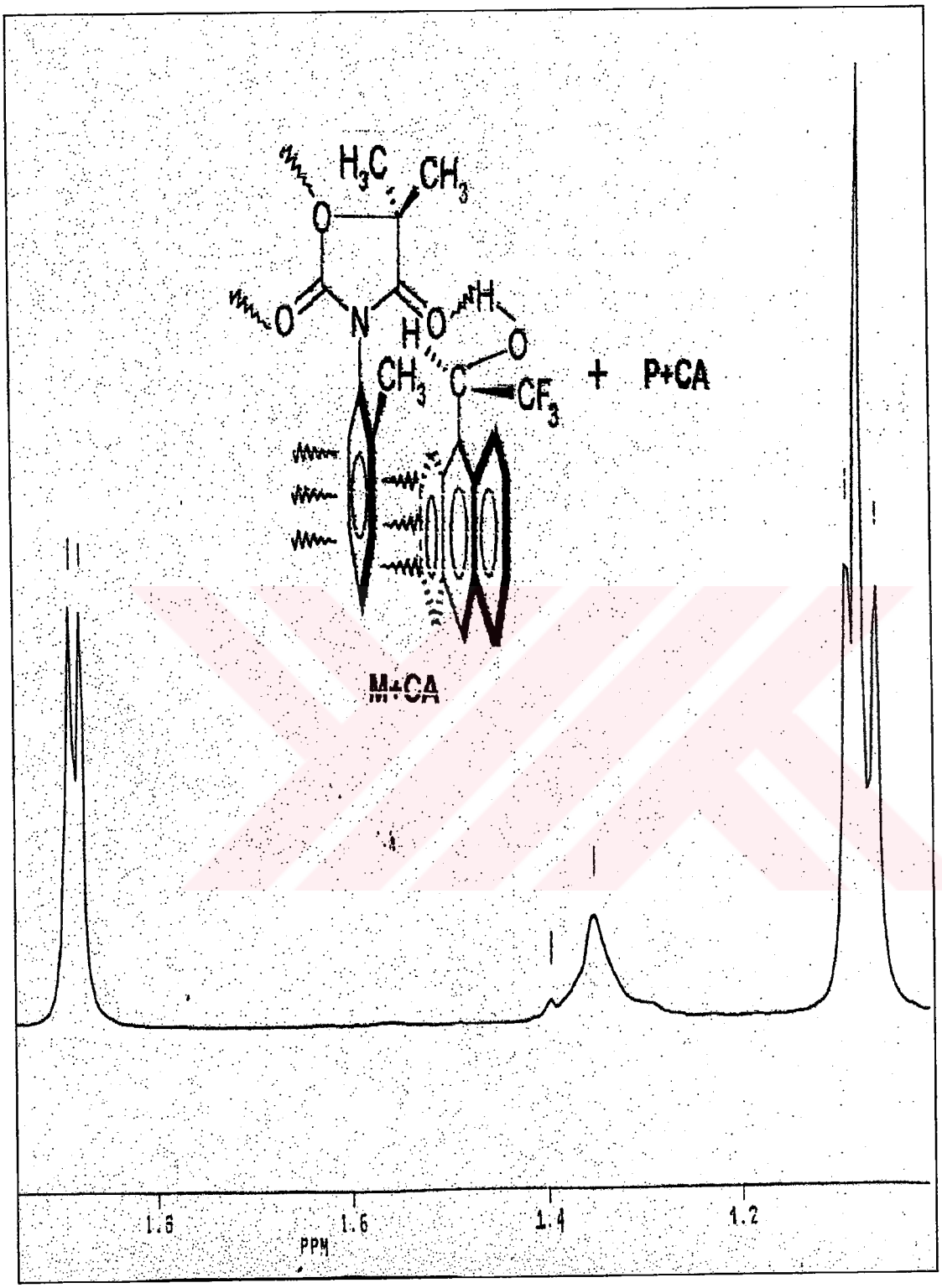

Figure 4.21. The 200 MHz ^{1}H NMR spectrum of the compound **2** taken in C_6D_6 in the presence of eight equivalents of (S)-(+)-TFAE

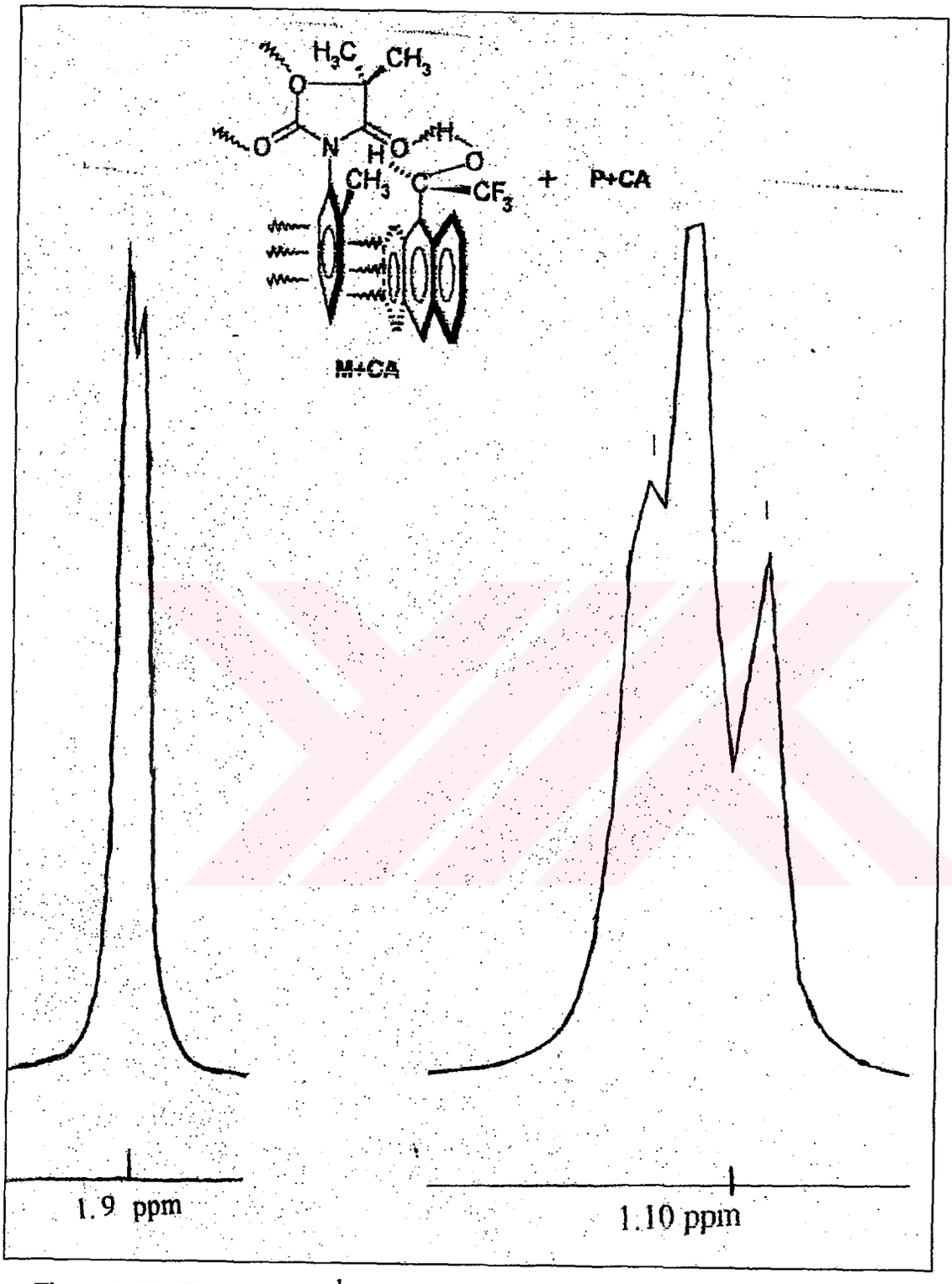

Figure 4.22. The 200 MHz ^{1}H NMR spectrum of the compound **2** taken in C_6D_6 in the presence of six equivalents of (S)-(+)-TFAE

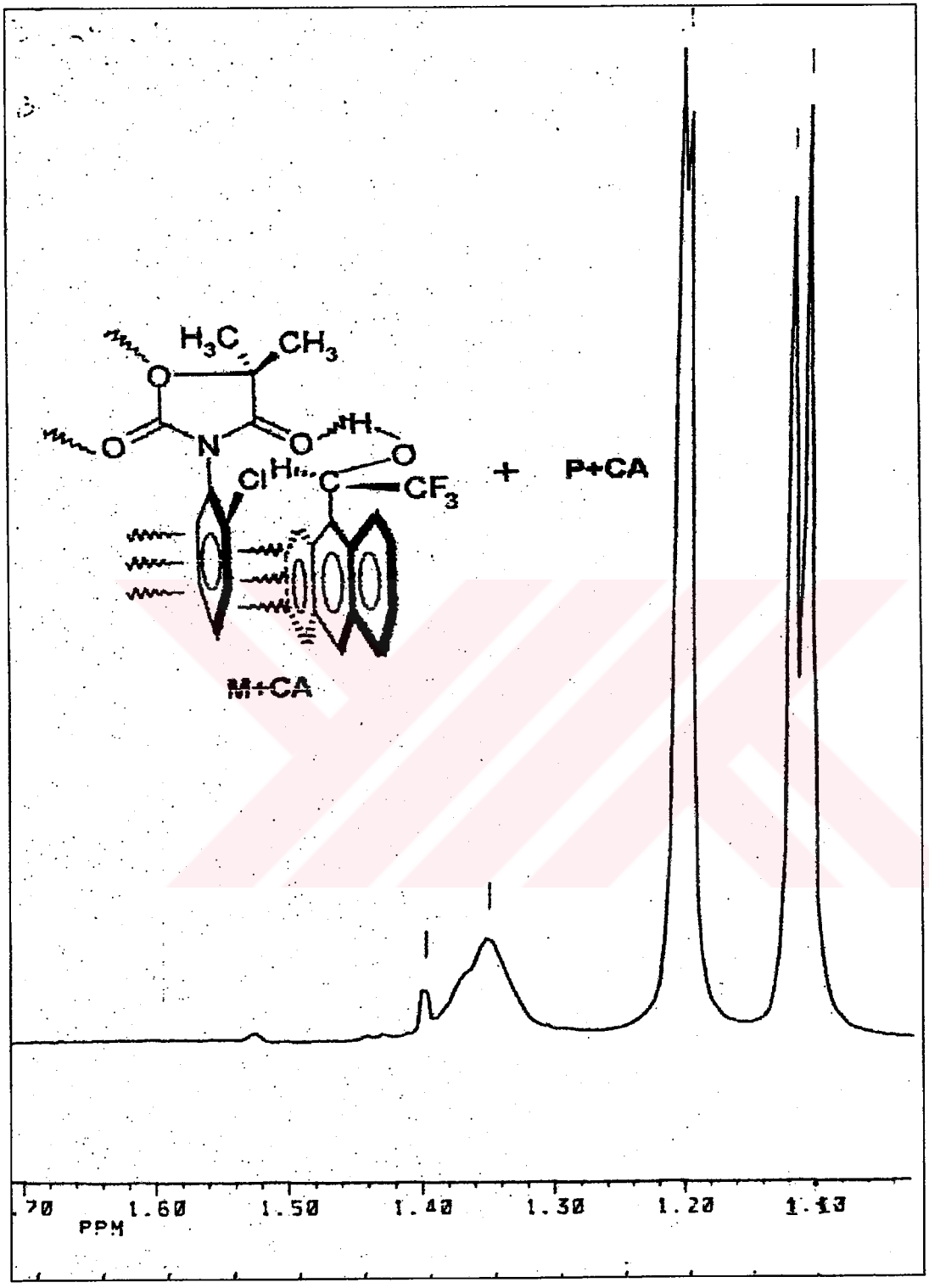

Figure 4.23. The 200 MHz ^{1}H NMR spectrum of the compound **4** taken in C_6D_6 in the presence of six equivalents of (S)-(+)-TFAE

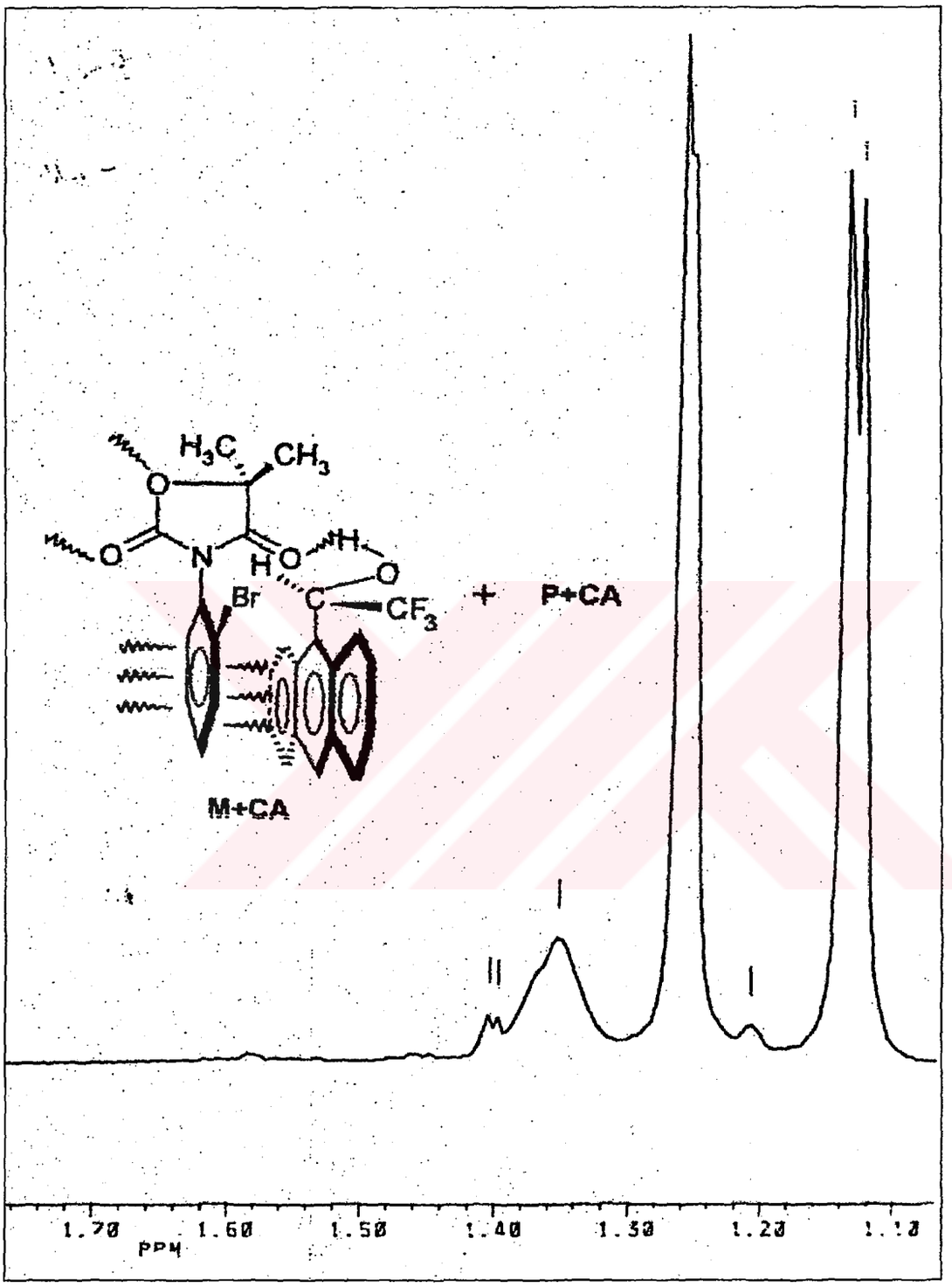

Figure 4.24. The 200 MHz ^{1}H NMR spectrum of the compound **8** taken in C_6D_6 in the presence of six equivalents of (S)-(+)-TFAE

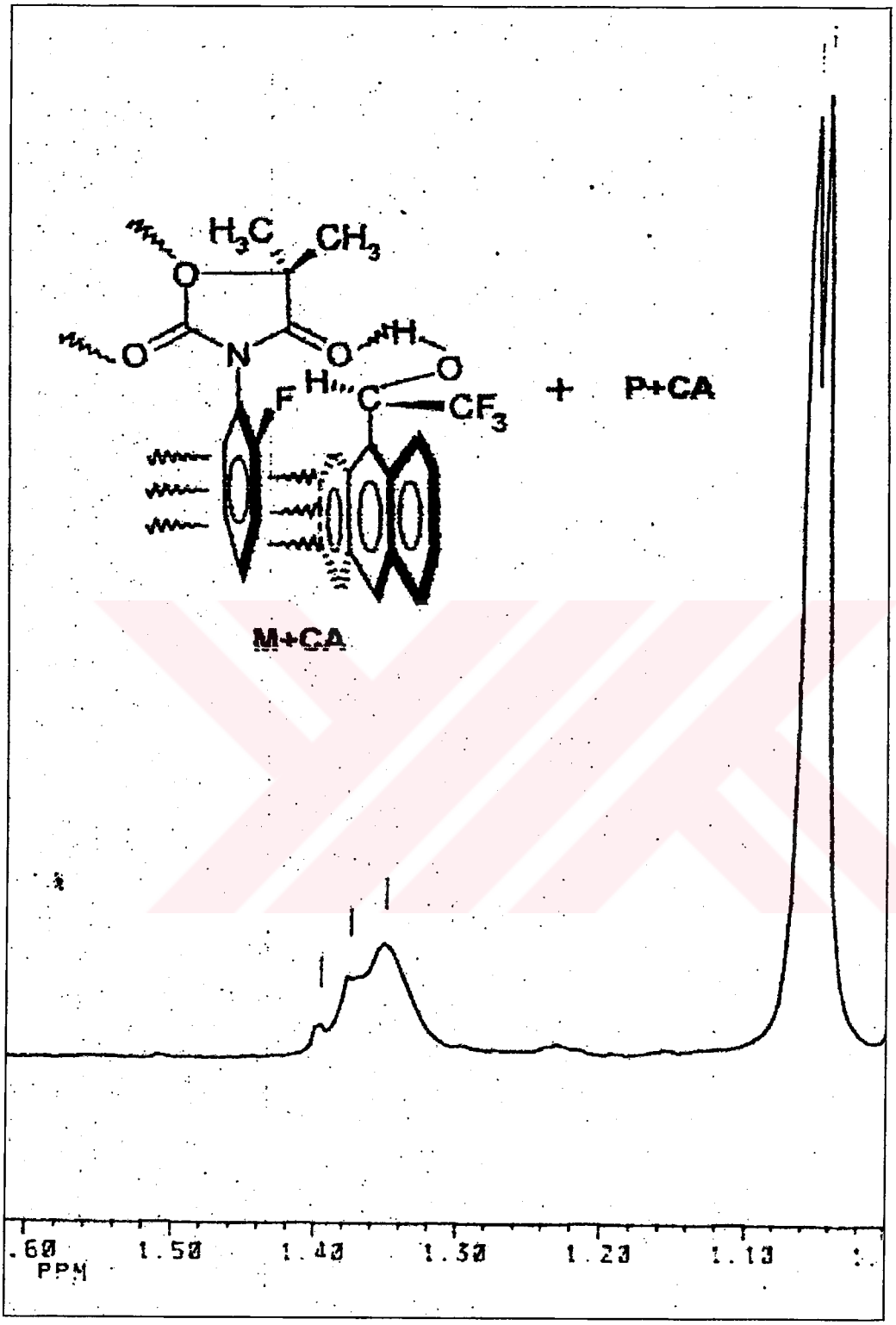

Figure 4.25. The 200 MHz ^{1}H NMR spectrum of the compound **6** taken in C_6D_6 in the presence of six equivalents of (S)-(+)-TFAE

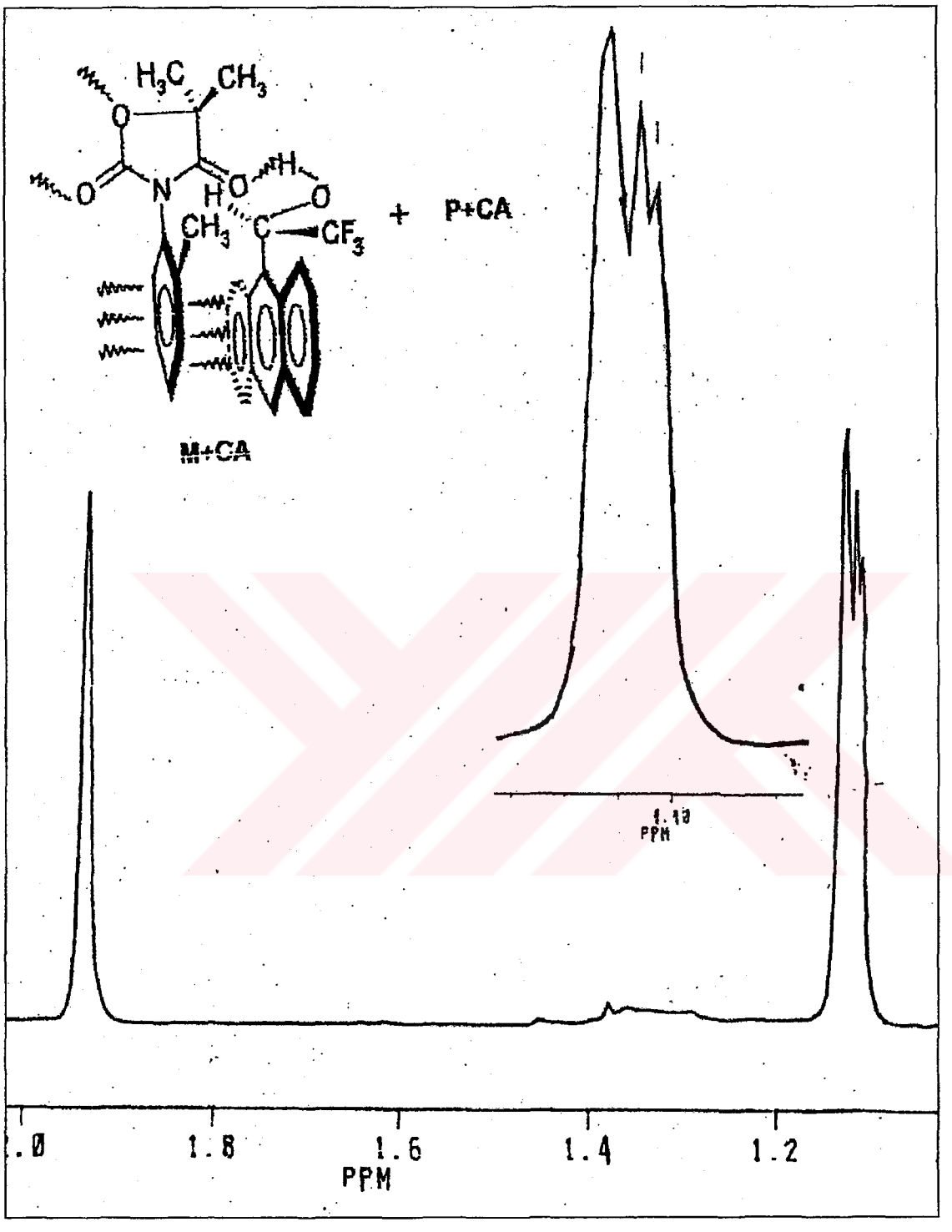

Figure 4.26. The 200 MHz ^{1}H NMR spectrum of compound **2** (with an expansion of the signal at 1.1 ppm) in the presence of six equivalents of the CA after keeping the solution at room temperature for three weeks

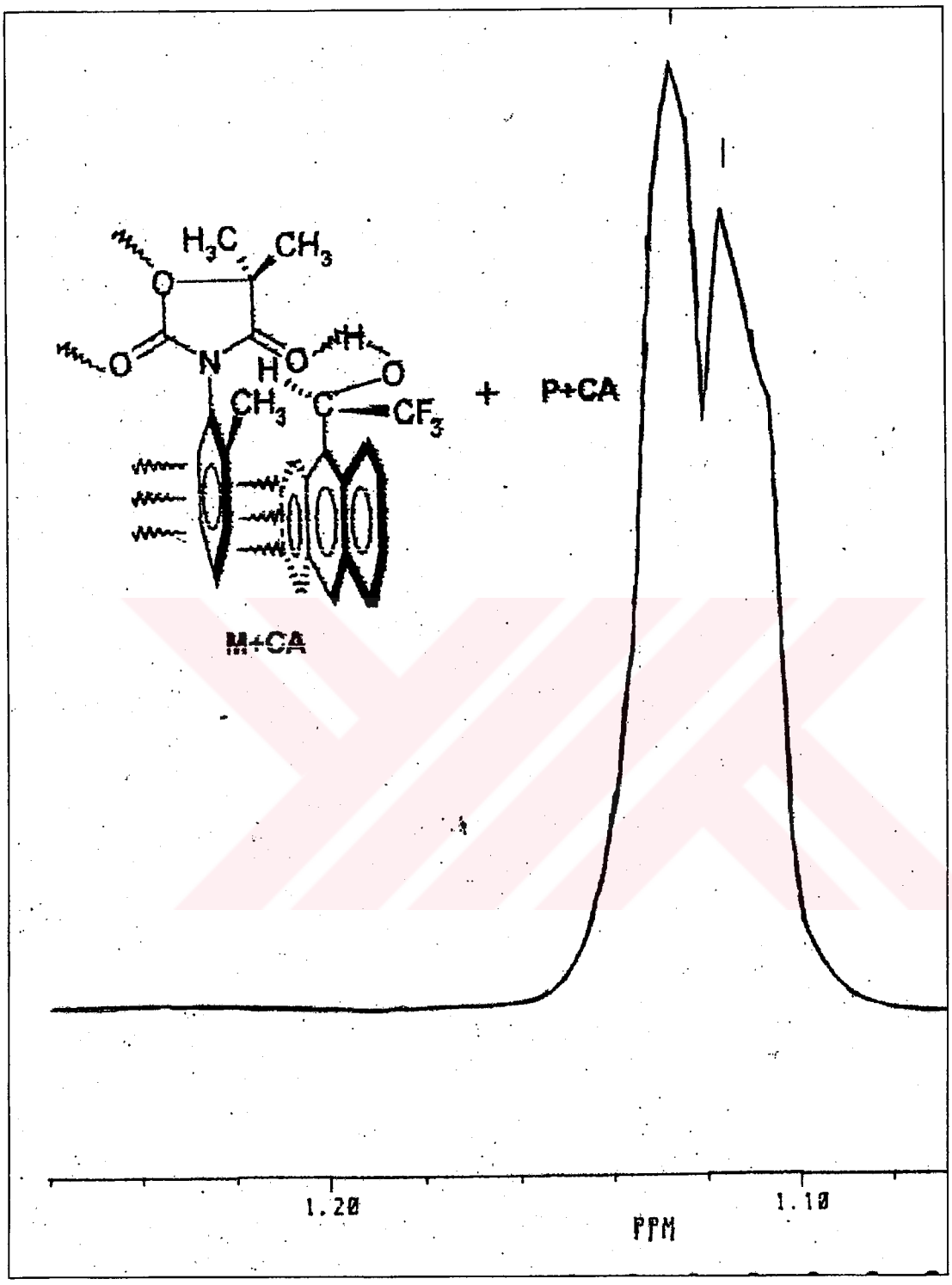

Figure 4.27. The expansion of the signal at 1.1 ppm of compound **2** in the presence of six equivalents of the CA after keeping the solution at 35 °C for 7.5 hours

4.3. Determination of Activation Barriers for Hindered Rotation by Dynamic NMR

Activation barriers to hindered internal rotation about the C-N single bond were determined by complete line shape analysis of the signals for the diastereotopic 5-methyl protons in compound **2** and **4** as a function of temperature. From the temperature-dependent behavior of the ^1H resonances, it was observed that at room temperature (22 °C), the two methyl groups were differently shielded, whereas at some higher temperatures, they became equivalent. The reason was that the rotation around C-N single bond was slow at 22 °C, therefore the methyl groups on the C-5 were in different magnetic environments (Figures 4.28 and 4.29). When the temperature was raised to overcome the barrier to rotation, they were no longer be distinguished by NMR spectroscopy. Then, only one signal was observed in the spectrum at higher tempeartures (Figures 4.28 and 4.29).

4.3.1. The Calculation of Activation Barrier for Compound 2

From the ^1H NMR spectrum of compound **2** (Figure 4.3), the separation in Hertz between the signals at slow rotation at 22 °C ($\Delta\nu$) was measured as 3.111 Hz (for 200 MHz instrument). The coalesence temperature was measured as 48 °C (321 K) from the temperature-dependent ^1H NMR spectrum (Figure 4.28). By using Eyring equation, the barrier to rotation was found as 75.78 kJ/mol. The calculations are as follows:

The rate constant at coalesence temperature, Tc:

$k_c = 2.22\ \Delta\nu$

$k_c = 2.22(3.111\ Hz) = 6.91\ s^{-1}$

Therefore, ΔG_{321}:

$\Delta G_{321} = 19.14\ Tc\ (10.32 + \log Tc/k_c)$

$\Delta G_{321} = 19.14\ (321)\ (10.32 + \log 321/6.91)$

$\Delta G_{321} = 75.776\ j/mol = 75.78\ kJ/mol$

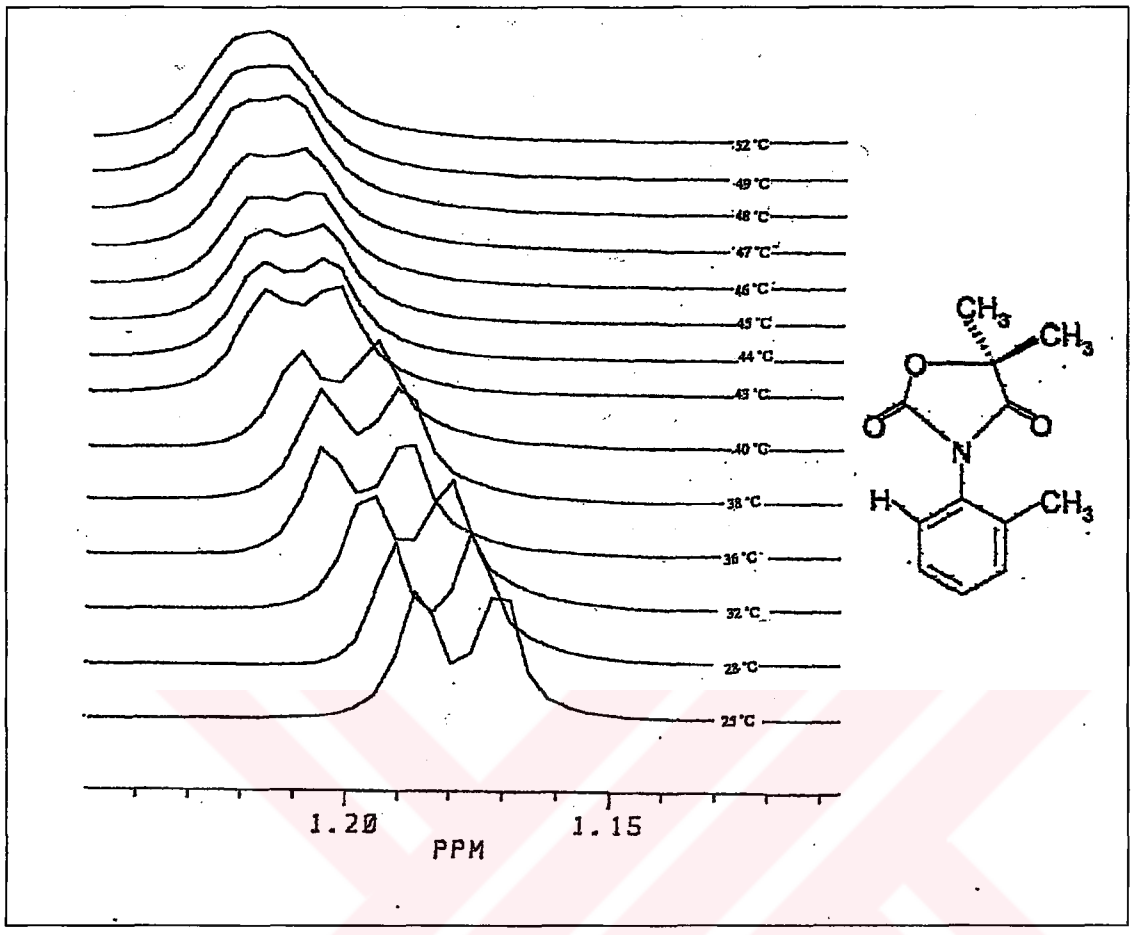

Figure 4.28. The temperature-dependent 200 MHz ^{1}H NMR spectrum of compound **2**

4.3.2. The Calculation of the Activation Barrier for Compound 4

For 5,5-dimethyl-3-(*o*-chlorophenyl)-2,4-oxazolidinedione (compound **4**) (Figure 4.5), the separation in Hertz between the signals in the absence of rapid rotation ($\Delta\nu$) was found as 10.349 Hz (for 200 MHz instrument). The coalesence temperature was measured as 104 °C (377 K) from the temperature-dependent ^{1}H NMR spectrum (Figure 4.29). By using the Eyring equation, the barrier to rotation was found as 83.24 kJ/mol.

The two values of activation barriers for compound **2**, 5,5-dimethyl-3-(*o*-tolyl)-2,4-oxazolidinedione, and compound **4**, 5,5-dimethyl-3-(*o*-chlorophenyl)-2,4-oxazolidinedione showed that the rotation around the C-N bond was slow enough to enable the detection of the rotational isomers by NMR. However, the barrier to rotation was not enough to make them separable at room temperature. The barrier was found to be higher for the *o*-chloro derivative than the *o*-methyl derivative. The greater steric requirement for the chlorine

atom is attributed to the presence of lone pair electrons that interacted with that of the carbonyl oxygen.

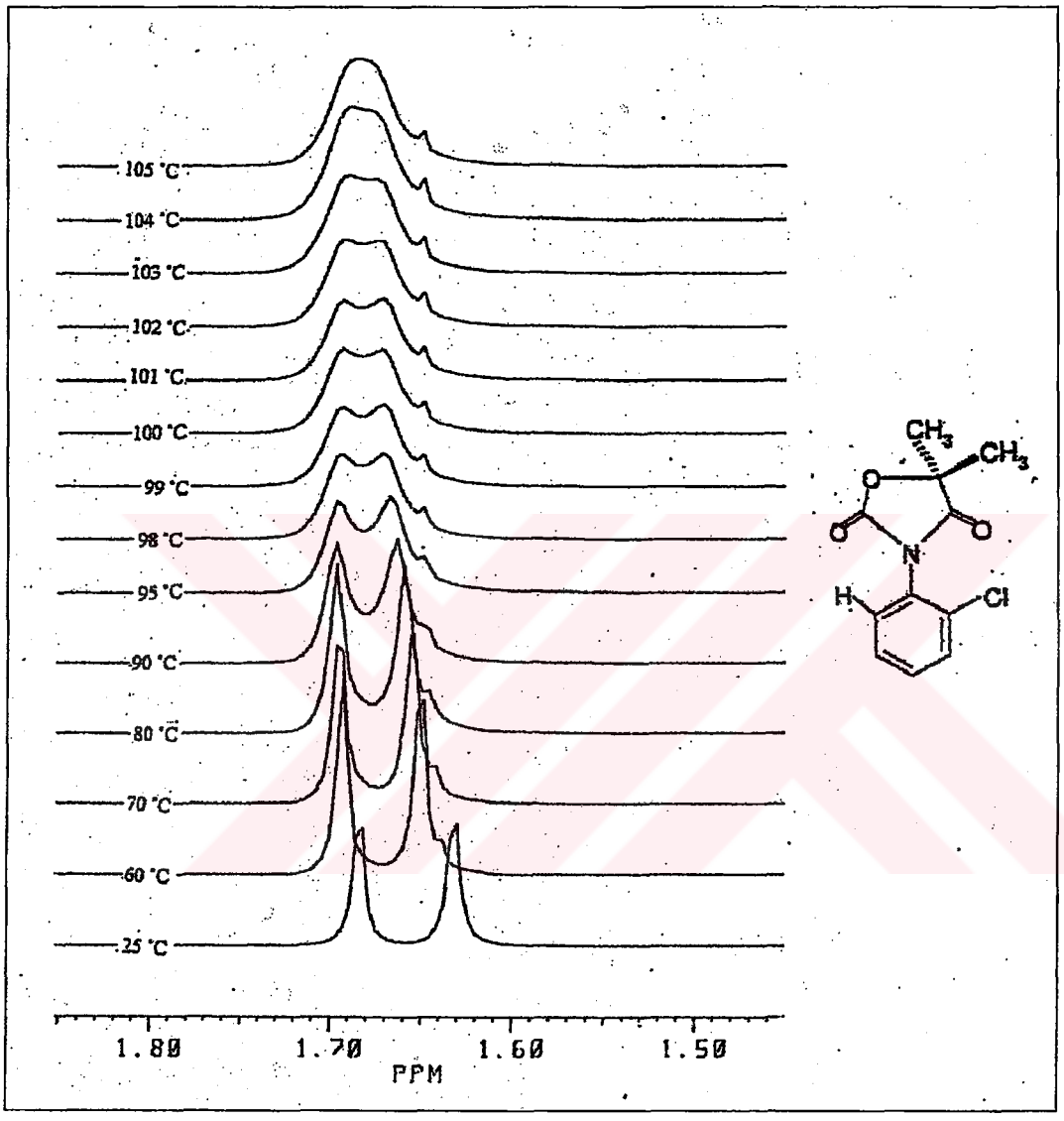

Figure 4.29. The temperature-dependent ^{1}H NMR spectrum of compound **4**

4.4. The Conformational Stability of Diastereomeric 2,4-Oxazolidinedione Derivatives

Normal work-up procedures after synthesis of 5-methyl-3-(*o*-aryl)-2,4-oxazolidinediones yielded unequal isomer compositions of the two diastereomers which were differentiated in 200 MHz ^{1}H NMR spectra (Figures 4.10, 4.13, 4.15). In order to identify which conformation is produced dominantly, through-space interactions between

the *o*-substituent and the methyl group or hydrogen atom on C-5 were considered. In the case of M conformation, the chlorine or bromine atom and methyl group are on the same side (Figure 4.30). Since the chlorine and bromine atoms are large and electronegative, they can cause a deshielding effect on the protons of the methyl group by withdrawing electrons. Therefore, the methyl protons in M conformation are expected to give a doublet that is more deshielded. Since in the spectra of 7S and 3S, the intensity of the deshielded doublet was higher than the other (Figure 4.16 and Figure 4.14, respectively), the conformations of the excess isomers of the compounds 3S and 7S were assigned as M conformation. The percentages of the dominant conformation M in compound 7S and 3S were 70 per cent and 60 per cent, respectively. In compound 1S, however, where the *ortho* substituent is methyl, an opposite electronic effect is expected, causing the P conformation (Figure 4.30) to have a more deshielded doublet for the 5-methyl protons than that of the M conformation. Based on this argument, the higher intensity doublet which appeared more deshielded has been assigned to conformation P, and the lower intensity doublet (which appeared more upfield) to conformation M. The ratio of the two diastereomers 1SP: 1SM was determined from the integral ratios as 57:43.

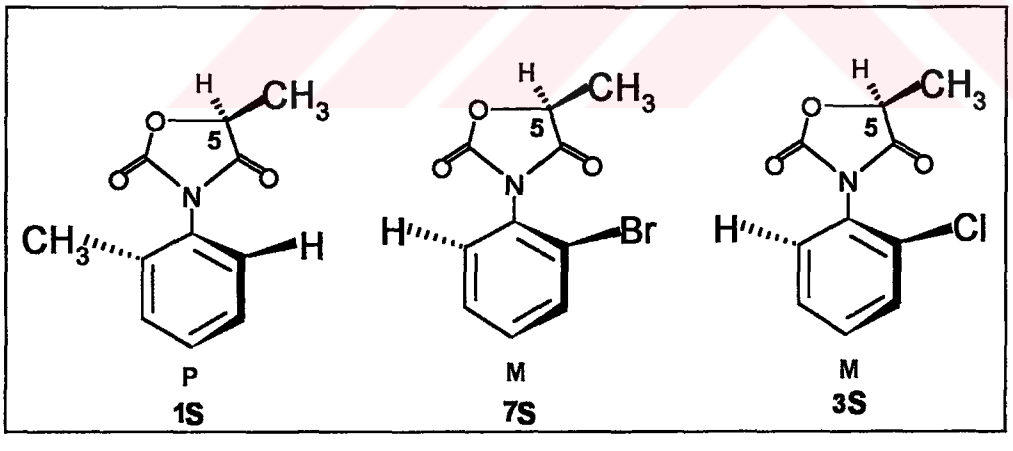

Figure 4.30. The conformations of the compounds formed in excess

The synthesis of compound 7S had yielded the M conformation in excess. However, when this isomeric mixture (7SM:7SP ratio being 62.5:32.5) was kept in a constant temperature bath, the conversion of M to P conformation was observed, by following the HPLC chromatograms (Figure 4.31, Table 4.4) on cellulose carbamate column, using UV detection at 240 nm.

Table 4.4. The change in isomer composition versus time of compound **7S** followed by HPLC [a]

Temperature (°C)	Time (h)	The percentage of the conformation P (%)	The percentage of the conformation M (%)
Room temperature	-	37.5	62.5
40	2	60.3	39.7
40	4	68.6	31.4
40	6	71.3	28.7
50	7	74.6	25.4
60	7.5	77.2	22.8

[a]: column: cellulose carbamate OD-H, Eluent: Hexane:Ethanol (80:20), flow rate: 0.5 ml/min, k_P'= 0.362, k_M'=0.655, α= 1.81, detection: UV at 240 nm

The synthesis of **7S** had yielded the **M** conformation in excess, as seen in the Figure 4.31. However, after keeping the mixture 2 hours at 40 °C in ethanol (Figure 4.31), the concentration of the **P** conformation increased and exceeded that of **M**. Increasing temperature increased the **P** concentration further. The increase in **P** continued until equilibrium. These results are interpreted in the following way:

During the ring closure step the carbonyl shows a facial selectivity (Figure 4.33) leading to an unequal distribution of the isomers **7SP** and **7SM** (37.5%: 62.5 %). This is probably the kinetically controlled pathway (Figure 4.32) during which the nitrogen ion approaches the ester carbonyl preferentially from the unhindered face forming the **M** conformation. However, when this diastereomeric mixture was heated at constant temperature, the conversion of the less stable conformer (**M**) to the more stable one (**P**) was realized via rotation around C-N single bond. Increasing temperature increases the equilibrium constant for the conversion, which is an endothermic process.

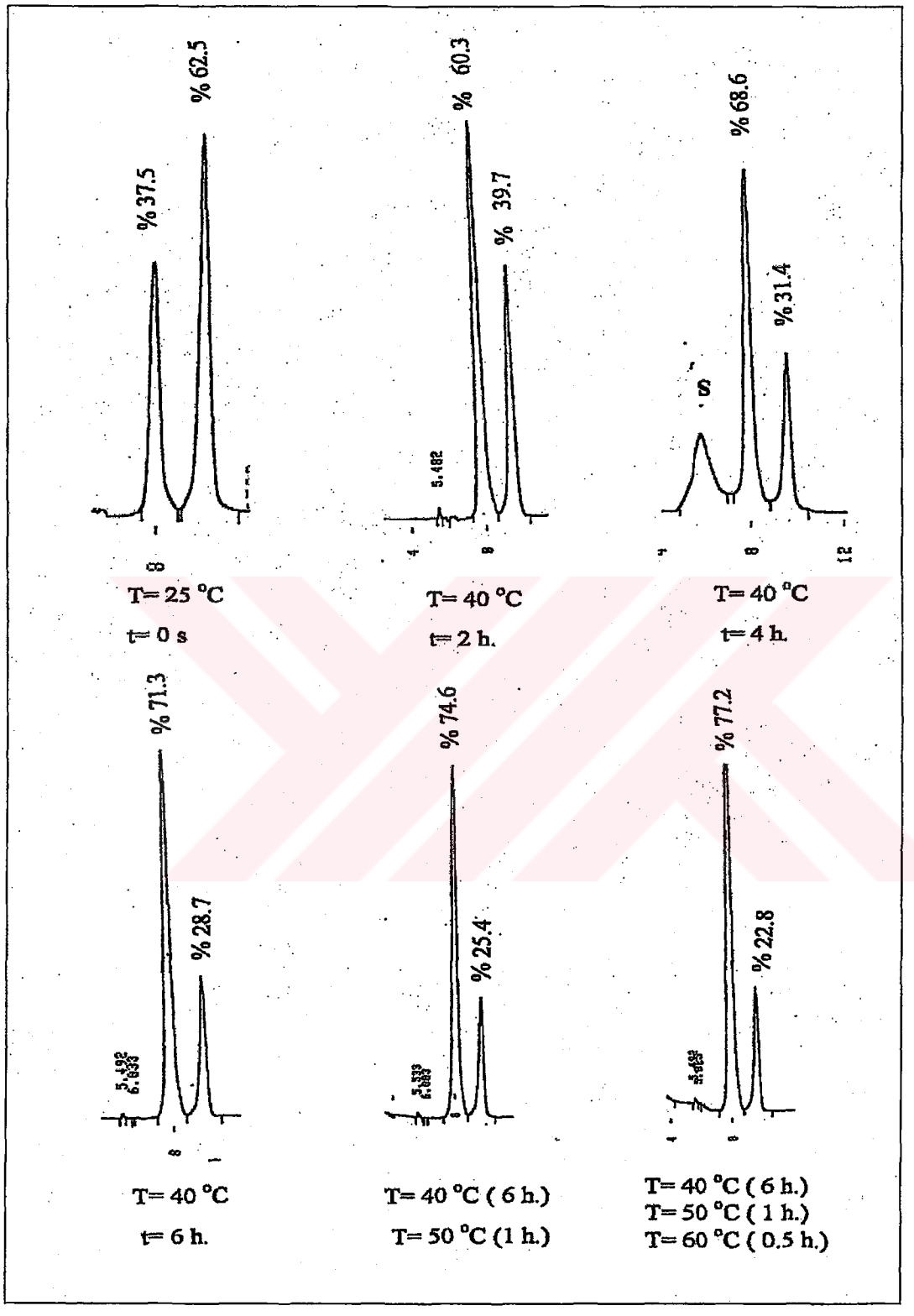

Figure 4.31. The chromatograms taken to follow the thermal equilibration of the rotational isomers of 7S. S: peak due to the water

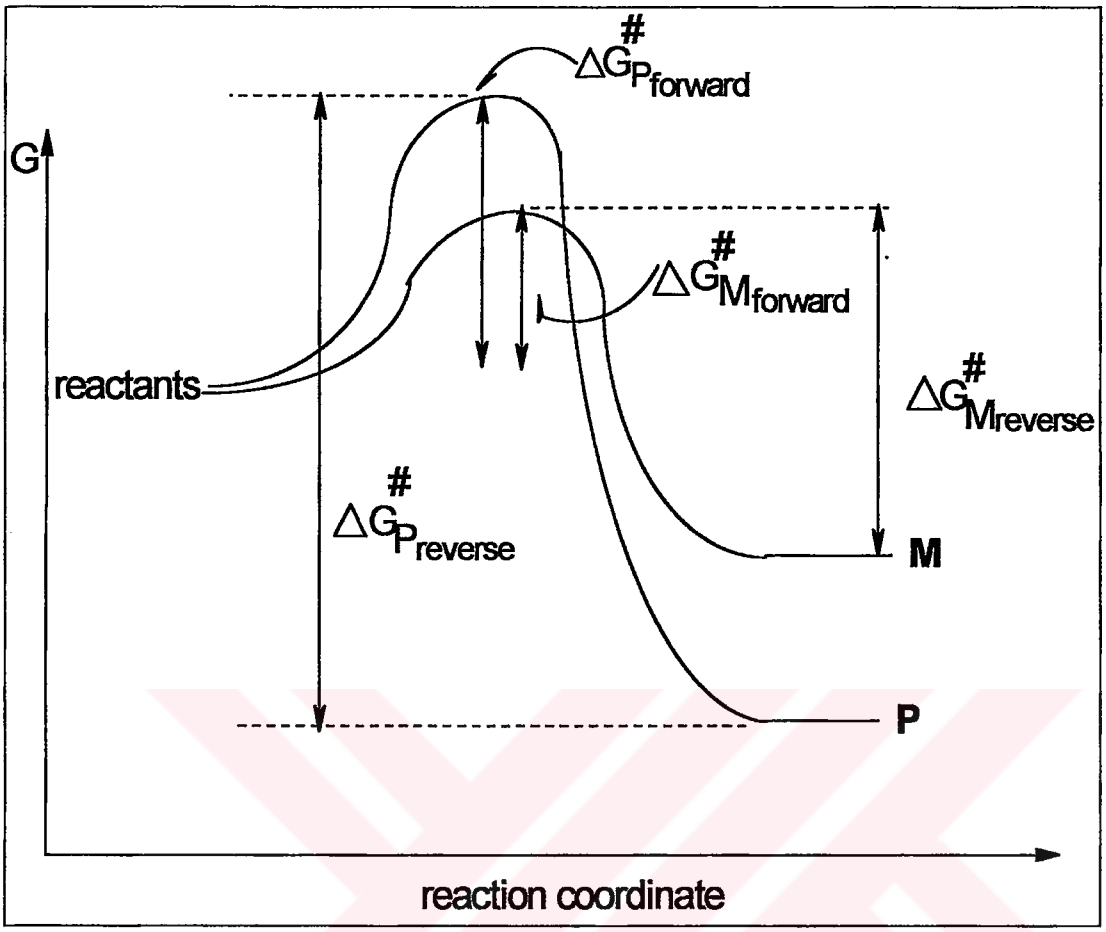

Figure 4.32. Activation barriers for the formation of two conformations

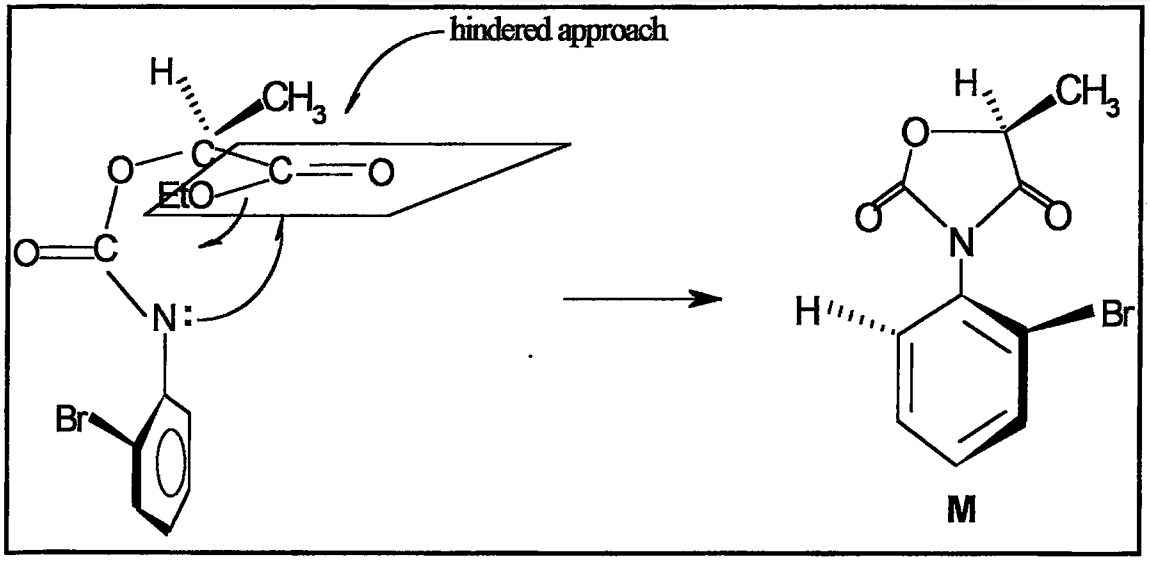

Figure 4.33. The ring closure for the M conformation

4.5. Determination of the Kinetic and Thermodynamic Constants of the Internal Rotation by HPLC

4.5.1. Determination of the Rate Constants and the Equilibrium Constants

The rate constants k_f and k_r for the internal rotation around the C-N single bond (Figure 2.11) for 5-methyl-3-(*o*-bromophenyl)-2,4-oxazolidinedione (**7S**) have been determined at 313, 323 and 333 K by following the equilibration of the diastereomers by the integration of the signals obtained from HPLC. The chromatograms are shown in the Figures 4.37,4.38 and 4.39 for 313 , 323 and 333 K, respectively.

The ratio of the integrals in percentage at equilibrium at a definite temperature have been taken as the equilibrium constant at that temperature (Tables 4.5, 4.6 and 4.7).

For compound **7S**, the thermodynamically less stable **M** conformation has been converted to the more stable one until equilibrium was reached. The rate constants were calculated by using the Equation 2.13. The slope of the line obtained from the plot of ln $([M]- [M]_{eq}/[M]_0-[M]_{eq}$ versus time gave k_r+k_f . When this value was combined with that calculated from equilibrium constant, $K= k_f / k_r$, the values for the rate constants were obtained.

The slopes for each temperature are shown in the Figures 4.34, 4.35 and 4.34. The percentages of conformations **M** and **P** are shown in the Tables 4.5, 4.6 and 4.7 for each temperature. The values for the forward and the reverse rate constants, and the equilibrium constants are given in the Table 4.8.

As seen in the Table 4.8, the rate constant for the forward reaction was found to be greater than that of the reverse reaction for equilibrium M $\rightleftharpoons$ P at all temperatures. Therefore, at equilibrium, the **P** conformation accumulated.

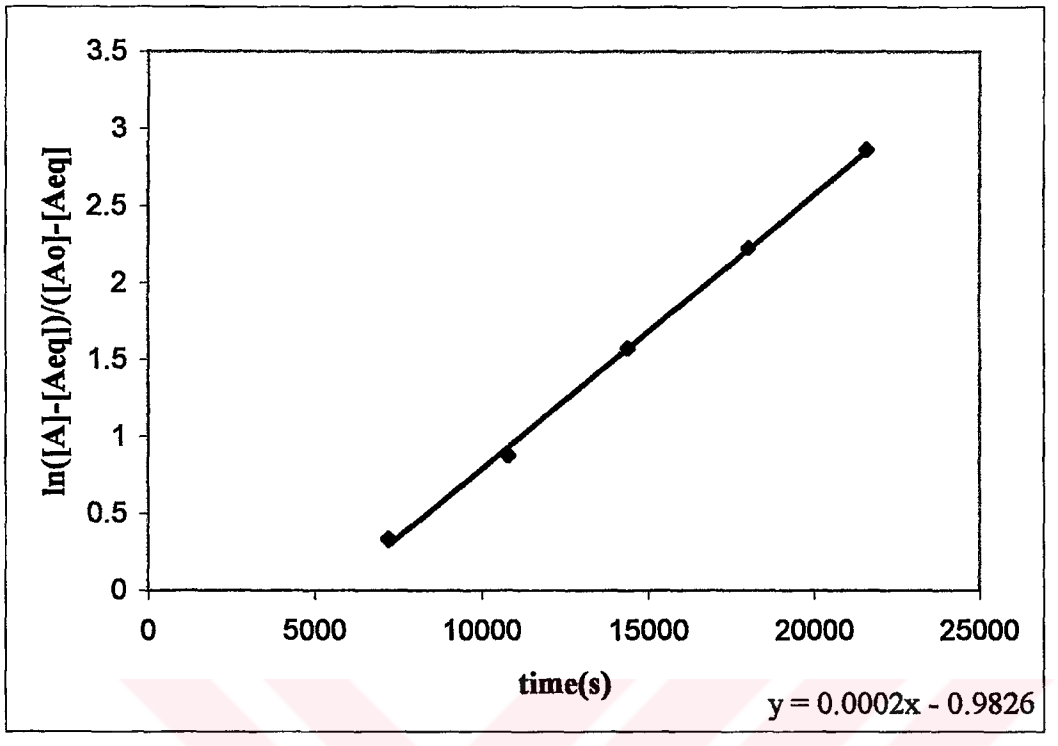

Figure 4.34. The plot of ln ([M]- $[M]_{eq}$/$[M]_{0}$-$[M]_{eq}$ versus time at 313 K

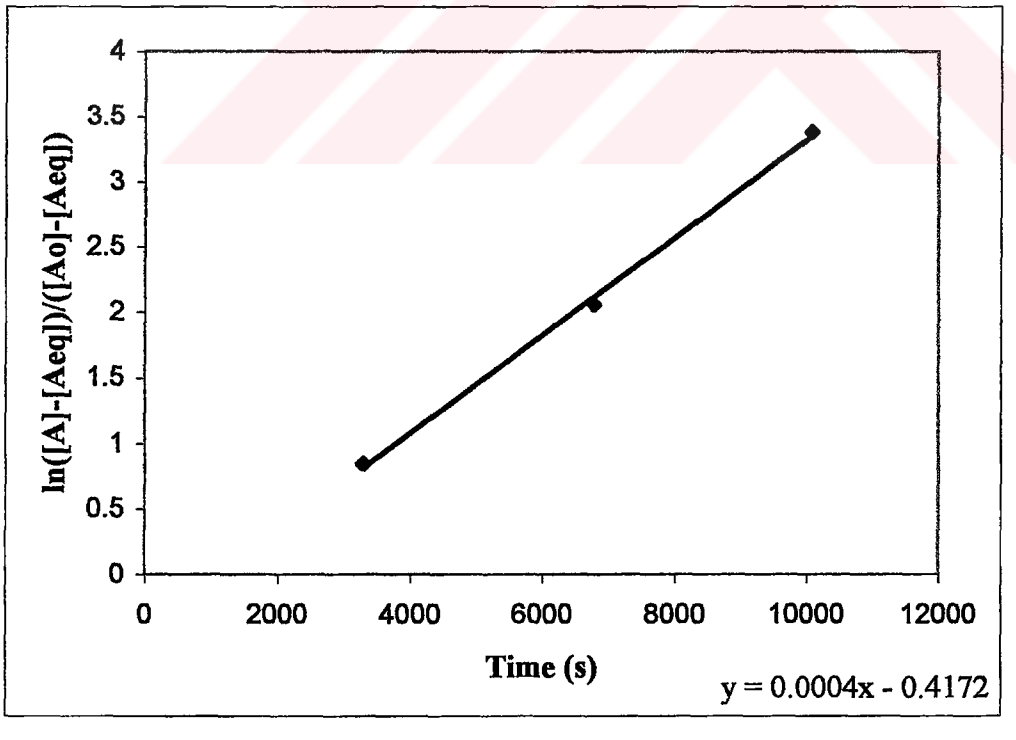

Figure 4.35. The plot of ln ([M]- $[M]_{eq}$/$[M]_{0}$-$[M]_{eq}$ versus time at 323 K

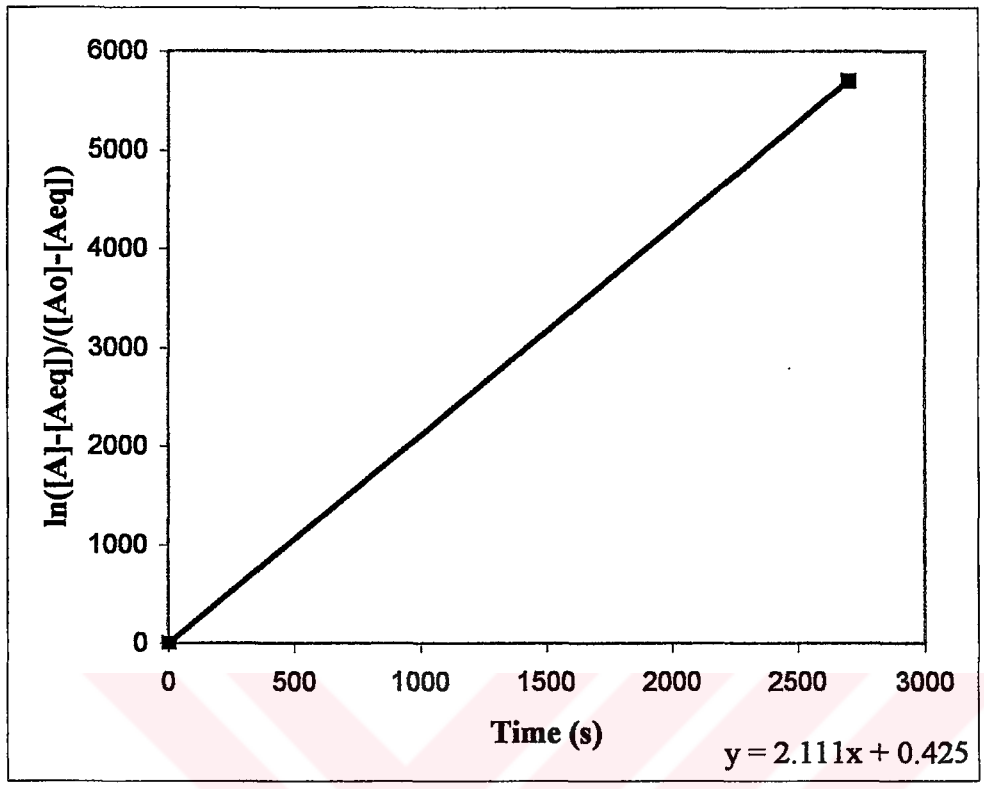

Figure 4.36. The plot of ln ([M]- $[M]_{eq}$ /$[M]_{0}$-$[M]_{eq}$ versus time at 333 K

Table 4.5. The change in isomer composition versus time of compound 7S followed by HPLC [a] for 313 K

Time (s)	The percentage of the conformation of **P**, (%)	The percentage of the conformation of **M**, (%)
0	54.52	45.48
7200	58.7	41.3
10800	63.04	36.96
14400	66.07	33.93
18000	67.51	32.49
21600	68.25	31.75
25200	69.08	30.92

[a]: Column: cellulose carbamate OD-H, eluent: ethanol, flow rate: 0.2 ml/min, k_P'=0.31, k_M'=0.53, α =1.71, t_P=19 min, t_M= 22.2 min, detection: UV at 240 nm

Table 4.6. The change in isomer composition versus time of compound 7S followed by HPLC [a] for 323 K

Time (s)	The percentage of the conformation of P, (%)	The percentage of the conformation of M, (%)
0	52.9	47.1
3300	66.3	33.7
6780	72.9	27.1
10080	75.6	24.4
13440	77.2	22.8
16020	76.4	23.7
[a]: Column: cellulose carbamate OD-H, eluent: ethanol, flow rate= 0.2 ml/min, k_P'=0.31, k_M'=0.53, α=1.71, t_P= 19 min, t_M= 22.2 min, detection: UV at 240 nm		

Table 4.7. The change in isomer composition versus time of compound 7S followed by HPLC [a] for 333 K

Time (s)	The percentage of the conformation of P, (%)	The percentage of the conformation of M, (%)
0	52.9	47.1
2700	66.3	33.7
5700	73.99	26.01
9300	76.7	23.3
12660	76.6	23.3
[a]: Column: cellulose carbamate OD-H, eluent: ethanol, flow rate= 0.2 ml/min, k_P'=0.31, k_M'=0.53, α=1.71, t_P= 19 min, t_M= 22.2 min, detection: UV at 240 nm		

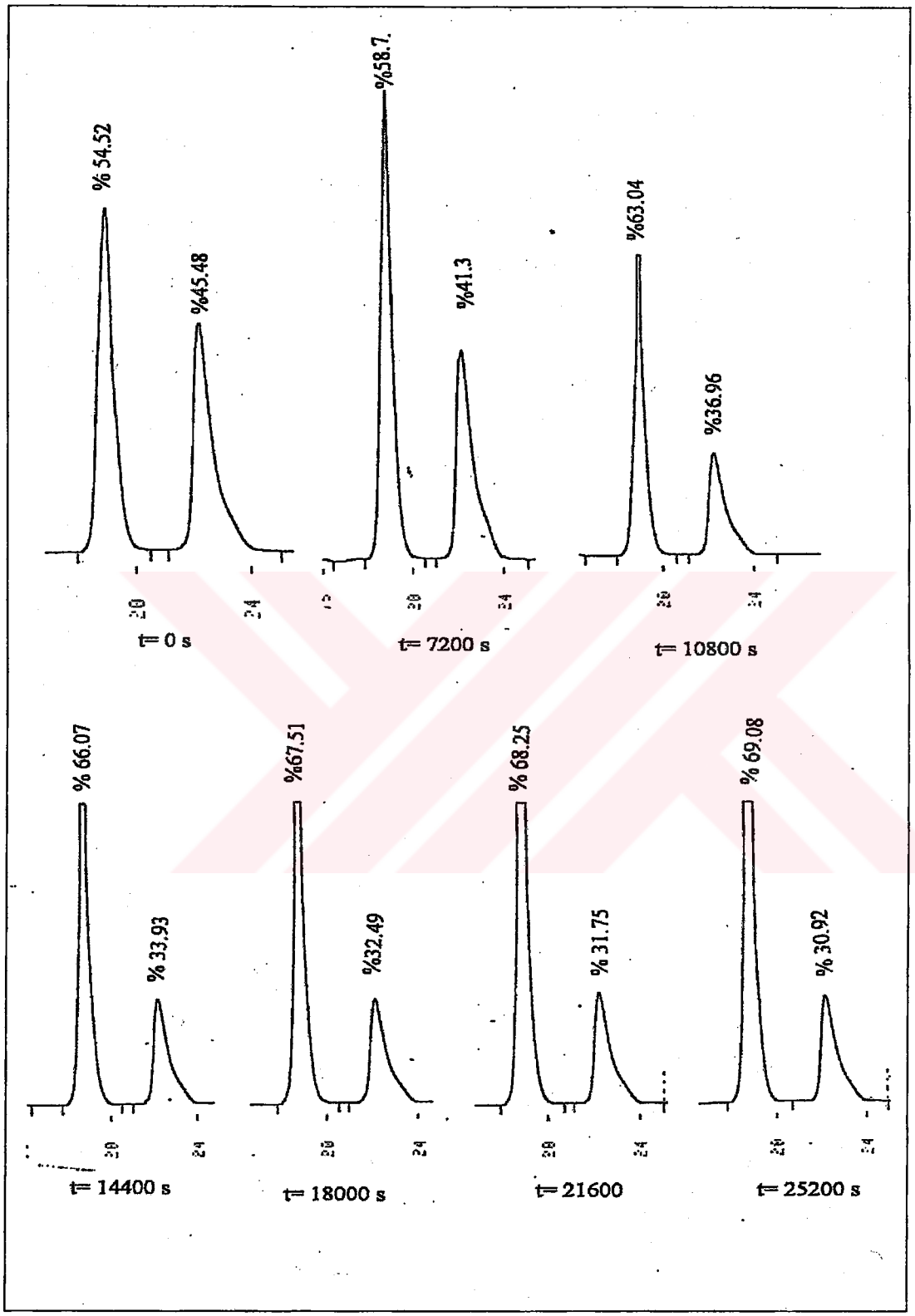

Figure 4.37. The chromatograms taken to follow the thermal equilibration of the rotational isomers of 7S at 313 K

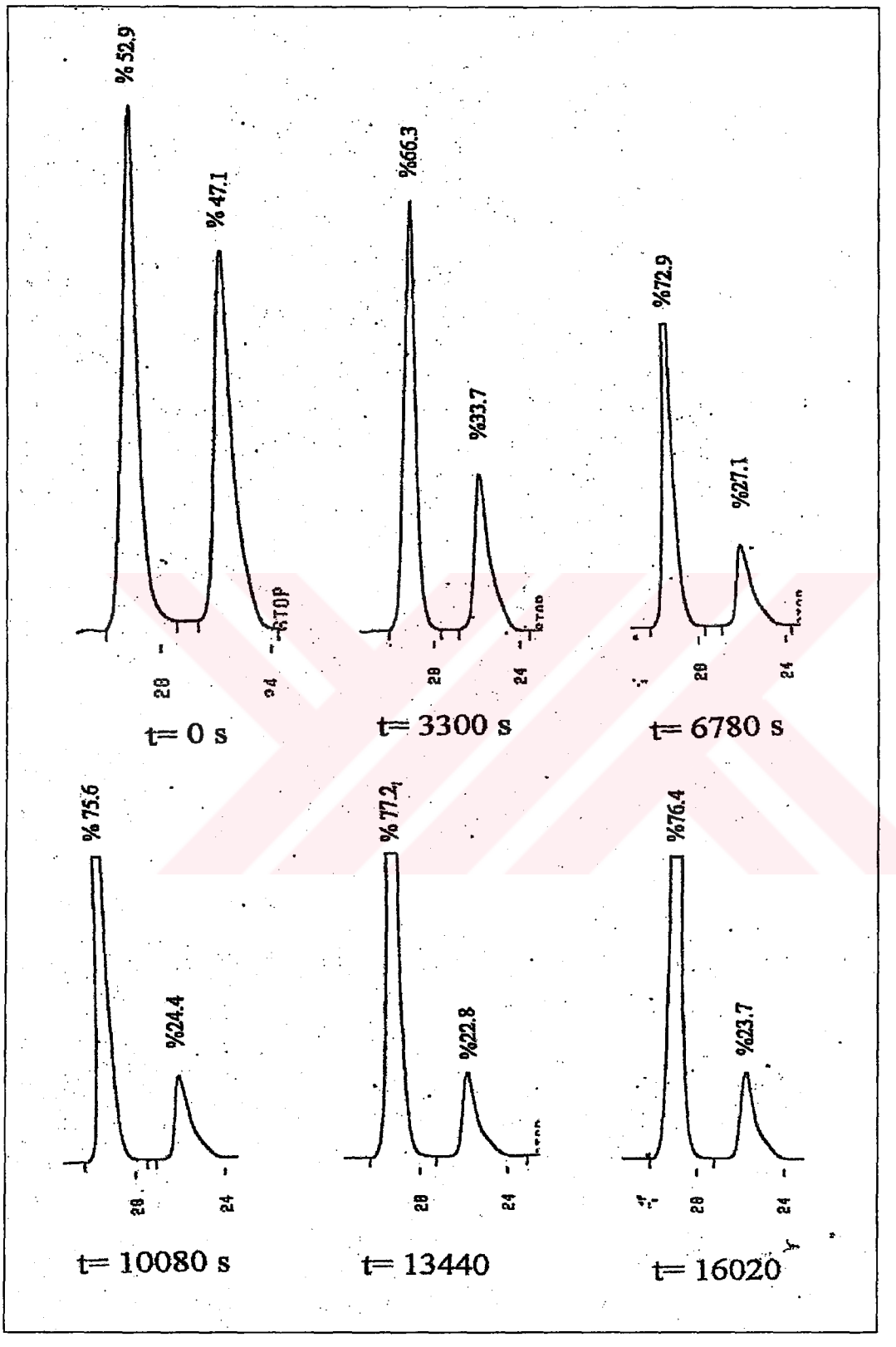

Figure 4.38. The chromatograms taken to follow the thermal equilibration of the rotational isomers of **7S** at 323 K

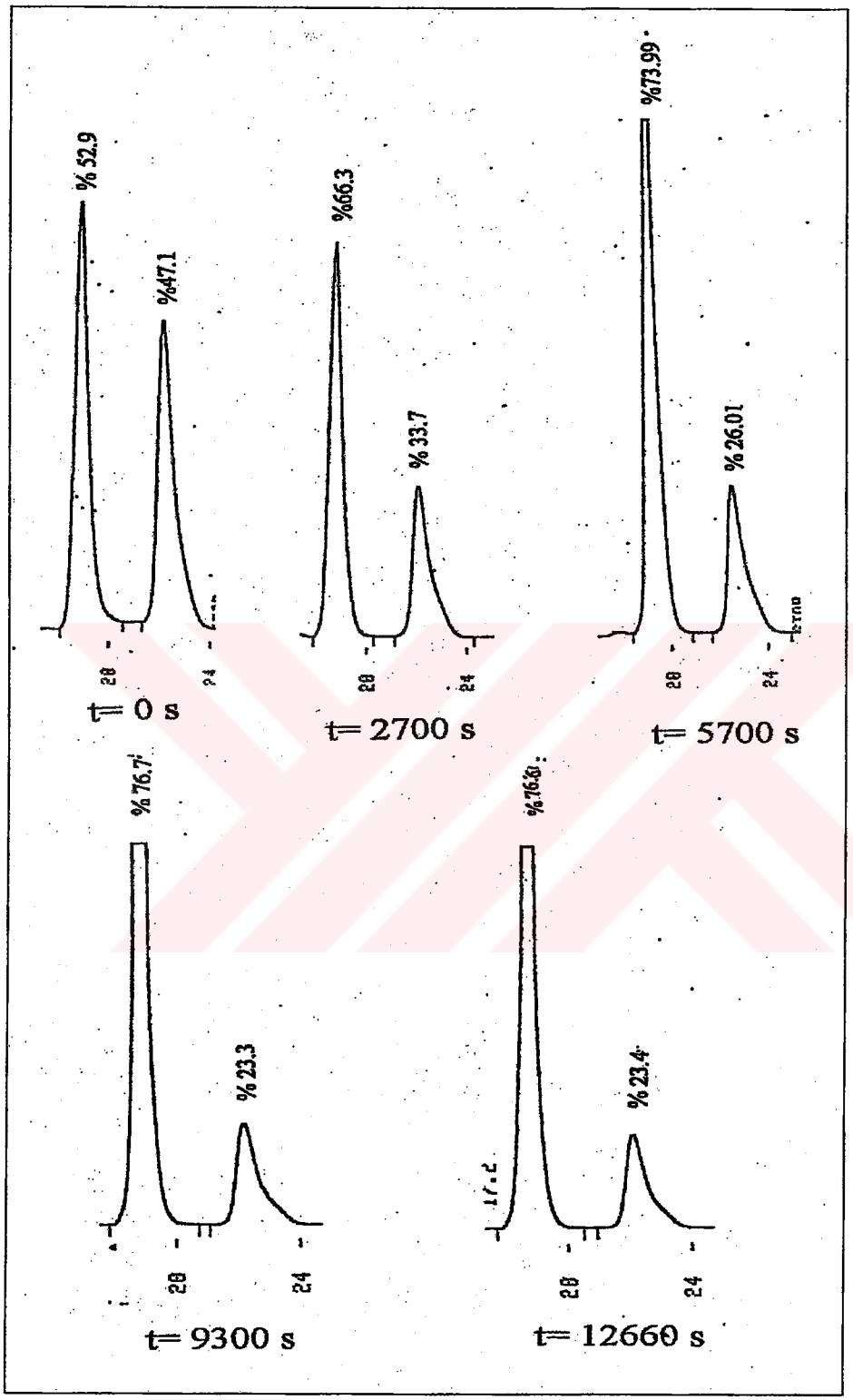

Figure 4.39. The chromatograms taken to follow the thermal equilibration of the rotational isomers of 7S at 333 K

4.5.2. Determination of the Activation Energy $\Delta G^{\#}$ for Hindered Rotation

$\Delta G^{\#}$ for the interconversion between the rotational isomers has been determined for compound **7S** using the values for the rate constants found in Section 4.5.1 and Eyring Equation 2.14. The results are given in the Table 4.8.

The barrier was found approximately 100 kJ/mol at 40 °C and 50 °C, which enabled the rotational isomers of 5-methyl-3-(*o*-bromophenyl)-2,4-oxazolidinedione (**7S**) to be separable at room temperature.

4.5.3. Determination of the ΔG°, ΔH° and ΔS° Values

ΔG° value for the interconversion of **M** to **P** (Figure 2.12) was found using the value of the equilibrium constant using the Equation 2.15 for each temperature. The negative value of ΔG° (Table 4.8) showed that the interconversion took place from the less stable conformation to the more stable one. ΔH° and ΔS° values have been determined by using Equation 2.16. From the slope and intercept of the ln K versus 1/T plot (Figure 4.40), the ΔH° and ΔS° values were calculated, respectively.

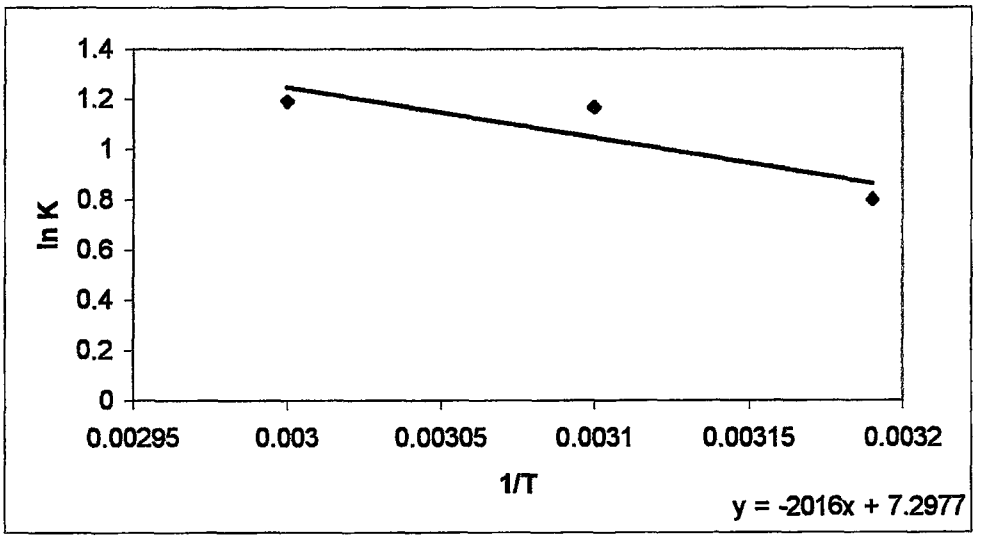

Figure 4.40. The plot of ln K versus 1/T

Table 4.8. Kinetic and thermodynamic constants of the internal rotation in compound **7S**

kinetic/thermodynamic constants for M ⇌ P	40 °C	50 °C	60 °C
k_f, (s^{-1})	$1.38*10^{-4}$	$3.05*10^{-4}$	1.62
k_r, (s^{-1})	$6.19*10^{-5}$	$9.48*10^{-5}$	0.49
$\Delta G^{\#}$,(kJ/mol) [a]	99.9	101.1	80.5
$\Delta G^{\#}$,(kJ/mol) [b]	102.003	104.2	83.8
ΔG^{o},(kJ/mol)	-2.09	-3.1	-3.3
K	2.2	3.2	3.3
ΔH^{o}, (kJ/mol)	16.8	-	-
ΔS^{o},(J/K)	60.7	-	-
[a]: Forward direction; [b]: reverse direction			

4.6. ^{13}C NMR Spectra of the Compounds

The (APT) ^{13}C NMR spectra of the compounds **2**, **4**, **6** and **8** were studied for identification and for the further proof for the chiralty of the molecules. The (APT) ^{13}C NMR spectra of these compounds have been taken in hexadeuterobenzene. The spectra indicated the presence of anisochronous carbon nuclei for the diastereotopic methyl groups in all compounds except compound **6** (Figures 4.41-4.44).

For the compounds **2**, **4** and **8**, two signals were observed for the two diastereotopically related carbons resonating between 22.9-23.7 ppm. The C-5 carbons gave peaks around 83 ppm. The carbonyl carbons resonated at around 174 and 153 ppm. The more deshielded peak for the cabonyl carbon has been assigned to the C-4 based on comparison with the values in the tables [26]. The aromatic carbons resonated between 122-136 ppm. All the chemical shift values are shown in Table 4.9.

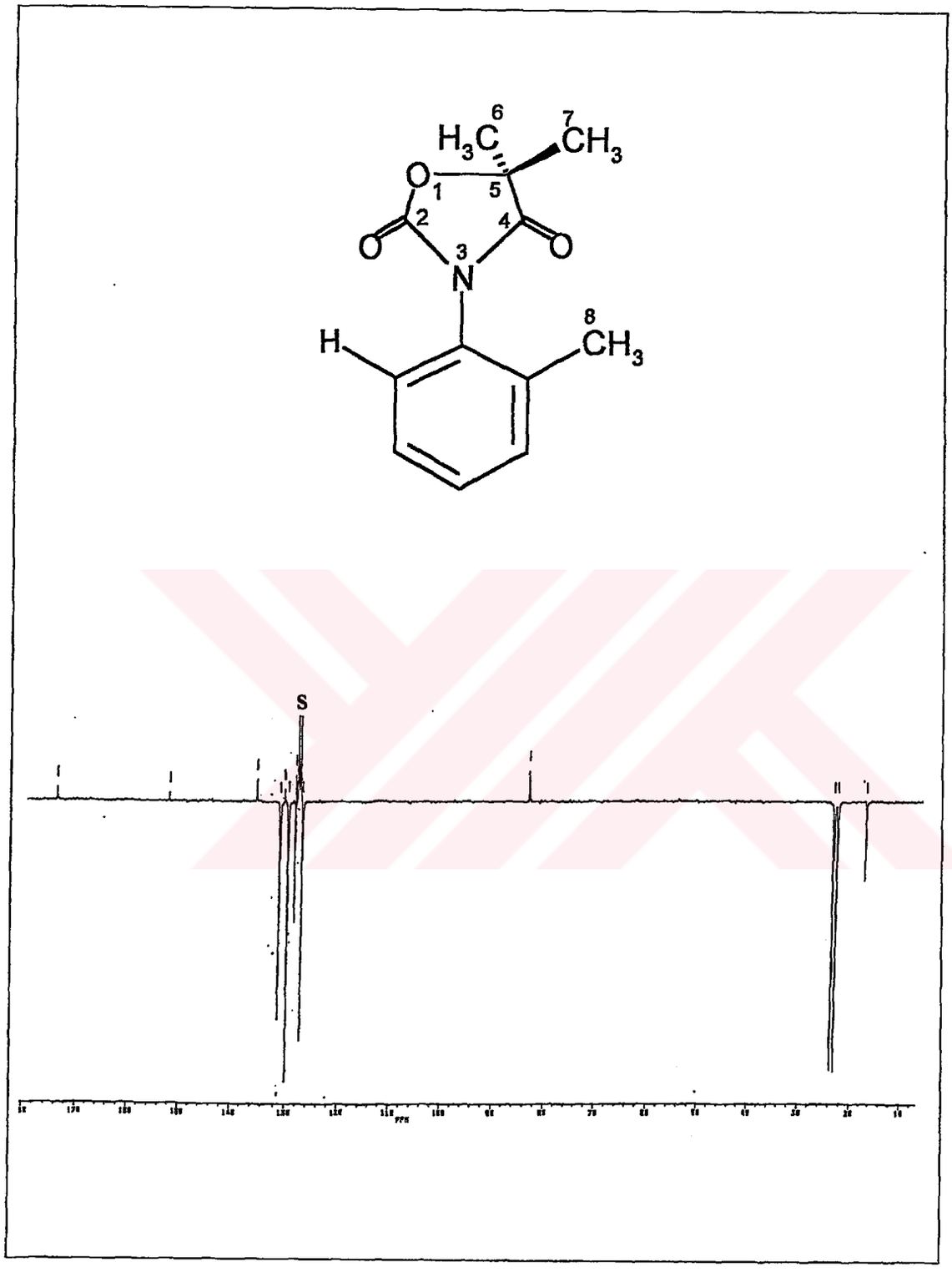

Figure 4.41. The (APT) ^{13}C NMR spectrum of the compound **2**. Solvent: C_6D_6 .

S: peaks due to the solvent

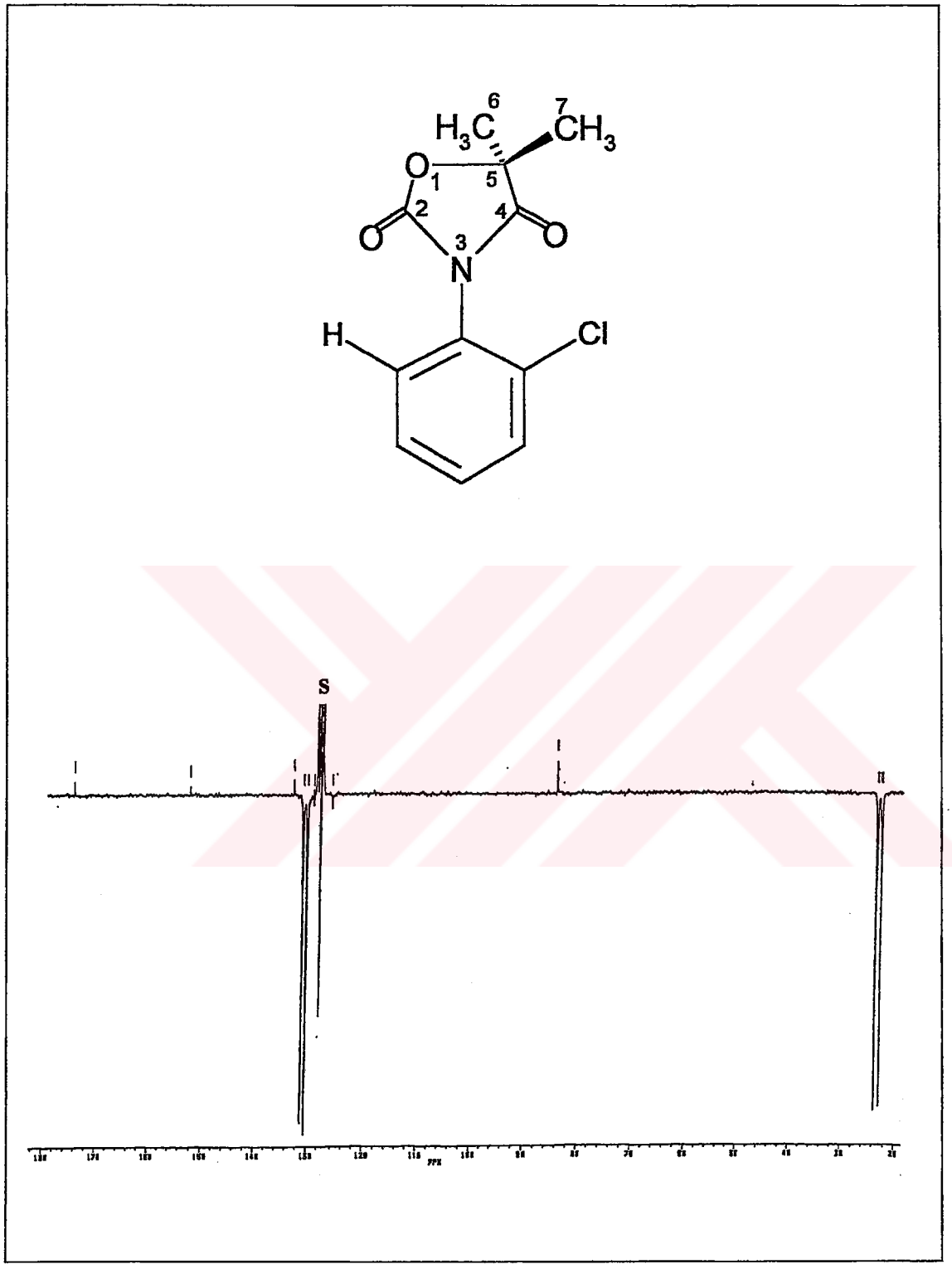

Figure 4.42. The (APT) ^{13}C NMR spectrum of the compound **4**. Solvent: C_6D_6 .

S: peaks due to the solvent

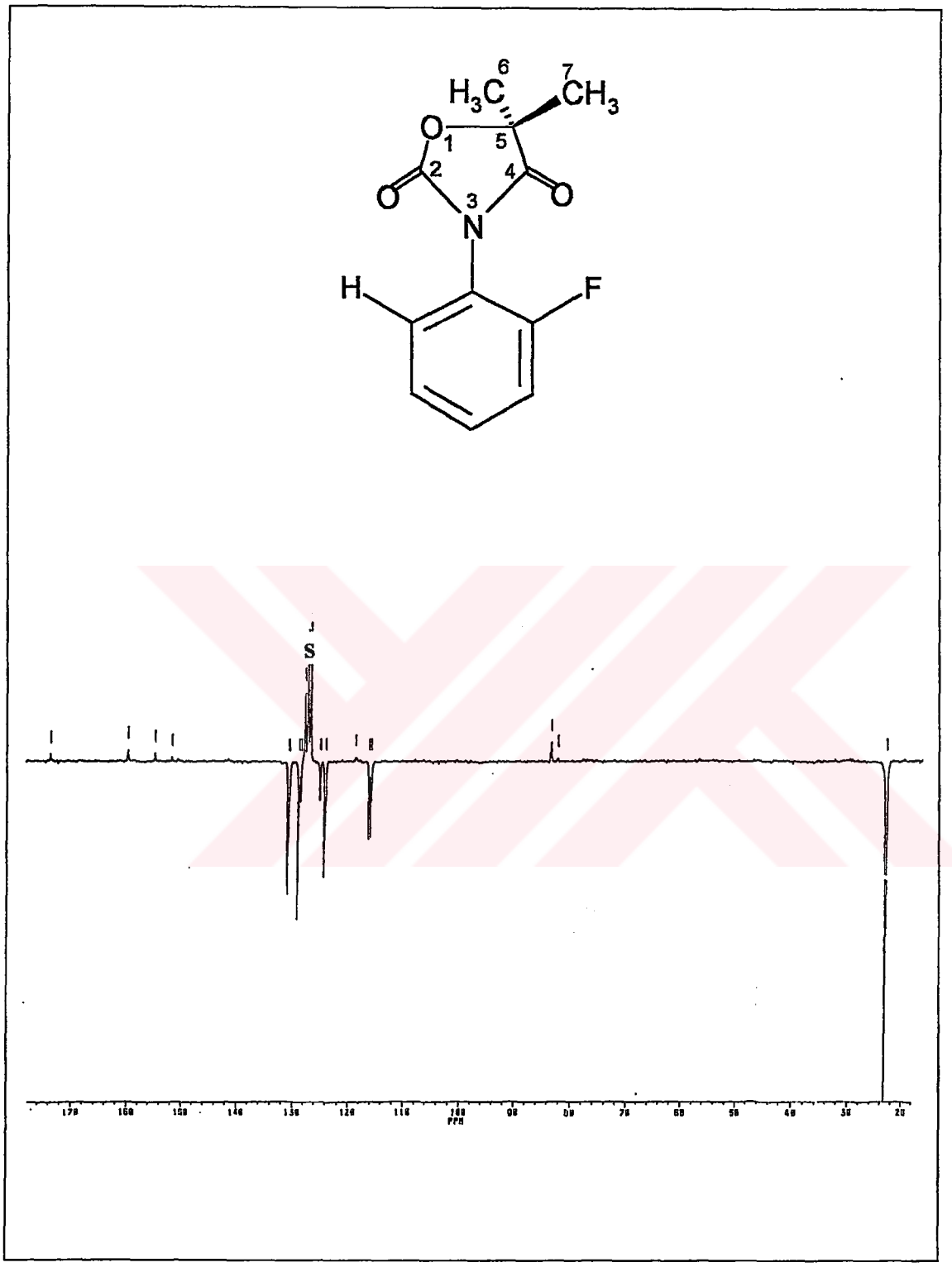

Figure 4.43. The (APT) ^{13}C NMR spectrum of the compound **6**. Solvent: C_6D_6 .

S: peaks due to the solvent

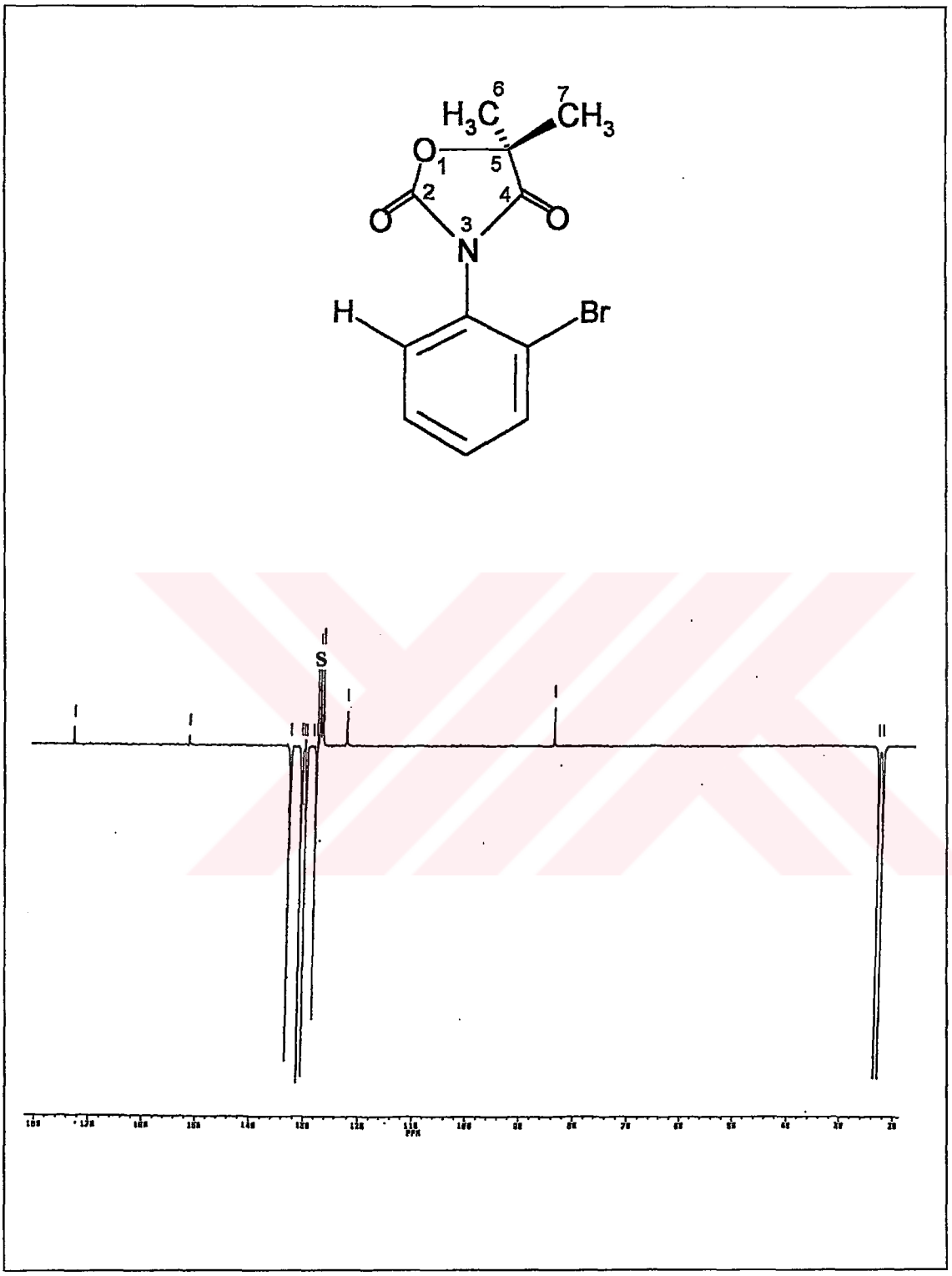

Figure 4.44. The (APT) ^{13}C NMR spectrum of the compound **8**. Solvent: C_6D_6 .

S: peaks due to the solvent

Table 4.9. The (APT) ^{13}C NMR chemical shifts (ppm) of the compounds **2, 4 , 6** and **8** in C_6D_6

Carbon No[a]	Compound **2**	Compound **4**	Compound **6**	Compound **8**
2	153.1	152.3	155.4 or 152.4	152.3
4	174.8	174.2	174.2 or 160.5	174.1
5	83.5	84.1	84	84.2
6 and 7	23 and 23.7[b]	22.9 and 23.8[b]	23.3	22.9 and 23.8[b]
8	17.4	-	-	-
aromatics	127.1-136.2	127.8-132.9	116.5-125.7	122.9-133.5
[a]: See Figures 4.39-4.42 for numbering; [b]: Signals due to the diastereotopic methyl carbons				

As seen in the Figure 4.43, for 5,5-dimethyl-3-(*o*-fluorophenyl)-2,4-oxazolidinedione (**6**), four more aromatic carbons and two more carbonyl carbons were observed with chemical shift values very close to that of the original compound. This observation was surprising because the compound seemed pure based on its elemental analysis, ^1H NMR and melting point. This point needs to be clarified by further investigations.

4.7. Reaction of 5-Methyl-3-(*o*-aryl)-2,4-oxazolidinediones with Methanol

The reaction of 5-methyl-3-(*o*-aryl)-2,4-oxazolidinediones with methanol was followed using the 60 MHz ^1H NMR spectrometer. The 5-methyl-3-(*o*-tolyl)-2,4-oxazolidinedione gave no reaction with methanol within five days under reflux. The ^1H NMR spectra taken after *o*-chloro, *o*-bromo and *o*-fluoro substituted 2,4-oxazolidinediones were refluxed in methanol for 5 days, followed by evaporation of the methanol, however, showed that these compounds reacted with methanol. The reaction was best followed for the *o*-fluoro substituted compound (**5S**). From the analysis of the ^1H NMR spectrum (Figure 4.47, A denotes the peaks due to the unreacted **5S**, B denotes due to the open chain product (Hydroxy amide) (see Figure 4.45), C denotes the peak due to methanol and methyl carbonate), it was concluded that a ring opening reaction took place from the lactone carbonyl followed by an elimination of methyl carbonate (Figure 4.45). The quartet at around 4.4 ppm has been assigned to the C-H proton, the doublet at around 2 ppm to the methyl protons of the open chain structure (the hydroxyamide). The N-H proton was observed at 8 ppm. The methyl carbonate protons resonated at 4 ppm. The products were

present together with some unreacted **5S**, where the florine atom has been associated with methanol. This structure (Figure 4.46) is thought to increase the barrier to rotation so that the two diastereomers became observable (Figure 4.47).

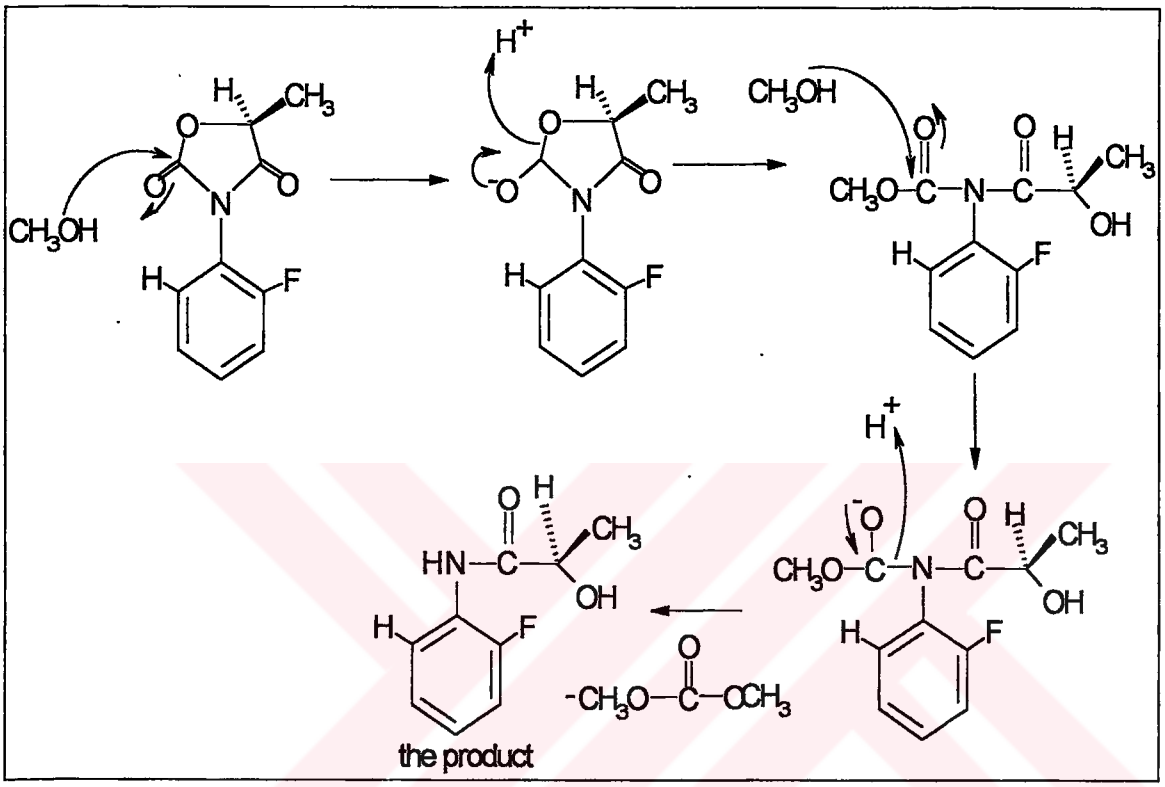

Figure 4.45. The structure of the product and the mechanism of the reaction of methanol with 5-methyl-3-(*o*-fluorophenyl)-2,4-oxazolidinedione

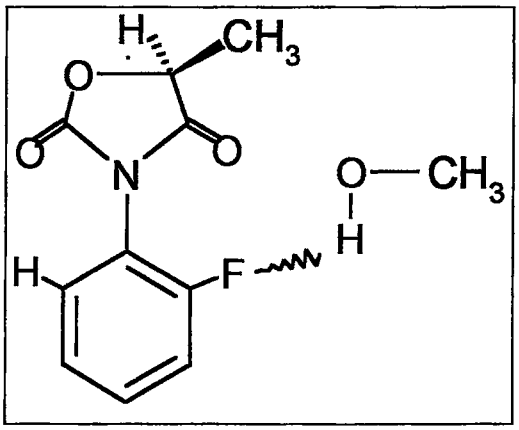

Figure 4.46. The association complex formed with methanol

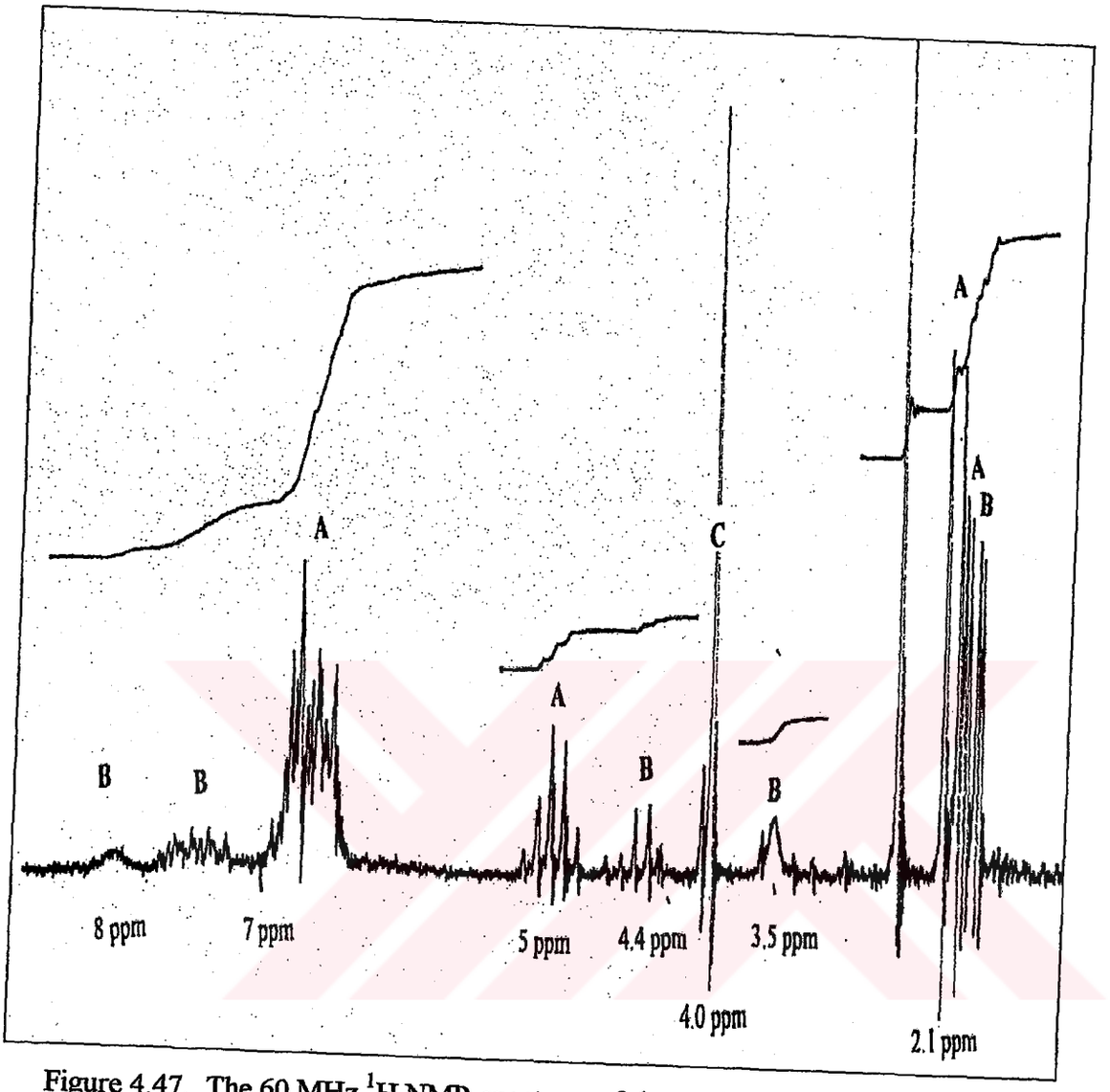

Figure 4.47. The 60 MHz ^{1}H NMR spectrum of the crude product obtained after 5S was refluxed in methanol for five days

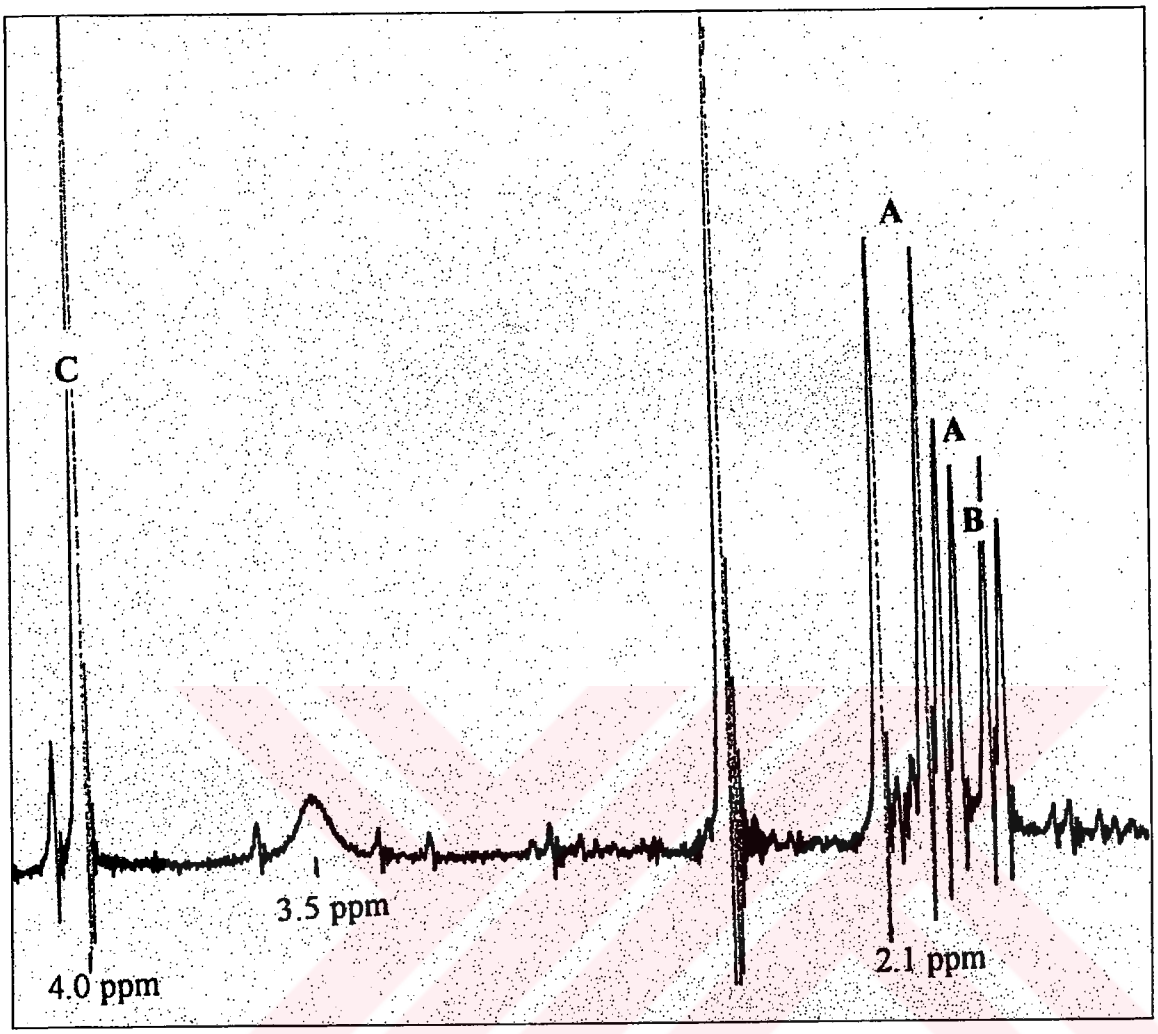

Figure 4.48. The upfield portion of the spectrum (Figure 4.47) expanded with sweep width of 250 Hz

5. CONCLUSION

In this project N-*o*-aryl substituted 2,4-oxazolidinedione derivatives (Figure 1.9) where the hindered molecular rotation around the C-N single bond causes axial chirality have been studied. The molecules have been synthesized (Table 1.1), chirality in their ground states has been investigated and the barriers to interconversion have been determined using dynamic ^{1}H NMR and thermal equilibration using HPLC on cellulose carbamate.

The synthesis of the compounds were done by the reaction of S-ethyl lactate or ethyl α-hydroxyisobutyrate with the appropriate *o*-arylisocyanate. The 5,5-dimethyl-3(*o*-aryl)-2,4-oxazolidinedione derivatives (**2,4,6,8**) formed enantiomers by 180 ° rotation around the C-N single bond, whereas the 5-methyl-3-(*o*-aryl)-2,4-oxazolidinediones (**1S,3S,5S,7S**) containing the C-5 chiral carbon formed diastereomers. In these molecules the N-*o*-aryl substitution should determine the barrier to internal rotation. The substituents chosen were fluoro, chloro, bromo and methyl groups. It has been observed that when the *o*-substituents is F, which is the smallest in the series (Table 4.1), the rotational isomers could not be detected on the NMR time scale at the ordinary probe temperature. When the substituent is changed to chlorine and methyl , the rotational isomers became detectable on ^{1}H and ^{13}C NMR but not on HPLC on an optically active column. For the *o*-methyl and *o*-chloro derivatives forming enantiomers (where the barriers were less than 100 kJ/mol), the barriers could be determined by dynamic NMR as 75.8 and 83.2 kJ/mol, respectively. The magnitude of the barriers showed that the Cl substituent causes a larger steric effect than the methyl substituent despite its smaller size. This effect which is consistent with the previous studies [18] is explained in terms of the interaction of the lone pairs electrons of chlorine with that of carbonyl oxygen atoms of the heterocyclic ring. Dynamic NMR could not be used to determine the energy of activation of *o*-methyl and *o*-chloro substituted diastereomers because of the unequal line intensities.

When the *ortho* substituent was bromine , the rotational isomers become separable by HPLC on cellulose carbamate and the activation barrier was determined as 100 kJ/mol at 40 °C.

The stereostructures of the diastereomers were identified by examining the ^{1}H NMR spectra.

The initial formation of the oxazolidinedione ring is thought to involve a facial selectivity of the ester carbonyl leading to the formation of the **M** conformation. However, when the **M** conformation was kept at constant temperature (40 °C) thermodynamic enrichment of the **P** conformation was observed while equilibrium was reached. The equilibrium constant and the free energy of activation between the diastereomers of the *o*-bromo derivative have been determined in addition to the free energy of activation for rotation.

A slow ring opening reaction of the halogen substituted diastereomers have been observed on treatment of the compounds with methanol under the reflux temperature.

6. REFERENCES

1. Crisitie, G.H. and J. Kenner, "Restricted Rotation about the C-N Single Bond of 1-Aryl-4,6-dimethylpyrimidine-2(1H)-ones and the Corresponding Thiones" , *Journal of American Chemical Society*, Vol. 55, No. 121, pp. 614, 1922.

2. Adams, R. and R.W. Stoughton, "Stereochemistry of Diphenyl Compounds. The Preparation and Resolutiom of 2-Methyl-6-nitro-2'-carboxydiphenyl", *Journal of American Chemical Society*, Vol. 52, pp. 5263-5267, 1930.

3. Shildneck and Adams, "Stereochemistry of Diphenylbenzenes. Meso and Racemic Hydroquinones and Quinones", *Journal of American Chemical Society*, Vol. 53, pp. 343, 1931.

4. Bock, L.H. and R. Adams, "Stereochemistry of Phenyl Pyrroles", *Journal of American Chemical Society*, Vol. 53, pp. 3519, 1931.

5. Bock, L.H. and R. Adams, "The Preparation and Resolution of N-2-caboxy-phenyl-2,5-dimethyl-3-carboxypyrolle", *Journal of American Chemical Society*, Vol. 53, pp. 374, 1931.

6. Chang, C. and R. Adams, "Stereochemistry of N,N'-dipyrryls. Resolution of N,N',2,5,2',5'-tetramethyl-3,3'-dicarboxydipyrryl", *Journal of American Chemical Society*, Vol. 53, pp. 2353-2357, 1931.

7. Bentz, W. E., L. D. Colebrook and J.R. Fehlner, "Hindered Rotation about C-N Bonds: Equilibration of Diastereomeric Rotational Isomers", *Chemical Communications*, pp. 974, 1970.

8. Colebrook, L. D. and H. G. Giles, "High Rotational Barriers About C-N Bonds in Aryl Substituted Heterocyclic Compounds Lacking Bulky *Ortho* Substituents", *Tetrahedron Letters*, No. 51, pp. 5236-5240, 1972.

9. Colebrook, L. D., H. G. Giles, A. Granata, J. R. Fehlner and S. Icli, "Restricted Internal Rotaion in 1-Arylhydantoins, 3-Arylhydantoins, and 3-Aryl-2-Thiohydantoins: Reversal of the Effective Sizes of Methyl and Chlorine", *Canadian Journal of Chemistry*, Vol. 51, pp. 3635-3639, 1973.

10. Raban, M. and K. Mislow, *Tetrahedron Letters*, No. 48, pp. 4249, 1965.

11. Colebrook, L. D., F. H. Hund and S. Icli, "Nuclear Magnetic Resonance Studies of Enantiomeric Internal Rotational Isomers of 1- and 3-Arylhydantoins in Achiral and Chiral Solvents", *Canadian Journal of Chemistry*, Vol. 53, pp. 1556-1562, 1975.

12. Dogan, I., T. Burgemeister, S. Icli and A. Mannschreck, "Sythesis and NMR Studies of Chiral 4-Oxazolidinones and Rhodanines", *Tetrahedron*, Vol. 48, pp. 7157-7164, 1992.

13. Berg, U., J. Sandström and A. Mannschreck, " Enantiomers of Polarized alkenes: Chromatographic Enrichment and Thermal Interconversion", *Tetrahedron Letters*, Vol. 23, No. 41, pp. 4237-4240, 1982.

14. Roussel, C. and A. Djafri, "Separation of Enantiomers on Triacetylcellulose and Barriers to Rotation in *m*-Substituted N-Phenyl-delta-4-thiazoline-2-thiones", *Nouveau de Chimie*, Vol. 10, No. 7, 1986.

15. Mintas, M., J. Vorkapic-Furac, A. Mannschreck, "Enantiomers and Barriers to Racemization of Hindered N-Aryl and N-Heteroarylpyrolles", *Journal of Heterocyclic Chemistry*, Vol. 29, pp. 327-333, 1992.

16. Roussel, C., J. L. Stein and F. Beauvais, "Separation of Atropisomers on CSP Microcrystalline Cellulosetriacetate and Barriers to Rotation in Some Polymethyl-3-phenyl-Δ-4-thioazoline-2-thiones and their Oxygen Analogues", *New Journal of Chemistry*, Vol. 14, No. 2, pp. 169-173, 1990.

17. Mintas M., J. Vorkapic-Furac and A. Mannschreck, "Sterically N-Aryl Pyrolles: Chromatographic Separation of Enantiomers and Barrier to Racemization", *Journal of Chemical Society Perkin Transaction II*, pp. 713-171, 1989.

18. Dogan, I. And A. Mannschreck, "The Enantiomers of N-Aryl-2-thioxo-4-oxazolidinones and N-Arylrhodanines. Investigation by Liquid Chromatography, Circular Dicroism and Thermal Racemization", *Journal of Chemical Society Perkin Transaction II*, pp. 1557-1560, 1993.

19. Icli, S. "^{1}H NMR and ^{13}C NMR Studies on 3-Aryl-5-alkyl-2,4-oxazolidinediones. The Magnetic Non-eqivalace of Isomeric Nuclei", *Organic Magnetic Resonance*, Vol, 12, No. 3, pp. 178-182, 1979.

20. Shapiro, S., F. C. Testa and L. Freedman, "N-Substituted Oxazolidinediones", *Journal of American Chemical Society*, Vol. 81, Dec. 20, pp. 6498-6504, 1959.

21. Cahn, R. S., C. Ingold and V. Prelog, "Specification of Molecular Chiralty", *Angewandte Chemie International Edition in English*, Vol. 5, No. 4, pp. 385-415, 1966.

22. Ernest, L. E. and H. W. Samuel, *Stereochemistry of Organic compounds*, John Wiley, New York, pp. 231-232, 1994.

23. Williams, T., P. Bommer and M. Uskokovic, "Diastereomeric Solute-Solute Interactions of Enantiomers in Achiral Solvents. Nonequivalence of the Nuclear Magneti Resonance Spectra of Racemic And Optically Active Dihydroqinine", *Journal of American Chemical Society*, Vol. 91, pp. 1871-1872, 1969.

24. Anet, F. A. l., L. M. Sweeting and D. J. Cram, "Diastereomeric Interactions in Solution", *Tetrahedron Letters*, No. 22, pp. 2617-2620, 1968.

25. Carey, A. F. and R. Sundberg, *Advanced Organic Chemistry*, Part-A: Structure and Mechanism, Plenum Press, New York-London, pp. 120, 1990.

26. Wehrli, F. W. and T. Wirthlin, *Interpretation of Carbon-13-NMR Spectra*, Hyden and Son Ltd, 1976.